Analytical Approximation Formulae for Hydrogen Diffusion in a Metal Slab

F. Pohl and J. Bohdansky

IPP 6/245 December 1984

MAX-PLANCK-INSTITUT FÜR PLASMAPHYSIK

8046 GARCHING BEI MÜNCHEN

MAX-PLANCK-INSTITUT FÜR PLASMAPHYSIK

GARCHING BEI MÜNCHEN

Analytical Approximation Formulae for Hydrogen Diffusion in a Metal Slab

F. Pohl and J. Bohdansky

IPP 6/245 December 1984

Die nachstehende Arbeit wurde im Rahmen des Vertrages zwischen dem Max-Planck-Institut für Plasmaphysik und der Europäischen Atomgemeinschaft über die Zusammenarbeit auf dem Gebiete der Plasmaphysik durchgeführt.

IPP 6/245 F. Pohl
J. Bohdansky

Analytical Approximation Formulae for Hydrogen Diffusion in a Metal Slab

December 1984 (in English)

Abstract:

This report treats hydrogen diffusion in the first wall of a fusion machine (INTOR, reactor, etc.), taking the thermal load into account. Analytical approximation formulae are given for the concentration and flux density of hydrogen diffusing through a plane metal slab. The re-emission flux, particularly during the dwell time(s) of machine operation, is also described with analytical formulae. The analytical formulae are compared with numerical calculations for steel as first wall material.

Contents page

C Temperature-Dependent Coefficients

Sec.5 Origin of the Parameters

Sec.6 Remarks on the Formulae 57

1. Introduction

Hydrogen diffusion through metal walls is a serious problem for DT fusion experiments with respect to both the tritium inventory and the tritium loss and has therefore often been investigated (see, for example, Ref./1/). Most reports on the subject essentially consist of numerical calculations using computer programms (DIFFUSE, PERI, Refs./11, /12/). These, however, do not readily show the influence of the parameters, e.g. the material constants, on the curves and/or data obtained. What is needed are analytical solutions of the diffusion problems involved in order to allow direct study of the influence of the various parameters. Exact solutions, however, only exist for special cases (sec. 2). This report uses these special solutions to construct analytical approximation solutions which are also valid for fusion-relevant conditions.

The treatment is concerned with the temperature variation (sec. 3) and hydrogen diffusion (sec. 4) in a plane slab with one side subjected simultaneously to hydrogen bombardment and a thermal load while the other side is cooled. The hydrogen bombardment and thermal load are periodically switched on and off to simulate the conditions on the first wall and on the divertor or limiter plates during the burn and dwell times of a fusion machine (e.g. INTOR or reactor). Some of the implanted hydrogen recombines on the surface of the slab to the coolant. This leads to nonlinear boundary conditions containing the recombination coefficient.

The calculations do not take into account the implantation profile of the hydrogen, this being admissible for most fusion-relevant conditions (low ion energy of approx. 10 to 1000 eV and high wall temperature of approx. 700 to 1200°K).

Hydrogen traps on the slab are also neglected. This leads to under-estimation of the hydrogen inventory (see eq.(4.29)) . By contrast, the diffusion behaviour in the steady state and hence the tritium losses after longer time of operation are scarcely affected by the traps

2. The functions erfc and eri

The functions erfc and eri feature here wherever the spatial dependence of the temperature or H concentration are being investigated. Their properties needed later are therefore set out in this section.

These functions are defined by

$$\mathrm{erfc}(V) = 1 - \frac{2}{\sqrt{\pi}} \int_0^V du\ e^{-u^2} \qquad (2.1a)$$

and

$$\mathrm{eri}(V) = 1 - \sqrt{\pi} \int_0^V du\ \mathrm{erfc}(u) \qquad b)$$

which can be rearranged to give

$$\mathrm{eri}(V) = e^{-V^2} - \sqrt{\pi}\, V\, \mathrm{erfc}(V)\ . \qquad (2.2)$$

The notation erfc stands for error function complement, i.e.

$$\mathrm{erfc} + \mathrm{erf} = 1$$

where erf denotes the GAUSSIAN error function;
eri stands for error function integrated.

Both functions are solutions of one-dimensional diffusion problems where a quantity (H-atoms, heat, temperature etc.) diffuses into a region $0 \leq x \leq \infty$. In this context a "problem" is defined by the

diffusion equation
boundary condition at x=0 ("left")
boundary condition at x=a ("right")
and initial condition at t=0

where x and t denote space and time and a is a value > 0 at which boundary condition "right" should be valid; required is the solution in the intervall $0 \leq x \leq a$ for all times $t \geq 0$. In the examples of this section a is assumed to be infinite, while in secs. 3 and 4 a is finite.

One of these diffusion problems can be described as follows: Let the region $0 \leq x \leq \infty$ be characterized by a diffusion constant D. At the time $t \leq 0$ let the density of the quantity be C=0. At time t=0 the density C at x=0 is abruptly raised from the initial value 0 to C_L and then kept constant for all times. The problem is defined by

Mass conservation $$\frac{\partial C}{\partial t} = - \frac{\partial F}{\partial x} \qquad (2.3a)$$

FICK's law $$F = - D \frac{\partial C}{\partial x} \qquad b)$$

Boundary cond."right" $$C\big|_{x \to \infty} = 0 \qquad c)$$

Boundary cond."left" $$C\big|_{x=0} = C_L \qquad d)$$

Initial cond. $$C\big|_{t=0} = 0 . \qquad e)$$

The solution is $$C = C_L \, \mathrm{erfc}\left(\frac{x}{H}\right) \qquad f)$$

$$F = \sqrt{\frac{D}{\pi t}} \, C_L \exp\left[-\left(\frac{x}{H}\right)^2\right] \qquad g)$$

with $$H = 2\sqrt{D\,t} \qquad h)$$

FIG.2-1
C versus x for two different t-values acc. to eq.(2.3)

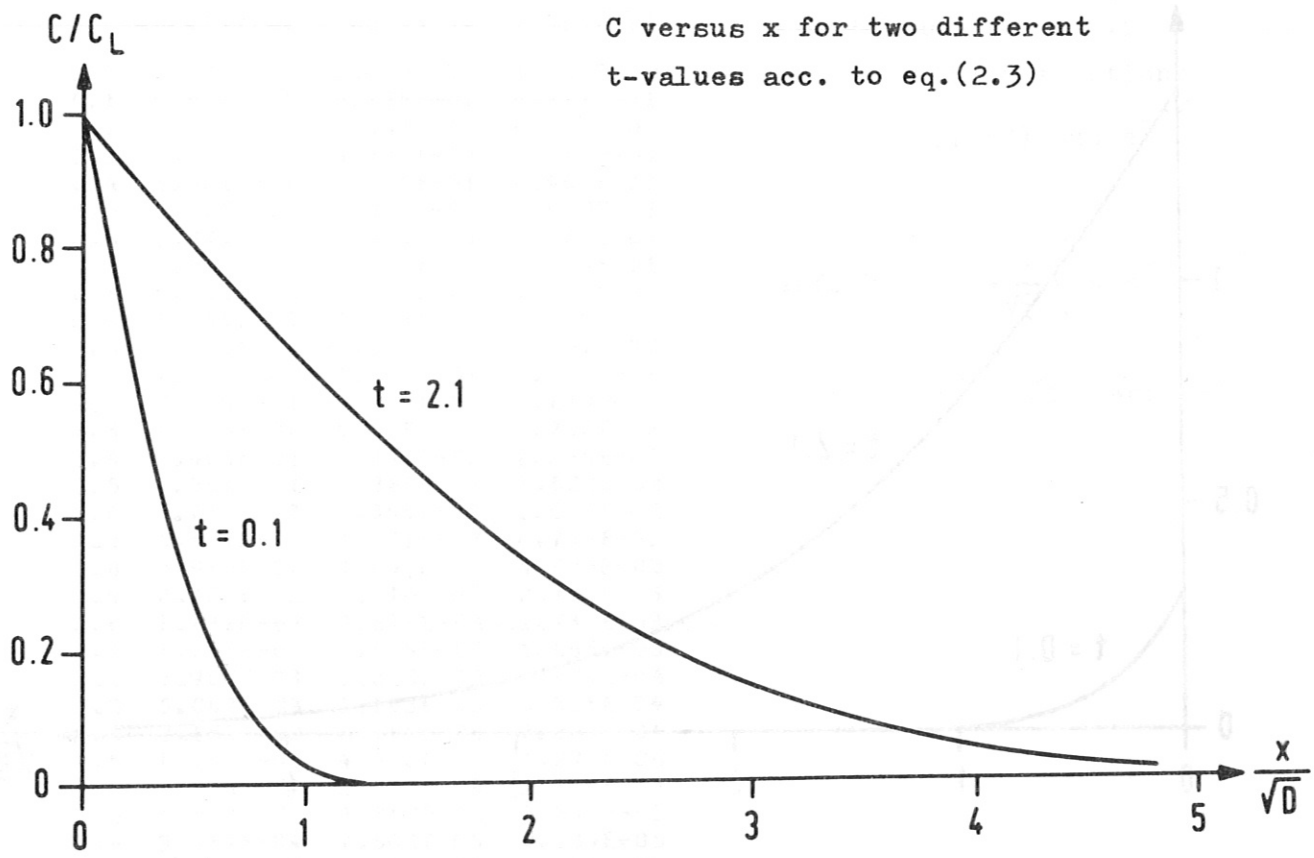

If flux constancy at the left boundary x=0 is reqired, the problem is changes, hence other function symbols are used. The use of T indicates that this problem will be used in sec.3 to calculate the temperature of the slab material. The problem is

$$\frac{\partial T}{\partial t} = -\frac{\partial Q}{\partial x} \qquad (2.4a)$$

$$Q = -U\frac{\partial T}{\partial x} \qquad b)$$

$$T\big|_{x\to\infty} = 0 \qquad c)$$

$$Q\big|_{x=0} = Q_L \qquad d)$$

$$T\big|_{t=0} = 0 \qquad e)$$

$$T = \frac{2}{\sqrt{\pi}}\sqrt{\frac{t}{U}}\; Q_L \operatorname{eri}\left(\frac{x}{2\sqrt{U\,t}}\right) \qquad f)$$

$$Q = Q_L \operatorname{erfc}\left(\frac{x}{2\sqrt{U\,t}}\right) \qquad g)$$

FIG.2-2
C versus x for two different t-values acc. to eq.(2.4)

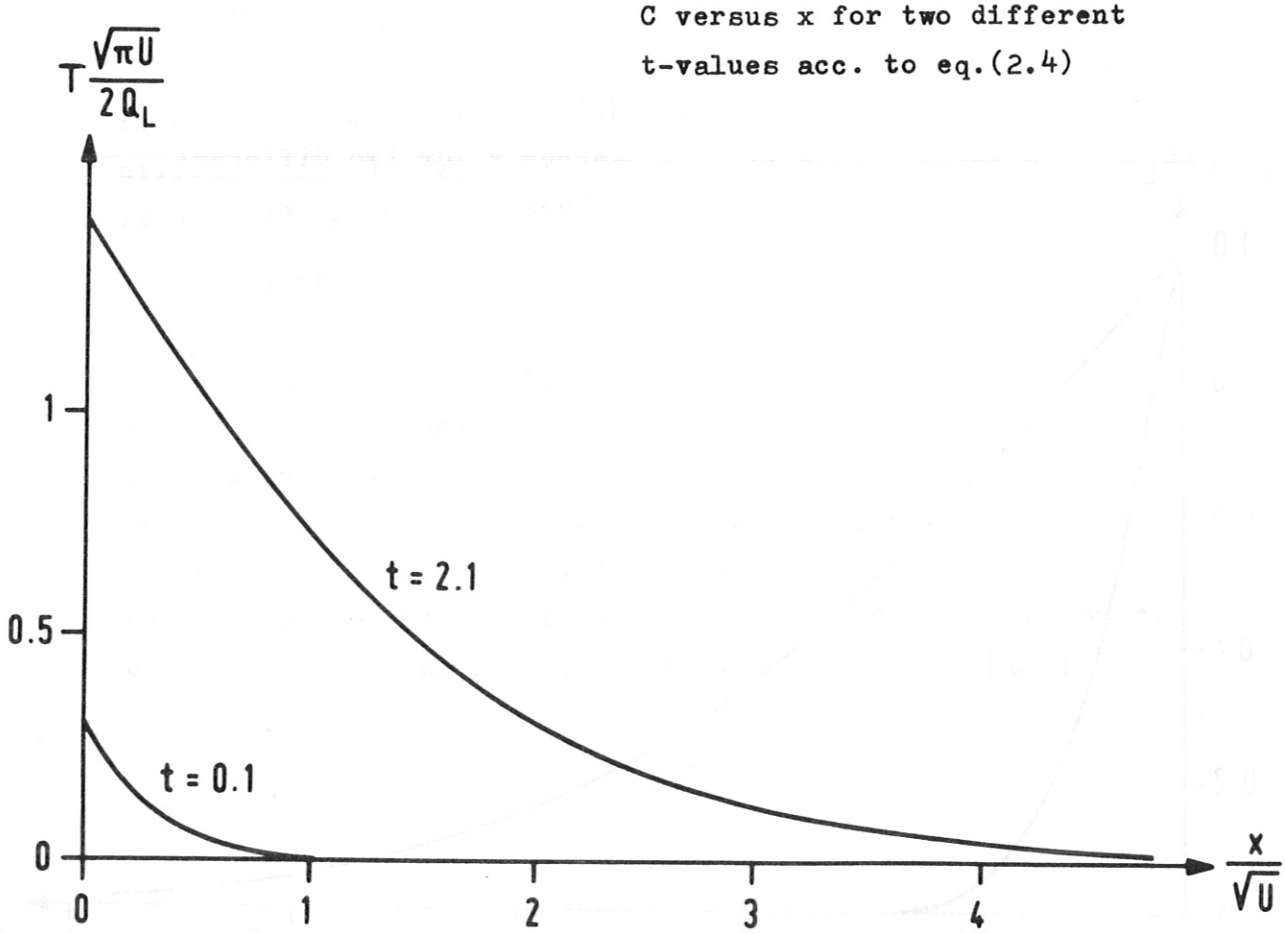

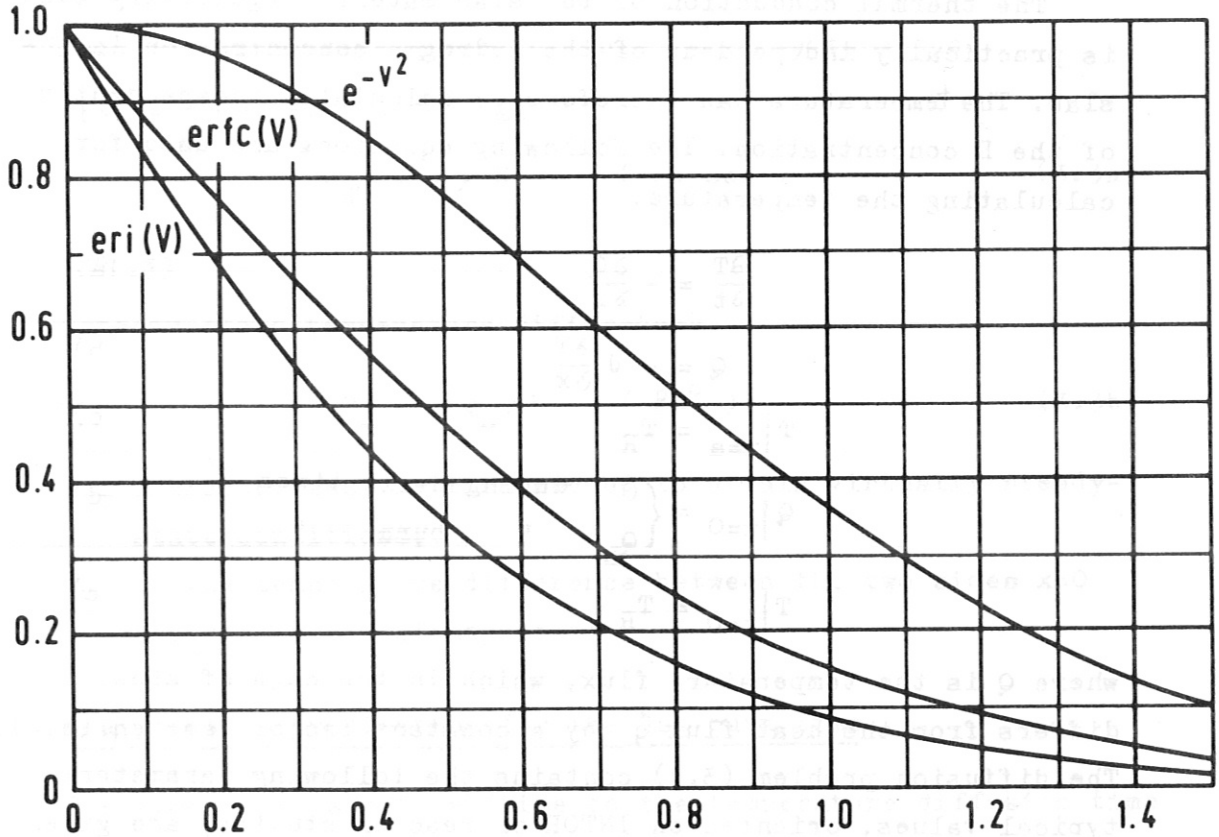

V	EXP(-V**2)	ERFC(V)	ERI(V)
0.0	1.000E 00	1.000E 00	1.000E 00
0.1	9.900E-01	8.875E-01	8.327E-01
0.2	9.608E-01	7.773E-01	6.852E-01
0.3	9.139E-01	6.714E-01	5.569E-01
0.4	8.521E-01	5.716E-01	4.469E-01
0.5	7.788E-01	4.795E-01	3.539E-01
0.6	6.977E-01	3.961E-01	2.764E-01
0.7	6.126E-01	3.222E-01	2.129E-01
0.8	5.273E-01	2.579E-01	1.616E-01
0.9	4.449E-01	2.031E-01	1.209E-01
1.0	3.679E-01	1.573E-01	8.907E-02
1.1	2.982E-01	1.198E-01	6.463E-02
1.2	2.369E-01	8.969E-02	4.617E-02
1.3	1.845E-01	6.599E-02	3.246E-02
1.4	1.409E-01	4.771E-02	2.246E-02
1.5	1.054E-01	3.389E-02	1.528E-02
1.6	7.730E-02	2.365E-02	1.023E-02
1.7	5.558E-02	1.621E-02	6.734E-03
1.8	3.916E-02	1.091E-02	4.358E-03
1.9	2.705E-02	7.210E-03	2.773E-03
2.0	1.832E-02	4.678E-03	1.734E-03
2.1	1.216E-02	2.979E-03	1.065E-03
2.2	7.907E-03	1.863E-03	6.431E-04
2.3	5.042E-03	1.143E-03	3.815E-04
2.4	3.151E-03	6.885E-04	2.223E-04
2.5	1.930E-03	4.070E-04	1.272E-04
2.6	1.159E-03	2.360E-04	7.150E-05
2.7	6.823E-04	1.343E-04	3.946E-05
2.8	3.937E-04	7.501E-05	2.139E-05
2.9	2.226E-04	4.110E-05	1.138E-05
3.0	1.234E-04	2.209E-05	5.947E-06

FIG.2-3 and Table 2.5
The normalized solutions eri(V), erfc(V) and e^{-V^2}

Definition:

$$\mathrm{erfc}(V) = 1 - \frac{2}{\sqrt{\pi}} \int_0^V du\, e^{-u^2}$$

$$\mathrm{eri}(V) = e^{-V^2} - \sqrt{\pi}\, V\, \mathrm{erfc}(V)$$

3. Temperature

The thermal conduction of the slab material (generally steel) is practically independent of the hydrogen concentration in the slab. The temperature can therefore be calculated independently of the H concentration. The following equations are used for calculating the temperature:

$$\frac{\partial T}{\partial t} = -\frac{\partial Q}{\partial x} \qquad (3.1a)$$

$$Q = -U\frac{\partial T}{\partial x} \qquad b)$$

$$T\big|_{x=a} = T_R \qquad c)$$

$$Q\big|_{x=0} = \begin{cases} 0 & \text{during dwell times} \\ Q_L & \text{" burn "} \end{cases} \qquad d)$$

$$T\big|_{t=0} = T_R \qquad e)$$

where Q is the temperature flux, which in the case of steel differs from the heat flux $\dot{q}$ by a constant factor, see eq.(5.2). The diffusion problem (3.1) contains the following parameters, typical values, oriented on INTOR or reactor studies, are given in parentheses (see §5):

Slab thickness	a	(1 cm)	(3.2a)
Temperature conductivity	U	(0.04 cm^2/sec)	b)
Coolant temperature	T_R	(600°K)	c)
Temperature flux density	Q_L	(3.2 degree $\frac{cm}{sec}$)	d)
Burn time	t_{burn}	(1-2 min)	e)
Dwell time	t_{dwell}	(4-10 sec)	f)

FIG.3-1 shows $Q\big|_{x=0}$ versus t for the first two burn-dwell periods and the time scales used here.

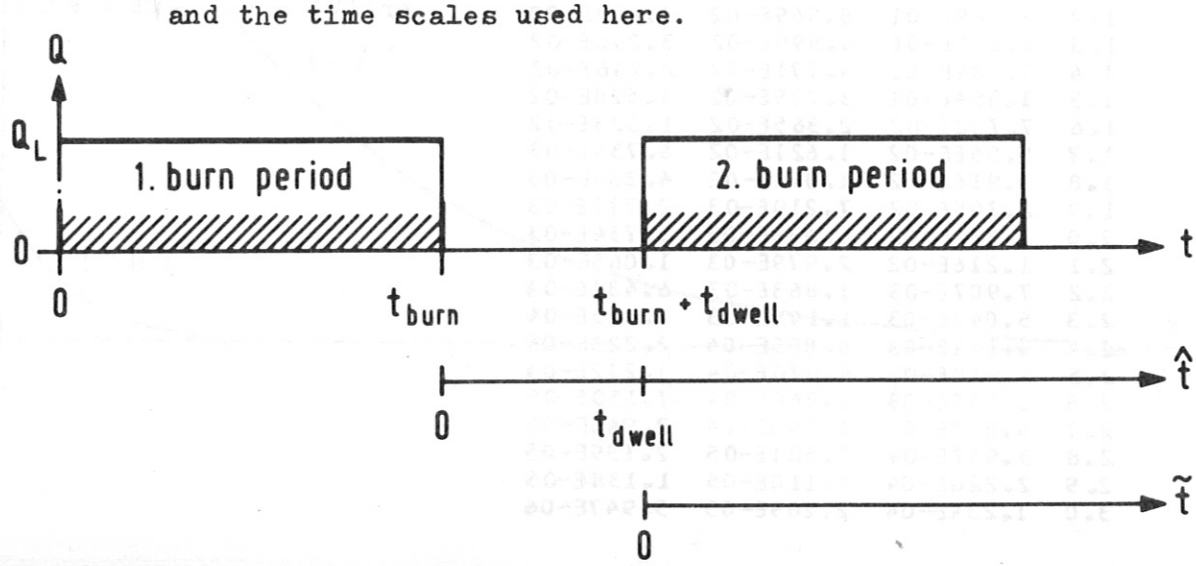

Characteristic time and temperature constants

From the parameters given in table (3.2) we form the

"temperature diffusion time"

$$t_{ST} = a^2 / U \qquad (25 \text{ sec}) \qquad (3.3a)$$

and the

"steady-state temperature difference"

$$T_D = a\, Q_L / U \qquad (80^\circ). \qquad (3.3b)$$

t_{ST} characterizes the time needed to attain virtually steady-state conditions;

T_D is the temperature difference between the two sides x=0 and x=a in the steady state.

Analytical approximation for the 1st burn time

For times very short relative to the temperature diffusion time ($t \ll t_{ST}$) the temperature T only differs significantly from the coolant temperature T_R, when $x \ll a$. It is therefore almost immaterial whether $T=T_R$ is postulated at x=a or at $x=\infty$ as boundary condition "right". We therefore use eq.(2.4) to get

$$T = T_R + \text{temp}(x,t) \qquad (3.4)$$

with

$$\frac{\text{temp}(x,t)}{T_D} = \frac{2}{\sqrt{\pi}} \sqrt{\frac{t}{t_{ST}}}\ \text{eri}\left(\frac{x/a}{2\sqrt{t/t_{ST}}}\right) \quad \text{for } t \ll t_{ST}. \qquad (3.5a)$$

For very long times we get the steady-state solution

$$\frac{\text{temp}(x,t)}{T_D} = 1 - \frac{x}{a} \qquad \text{for } t \gg t_{ST}. \qquad (3.5b)$$

The temperature is thus known for very long and very short times. For intervening medium times we rely on numerical calculations. The results of theses can be interpolated with the approximation formula

$$\frac{\text{temp}(x,t)}{T_D} = \frac{2}{\sqrt{\pi}} \sqrt{\frac{t}{t_{ST}}}\ \frac{\text{eri}\left(\frac{x/a}{2\sqrt{t/t_{ST}}}\right) - \text{eri}\left(\frac{2 - x/a}{2\sqrt{t/t_{ST}}}\right)}{1 + \text{erfc}(\sqrt{t_{ST}/t})} \qquad (3.5)$$

the values being at most 6% too small, see eq.(6.1). Eq.(3.5) contains both the short-time case (3.5a) and the steady-state case (3.5b) as special cases. This is seen for small t in eq. (3.5), where the second term in both the numerator and denominator vanishes. For large t the argument

$$V = \frac{x}{2\sqrt{U\,t}} = \frac{x/a}{2\sqrt{t/t_{ST}}}$$

of the functions erfc and eri is very small, so that the expansions

$$\mathrm{erfc}(V) = 1 - \frac{2}{\sqrt{\pi}} V \qquad (3.6a)$$

$$\mathrm{eri}(V) = 1 - \sqrt{\pi}\, V \qquad b)$$

are valid. Substitution of eq.(3.6a) in 0-order and eq.(3.6b) in 1-order approximation in eq.(3.5) yields the steady-state solution (3.5b).

Eq.(3.5) is not the only formula of this kind. For the special case x=0 the formula

$$\frac{\mathrm{temp}(0,t)}{T_D} = \sqrt{\frac{1}{\sqrt[3]{0.485\ (t_{ST}/t)^3 + 1}}} \qquad (3.7)$$

is much more exact (approx.1%) and will be used almost exclusively in sec.4 to treat processes in the vicinity of the irradiated surface x=0. Eq.(3.7) also contains the short-time case (3.5a) and the steady-state solution (3.5b) as special cases:

$$\frac{\mathrm{temp}(0,t)}{T_D} = \begin{cases} \sqrt[6]{\frac{1}{0.485}}\sqrt{\frac{t}{t_{ST}}} = \frac{2}{\sqrt{\pi}}\sqrt{\frac{t}{t_{ST}}} & \text{for } t \ll t_{ST} \\ 1. & \text{for } t \gg t_{ST} \end{cases}$$

Eqs.(3.5) and (3.7) are formulated to include only the dimensionless quantities x/a, temp/T_D and t/t_{ST} ; apart from theses three quantitites there are no other parameters in eqs.(3.5)-(3.7)

Arbitrary times, superposition

Having given the solution for the 1st burn time in eq.(3.5)-(3.7), we now describe how to obtain from it the solution for arbitrary times (1st dwell time, 2nd burn time, etc.). First we write down the result, explaining it later; it holds that

1st burn time: $T = T_R + \text{temp}(x,t)$ s.(3.4)

1st dwell time: $T = T_R + \text{temp}(x,t) - \text{temp}(x,t-t_{burn})$ (3.8a)

2nd burn time: $T = T_R + \text{temp}(x,t) - \text{temp}(x,t-t_{burn}) + \text{temp}(x,t-t_{burn}-t_{dwell})$ (3.8b)

etc. with

t_{burn} = length of burn time

t_{dwell} = " " dwell " .

Each line of eq.(3.8) solves the differential eq.(3.1a+b) for the boundary condition $Q\big|_{x=0} = \pm Q_L$ - except at the times $t=t_{burn}$; $t_{burn}+t_{dwell}$ etc, at which the flux jumps. The differential eq.(3.1a+b) is linear, therefore the sum of several solutions is also a solution. Each term $\text{temp}(x,t-t_o)$ produces at x=0 the flux Q_L. During the dwell times there are as many temp terms with positive sign as with negative sign, whose contributions to the flux at x=0 cancel out, so that boundary condition (3.1d) is fulfilled.

In the following figures (3-2 and 3-3) we represent the dimensionless temperature variation

$$\frac{T-T_R}{T_D} \quad \text{as a function of} \quad \frac{x}{a} \quad \text{and} \quad \frac{t}{t_{ST}} .$$

so the figures are independent of the choice of the parameters a, U, T_R, Q_L, t_{ST}, T_D .

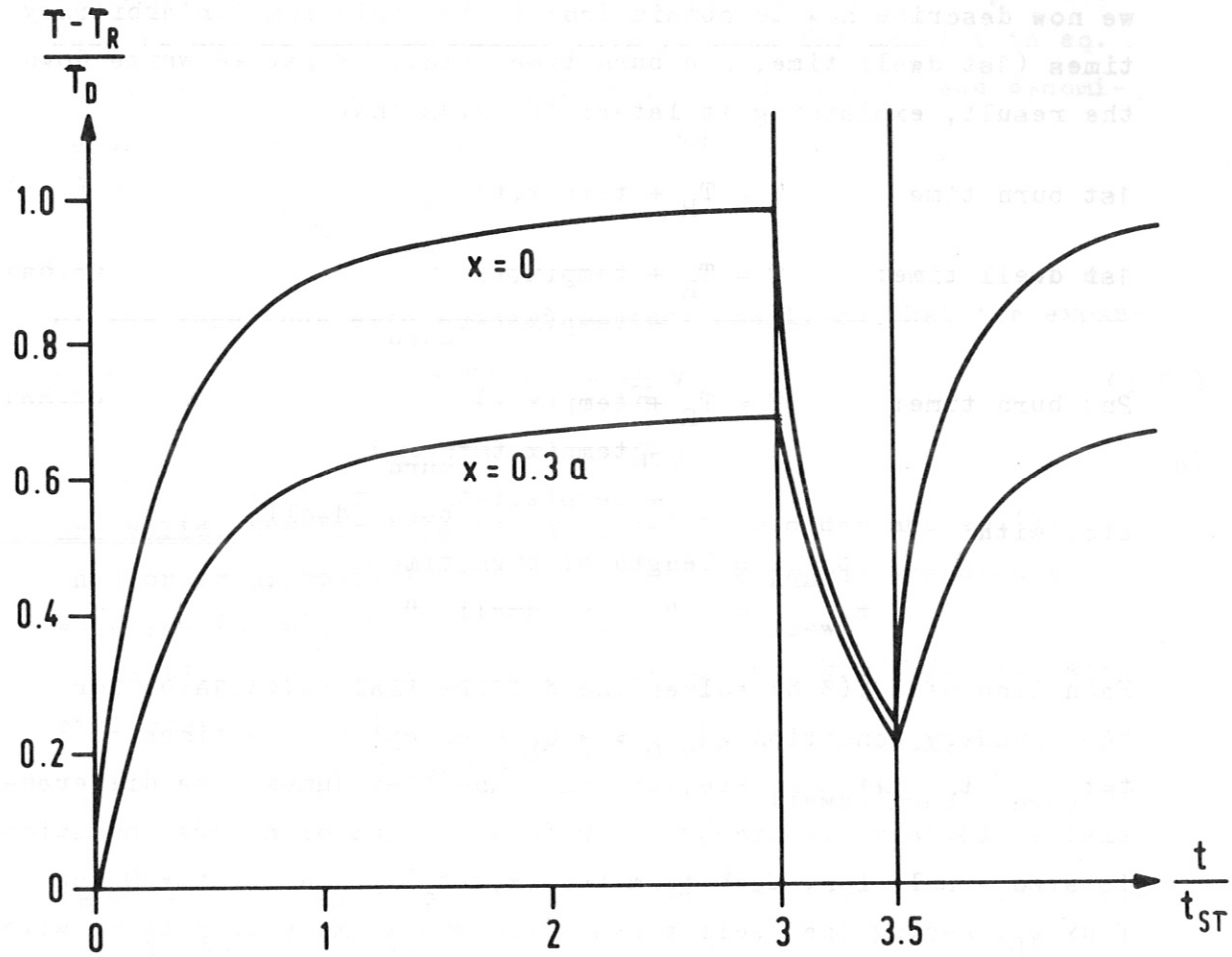

FIG.3-2

T versus t with x as parameter

for constant temperature diffusion coefficient U

calculated acc.to eq.(3.5) for $t_{burn}/t_{ST} = 3$

and $t_{dwell}/t_{ST} = 0.5$.

The normalization factors are $t_{ST} = a^2/U$

and $T_D = a\, Q_L / U$.

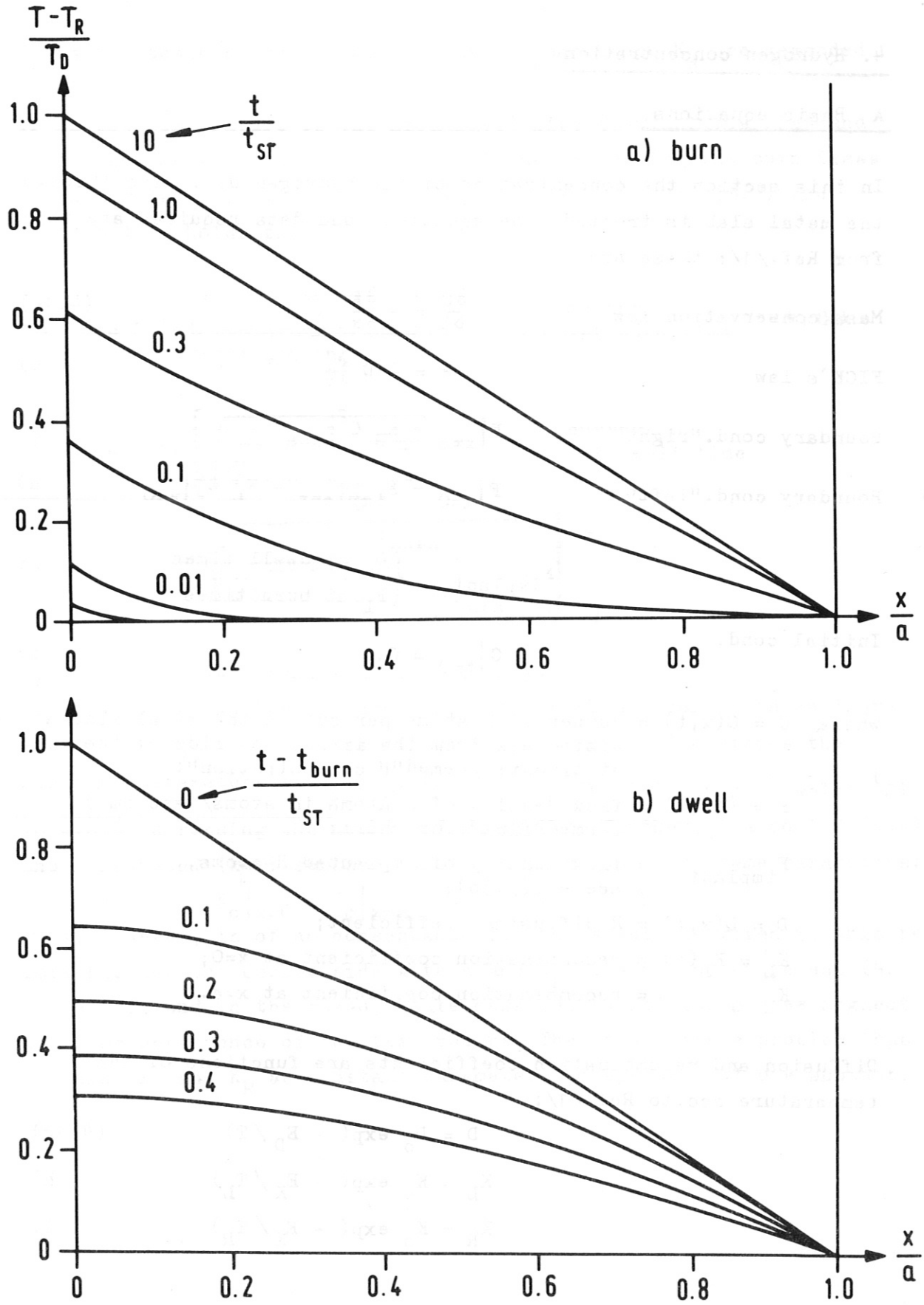

FIG.3-3 T versus x with t as parameter
a) during the 1st burn time
b) during a dwell time

4. Hydrogen concentration

A Basic equations

In this section the concentration of the hydrogen diffusing through the metal slab is treated. The equations and data required are taken from Ref./1/; these are

Mass conservation law

$$\frac{\partial C}{\partial t} = - \frac{\partial F}{\partial x} \qquad (4.1a)$$

FICK`s law

$$F = - D \frac{\partial C}{\partial x} \qquad b)$$

Boundary cond."right"

$$F\big|_{x=a} = K_R \, C^2\big|_{x=a} \qquad c)$$

Boundary cond."left"

$$F\big|_{x=0} = F_{implant} - K_L \, C^2\big|_{x=0} \qquad d)$$

$$F_{implant} = \begin{cases} 0 & \text{at dwell times} \\ F_L & \text{at burn times} \end{cases} \qquad e)$$

Initial cond.

$$C\big|_{t=0} = 0, \qquad f)$$

where $C = C(x,t)$ = number of H-atoms per cm^3 in the metal slab at distance x from the irradiated side of the slab at time t; termed"H concentration";

$F = F(x,t)$ = flux density of H atoms in atoms/(sec cm^2) termed"flux" for short;

$F_{implant}$ = flux density of implanted H-atoms, see eq.(5.3b);

$D = D(x,t)$ = H diffusion coefficient;

$K_L = K_L(t)$ = recombination coefficient at x=0;

K_R = recombination coefficient at x=a.

Diffusion and recombination coefficients are functions of the temperature acc.to Ref./1/:

$$D = D_o \exp(- E_D / T) \qquad (4.1g)$$

$$K_L = K_o \exp(- E_K / T_L) \qquad h)$$

$$K_R = K_o \exp(- E_K / T_R) \qquad i)$$

T_R is the temperature of the coolant; T_R and hence K_R are regarded as constants;

T_L is the temperature of the irradiated side (x=0) of the slab and depends on time because the slab is heated during the burn times and cooled during the dwell times. According to eq.(3.7) and (3.8a) it holds that

$$T_L = T_R + T_D \sqrt{\frac{t}{\sqrt[3]{0.485\, t_{ST}^3 + t^3}}} \qquad \text{during 1st burn time} \qquad (4.1k)$$

$$T_L = T_R + T_D \left[\sqrt{\frac{t}{\sqrt[3]{0.485\, t_{ST}^3 + t^3}}} - \sqrt{\frac{t - t_{burn}}{\sqrt[3]{0.485\, t_{ST}^3 + (t-t_{burn})^3}}} \right] ; \qquad \text{during 1st dwell time}$$

$T_L = T_L(t)$ is thus a function of time only.

$T = T(x,t)$ is the temperature inside the slab and can be taken from eq. (3.5-8). The diffusion problem (4.1) contains the constant parameters a, D_o, E_D, E_K, F_L, K_o, T_D, T_R, t_{burn}, t_{dwell}, t_{ST}. To avoid increasing the number of parameters further, the cooled (x=a) and irradiated (x=0) surfaces are assumed to have the same parameters:

$$K_o|_{x=0} = K_o|_{x=a} = K_o \quad \text{etc..}$$

This, however, is of no consequence for the solutions given in this report because the cooled side with a and K_R does not occur in eqs.(4.5) to (4.24), and in the steady-state case (eq.(4.25)-(4.36)) we neglect the time dependence of the temperature. The steady-state problem thus contains K_L and K_R as constant parameters independent of one another.

Typical values for the constant parameters are acc.to sec 5:

$a = 1$ cm — plate thickness (4.2a)

$D_o = 0.085\ cm^2/sec$ } for steel b)

$E_D = 7000^oK$ } for steel c)

$E_K = 6000^oK$ } for steel d)

$F_L = 1.5\ 10^{16}$ atoms/(sec cm^2) for INTOR e)

$K_o = \begin{cases} 1.6\ 10^{-16}\ cm^4/(atom\ sec) & \text{" clean surfaces} \\ 1.6\ 10^{-20} \quad \text{"} & \text{" dirty "} \end{cases}$ f)

$T_D = 80^o$ " INTOR g)

$T_R = 600^oK$ " NET or reactor h)

$t_{ST} = 25$ sec i)

$t_{burn} = 60$ sec k)

$t_{dwell} = 4$ sec . l)

K_o thus depends on the purity of the metal surface.

For $T=680^oK$ (INTOR, irradiated side of the slab)
the coefficients have the following values:

$D = 2\ 10^{-6}\ cm^2/sec$ (4.2m)

$K_L = \begin{cases} 2\ 10^{-20}\ cm^4/(atom\ sec) & \text{for clean surfaces} \\ 2\ 10^{-24} \quad \text{"} & \text{" dirty "} \end{cases}$ n)

$K_R = 0.3\ K_L$. p)

For the sake of clarity we introduce the following parameters characteristic of problem (4.1), with typical values given in parentheses:

"release time"

$$t_A = \frac{D}{F_L K_L} \quad \begin{pmatrix} 0.01 \text{ sec for clean surfaces} \\ 1 \text{ min} \quad " \quad \text{dirty} \quad " \end{pmatrix} \tag{4.3a}$$

"particle diffusion time"

$$t_{SC} = \frac{a^2}{D} \qquad (5 \text{ days}) \tag{4.3b}$$

"concentration limit"

$$C_L = \sqrt{\frac{F_L}{K_L}} \qquad \begin{pmatrix} 10^{18} \text{ cm}^{-3} \text{ for clean surfaces} \\ 10^{20} \quad " \quad " \quad \text{dirty} \quad " \end{pmatrix} \tag{4.3c}$$

"penetration depth" of C variation due to dwell time

$$H_{dwell} = 2\sqrt{D\, t_{dwell}} \ , \tag{4.3d}$$

We only treat cases in which t_{SC} is very large relative to all other characteristic times and assume everywhere in this report that

$$H_{dwell} \ll a \ . \tag{4.4}$$

We give approximation formulae for

the 1st burn time	(eqs.(4.5-8) and (4.18-22))
an arbitrary dwell time	(" (4.9-17) " (4.23-24))
the 2nd burn time	(" (4.15))
the steady-state solution without	(" (4.29-31))
and with SORET effect.	(" (4.32-36))

Here (eqs.(4.5-17)) we discuss in detail the case, where the coefficients D and K_L are constant because the approximation formulae obtained for this case are also important for temperature-dependent coefficients. The derivation of the approximation formulae presented in the following and their inaccuracy etc. are discussed in detail in sec.6. The attribute "approximated" is usually omitted since all equations from eq.(4.5) to eq.(4.36) are approximations.

B Constant coefficients D and K_L

1st burn time

For extremely short times immediately after the first switching on there is not yet any significant H concentration, so that the boundary condition (4.1d) on the irradiated side of the slab x=0 can be approximated by

$$F\Big|_{x=0} = F_L \quad . \tag{4.5a}$$

Problem (4.1) is then identical with problem (2.4). The solution is

$$\frac{C}{C_L} = \frac{2}{\pi}\sqrt{\tau}\ \mathrm{eri}\left(\frac{x}{H}\right) \qquad \text{for } t \ll t_A \tag{4.5b}$$

$$\frac{F}{F_L} = \mathrm{erfc}\left(\frac{x}{H}\right) \tag{4.5c}$$

with

$$\tau = \pi t / t_A \tag{4.5d}$$

and

$$H = 2\sqrt{D\,t} \quad . \tag{4.5e}$$

Solution (4.5) is only valid as long as time t is small relative to the release time t_A. The latter can attain the order of magnitude of the burn time, if the metal surfaces are dirty.

For finite times ($t \gtrsim t_A$) the flux F at x=0 cannot remain constant, as stated in eq.(4.5c), but decreases with time. This is because more and more of the constant flux F_L of the implanted particles is re-emitted with growing concentration C. The flux decrease can be described in crude approximation by

$$\frac{F}{F_L}\Big|_{x=0} = \frac{1}{\sqrt{1+\tau}} \quad . \tag{4.6a}$$

From boundary condition (4.1d+e) this yields for the concentration

$$\frac{C}{C_L}\Big|_{x=0} = \sqrt{1 - \frac{1}{\sqrt{1+\tau}}} \quad . \tag{4.6b}$$

A much more exact formula is given in eq.(4.8); for explanation see eq.(6.9). The function describing the spatial dependence in the equation for C is gradually transformed with increasing time

from the function eri to the function erfc. (4.6c)

For large times ($t \gg t_A$), about as many H-atoms are implanted as are re-emitted. The difference between the fluxes of the implanted and re-emitted particles becomes very small:

$$F\big|_{x=0} \ll F_L$$

so that the boundary condition (4.1d) at x=0 is reduced to

$$C\big|_{x=0} = C_L = \sqrt{\frac{F_L}{K_L}} \quad . \tag{4.7a}$$

Problem (4.1) is then identical with problem (2.3), the solution is

$$\frac{C}{C_L} = \operatorname{erfc}\left(\frac{x}{H}\right) \qquad \text{for } t \gg t_A \tag{4.7b}$$

$$\frac{F}{F_L} = \frac{1}{\sqrt{\tau}} \exp\left(-\left(\frac{x}{H}\right)^2\right) \quad . \tag{4.7c}$$

Solution (4.7) is valid beyond the 1st burn time up to times of the order of the particle diffusion time t_{SC} (see eq.(4.3b)) and describes how the slab is gradually filled with hydrogen if H traps are neglected, as is done in problem (4.1). We do not go further into this because in reality a large part of the hydrogen in the metal is bound in traps. For very clean metal slabs ($t_A \to 0$) solution (4.7) is already valid for short times ($t \ll t_{burn}$, see FIG.4-5a and 4-5c).

In FIG.4-1 various formulae are compared for the build-up of the H-concentration at x=0.

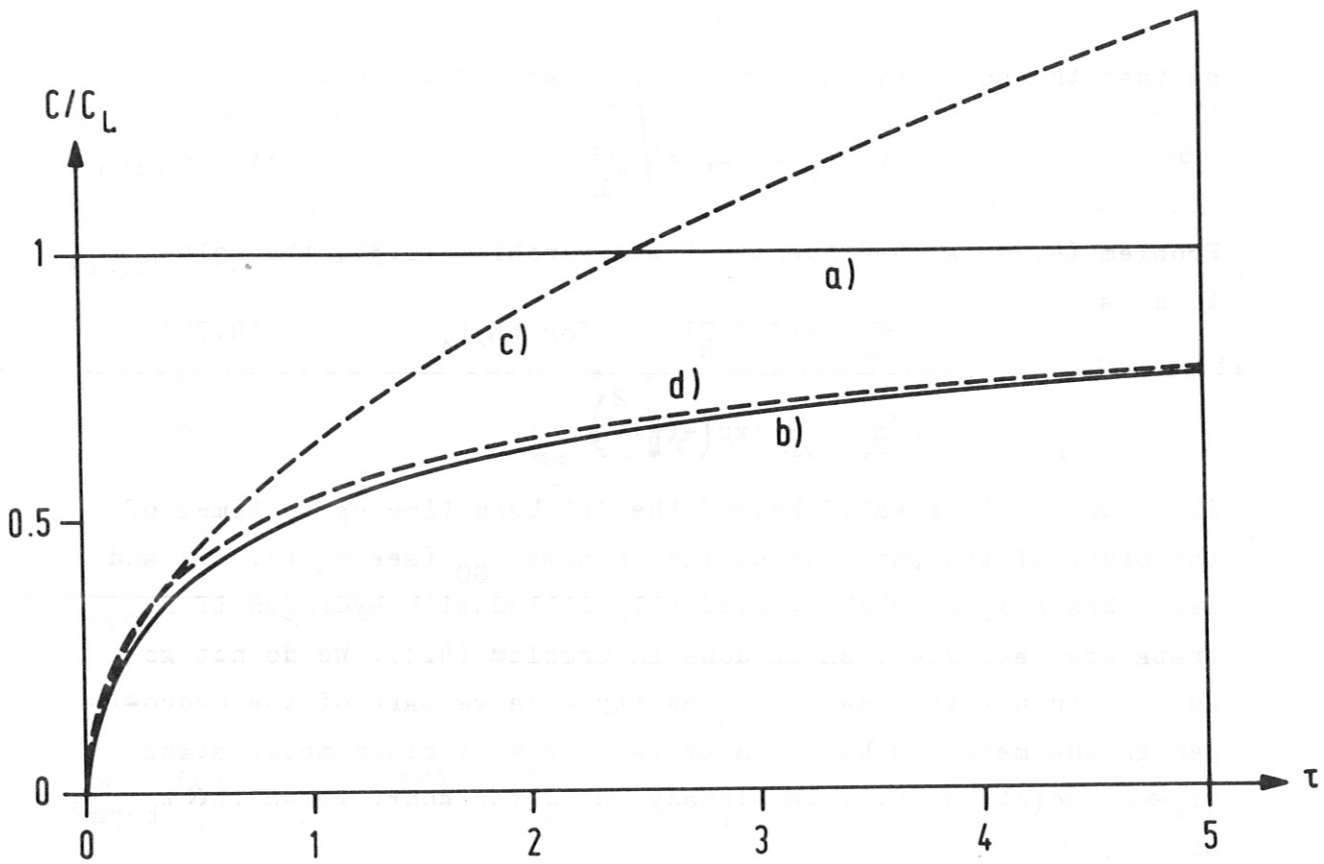

FIG.4-1

C/C_L versus τ at x=0 for the 1st burn time with constant coefficients

Solid curves:

a) Long-time solution $\quad C/C_L = 1$ s.(4.7b)

b) quasi-exact solution $\quad C/C_L = \sqrt{1 - 1/\sqrt{1 + b\tau}}$ (4.8a)

$b = 1 - 0.19/\sqrt{1 + \tau}$ b)

Dashed curves:

c) Short-time solution $\quad C/C_L = \frac{2}{\pi}\sqrt{\tau}$ s.(4.5b)

d) simplification of b) $\quad C/C_L = \sqrt{1 - 1/\sqrt{1 + \tau}}$. s.(4.6b)

The attribute "quasi-exact" for eq.(4.8) denotes that eq.(4.8) correctly reproduces the numerical results within the drawing accuracy (1%). The numerical factor 0.19 stands for $1 - 8/\pi^2$, see eq.(6.9) .

Dwell time

During the dwell time the boundary condition (4.1d+e) on the irradiated side of the slab is

$$F\big|_{x=0} = - K_L \, C^2\big|_{x=0} \quad ,$$

The negative sign means that hydrogen on the irradiated side x=0 is re-emitted from the slab. This re-emission flux leads to partial degassing, i.e. a decrease of the H-concentration, near the irradiated surface of the slab. This is described by the ansatz

$$C = C_{burn} - C_{var} \qquad (4.9)$$

where C_{burn} denotes the density profile built up at the end of the preceeding burn time acc.to eq.(4.5-7);

C_{var} describes the density drop due to degassing of the irradiated side, termed "dwell time variation".

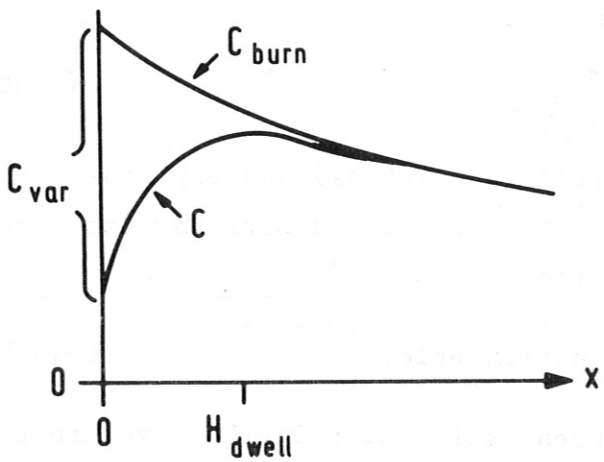

The sketch shows schematically C and C_{burn} versus x; C_{var} is the difference. For $x \gtrsim H_{dwell}$ one has $C_{var} \approx 0$; H_{dwell} is thus called the penetration depth of the dwell time variation, see eq.(4.3d) and eq.(4.9g) for $\hat{t}=t_{dwell}$.

To calculate C_{var} for a simple case, we choose as the initial condition at the beginning t=0 of the dwell time

$$C = C_{burn} = C_L = \text{const for all } x. \qquad (4.9a)$$

For extremely short times immediately after the start of the dwell time the H concentration has not yet significantly decreased, so that the boundary condition on the irradiated side x=0 of the slab can be approximated by

$$F\big|_{x=0} = - K_L C_L^2 = - F_L \quad . \qquad (4.9b)$$

Problem (4.1) in this case has the solution

$$\frac{C}{C_L} = 1 - \frac{2}{\pi}\sqrt{\hat{\tau}}\ \mathrm{eri}\left(\frac{x}{\hat{H}}\right) \qquad \text{for } t \ll t_A \qquad (4.9c)$$

$$\frac{F}{F_L} = -\ \mathrm{erfc}\left(\frac{x}{\hat{H}}\right) \qquad d)$$

$$\hat{\tau} = \pi \hat{t}/t_A \qquad e)$$

$$\hat{t} = t - t_{burn} \qquad \text{(s.FIG.3-1)} \qquad f)$$

$$\hat{H} = 2\sqrt{D\,\hat{t}} \qquad g)$$

$\hat{t}$ is the time elapsed since dwell time start.
For $\hat{t}=t_{dwell}$ one gets $\hat{H}=H_{dwell}$, the penetration depth of the dwell time variation C_{var}.

Solution (4.9) is only valid for the time immediately after the start of the dwell time. The flux decreases with time, which can be described in rough approximation by

$$\left.\frac{F}{F_L}\right|_{x=0} = -\ \frac{1}{1+\sqrt{\hat{\tau}}} \,. \qquad (4.10a)$$

A much more exact formula is given in eq.(4.12) and explained in eq.(6.9). With increasing time $\hat{t}$ the function describing the spatial dependence is transformed from

the function eri to the function erfc. (4.10b)

For large times ($\hat{t} \gg t_A$), the concentration at x=0 will have dropped to values small relative to C_L; it then holds that

$$\frac{C}{C_L} = 1 - \mathrm{erfc}\left(\frac{x}{\hat{H}}\right) \qquad \text{for } \hat{t} \gg t_A \qquad (4.11a)$$

$$\frac{F}{F_L} = -\ \frac{1}{\sqrt{\hat{\tau}}}\ \exp\left[-\left(\frac{x}{\hat{H}}\right)^2\right] \,. \qquad b)$$

FIG.4-2 shows the re-emission flux versus time according to eq.(4.10a) and the "quasi-exact" eq.(4.12) with error approx. 0.5%.

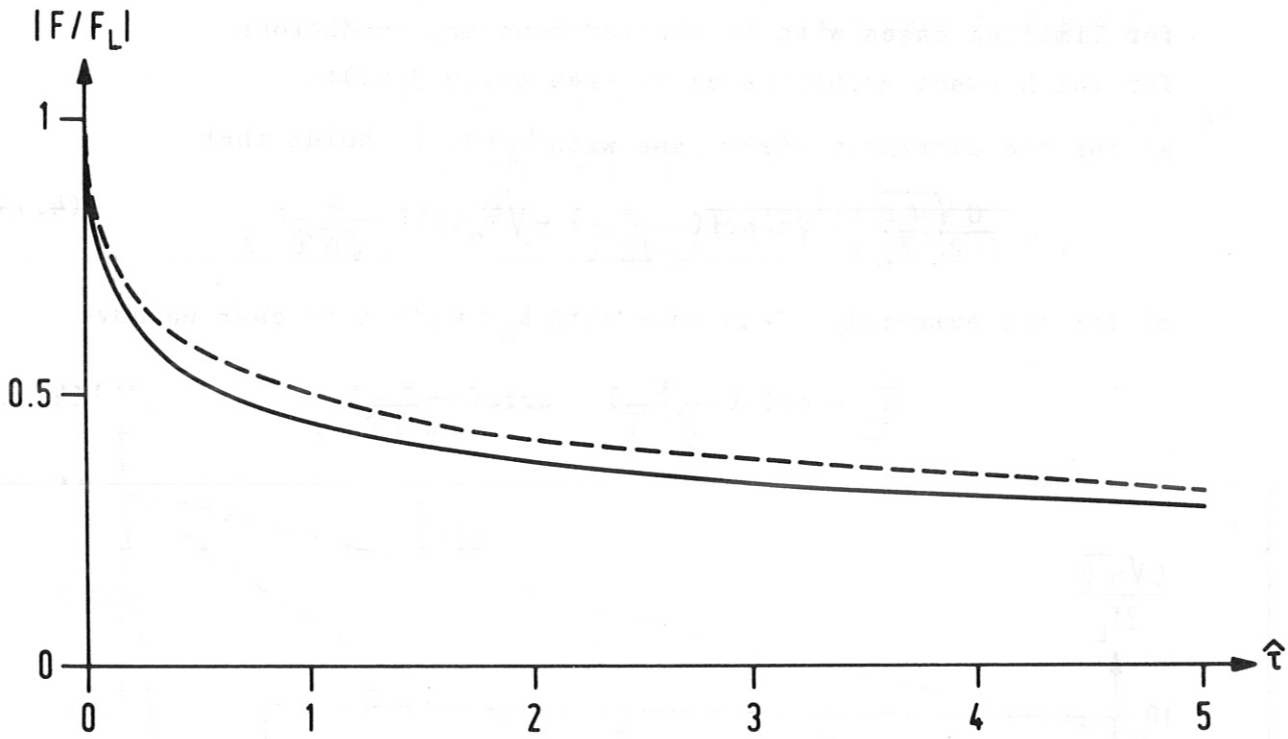

FIG.4-2

Re-emissionn flux $F/F_{L\ x=0}$ versus $\hat{\tau}$ during a dwell time for $\tau \to \infty$ i.e. after many burn-dwell cycles.

Dashed: according to eq.

$$\left|\frac{F}{F_L}\right|_{x=0} = \frac{1}{1+\sqrt{\hat{\tau}}} \qquad \text{s.(4.10a)}$$

Solid: according to eq.

$$\left|\frac{F}{F_L}\right|_{x=0} = \frac{1}{1+\hat{b}\sqrt{\hat{\tau}}} \qquad (4.12a)$$

$$\hat{b} = 1 + \frac{0.27}{\sqrt[6]{1+\hat{\tau}}} \qquad \text{b)}$$

Eq.(4.12) interpolates the numerical results with an accuracy of approx. 0.5%; the factor 0.27 stands for $4/\pi$, see eq.(6.9) .

Limiting cases with linearized boundary conditions

In FIG.4-3 we show concentration profiles for $t_{burn}=60$ C (normalized) versus x (normalized) during the 1st dwell time for limiting cases with linearized boundary conditions for which exact solutions exist (see eq.(6.3-6)):

a) for the extremely dirty case with $t_A \to \infty$; it holds that

$$\frac{C\sqrt{\pi D}}{2F_L} = \sqrt{t}\,\mathrm{eri}\left(\frac{x}{2\sqrt{D\,t}}\right) - \sqrt{\hat{t}}\,\mathrm{eri}\left(\frac{x}{2\sqrt{D\,\hat{t}}}\right); \qquad (4.13)$$

b) for the extremely clean case with $t_A \to 0$; in this case we have

$$\frac{C}{C_L} = \mathrm{erfc}\left(\frac{x}{2\sqrt{D\,t}}\right) - \mathrm{erfc}\left(\frac{x}{2\sqrt{D\,\hat{t}}}\right). \qquad (4.14)$$

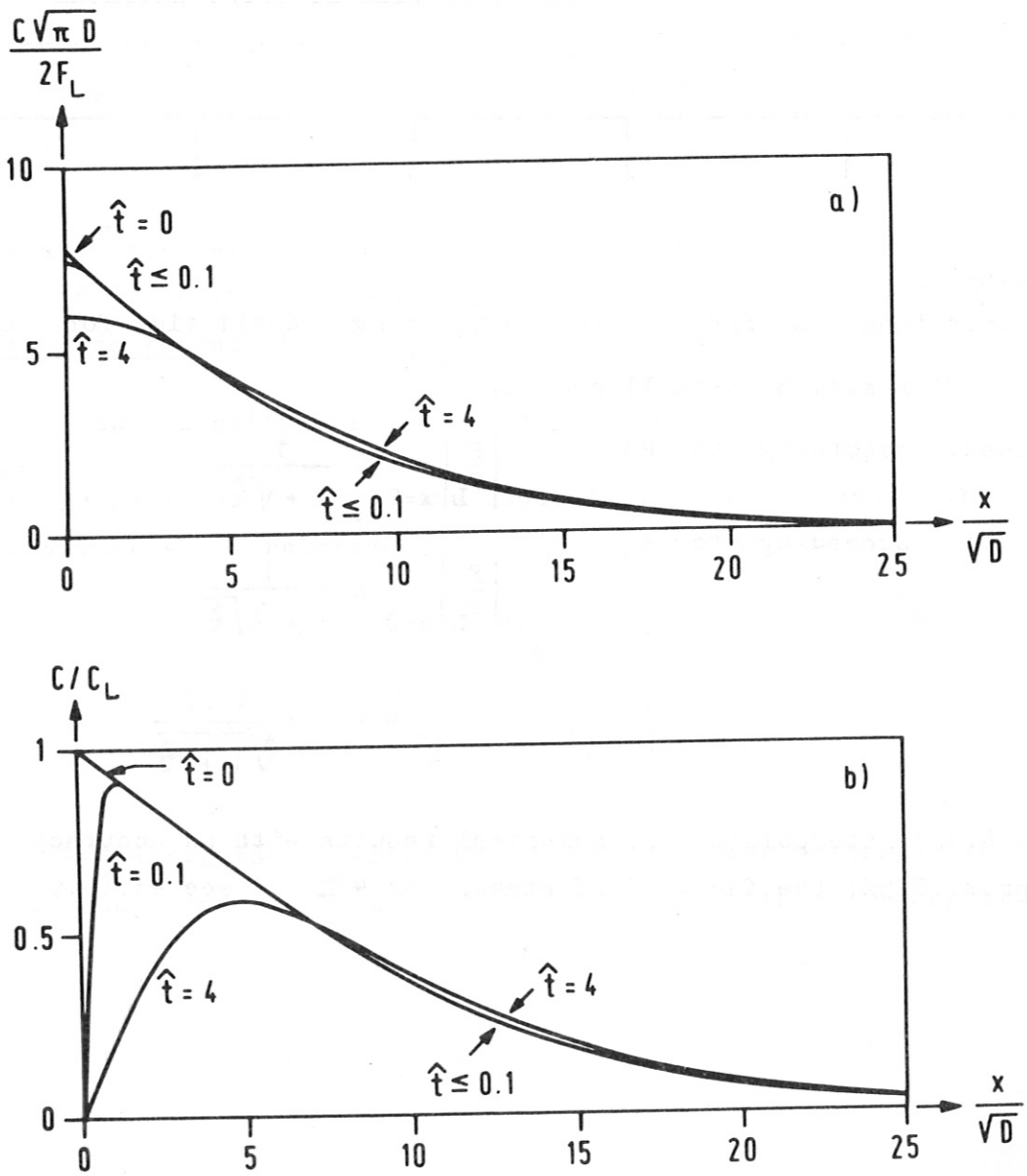

FIG.4-3

2nd burn time

For the 2nd burn time we present as an example the H concentration calculated for the extremely clean case $t_A \to 0$ acc.to the equation

$$\frac{C}{C_L} = \mathrm{erfc}\left(x / \left(2\sqrt{D\,t}\right)\right) + \\ - \mathrm{erfc}\left(x / \left(2\sqrt{D\,(t-t_{burn})}\right)\right) + \\ + \mathrm{erfc}\left(x / \left(2\sqrt{D\,(t-t_{burn}-t_{dwell})}\right)\right) . \qquad (4.15)$$

(see eq.(4.14))

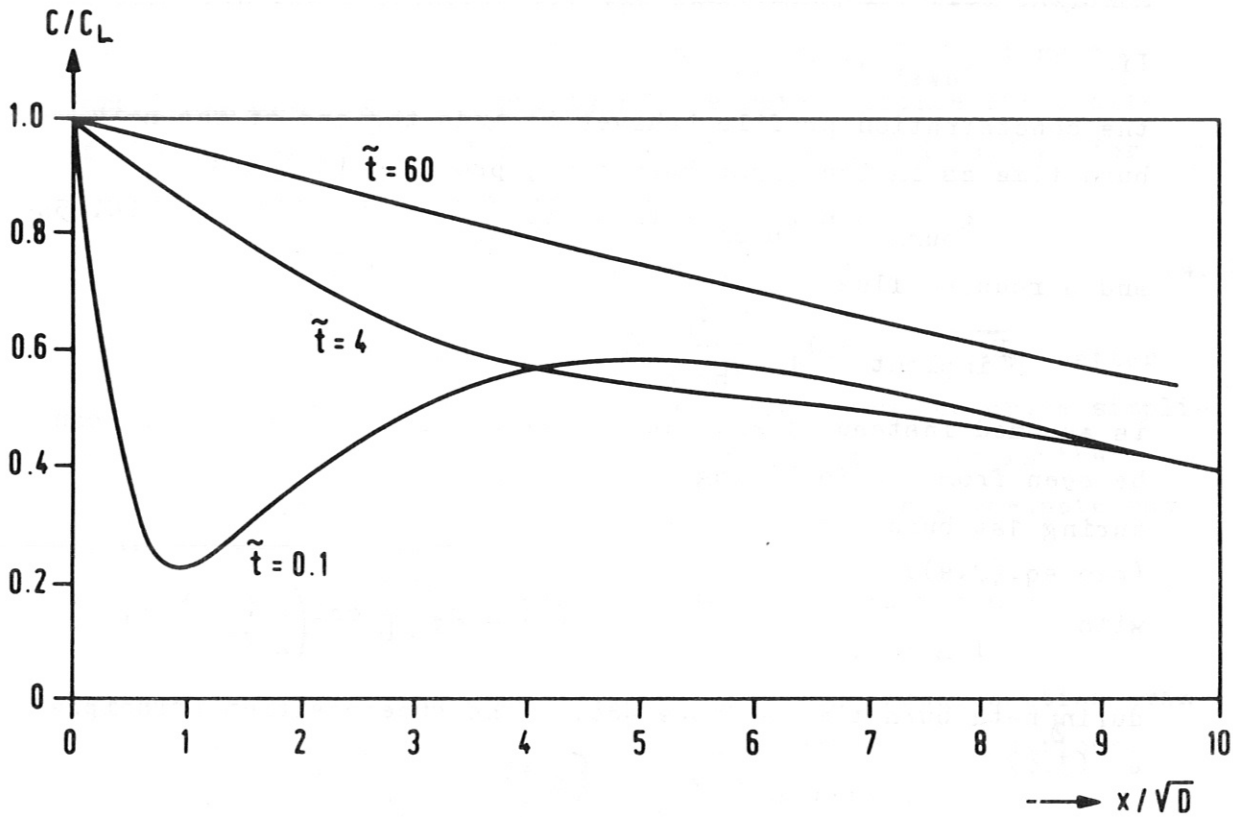

FIG.4-4
H-concentration C/C_L versus x during the 2nd burn time acc.to eq.(4.15) for $t_{burn}=60$ and $t_{dwell}=4$ at three different times. $\tilde{t}$ is defined by

$$\tilde{t} = t - t_{burn} - t_{dwell}$$

and stands for the time elapsed since 2nd burn time start, see FIG.3-1

A characteristic feature of the C-profile during the 2nd burn time is the distinct dip at small $\tilde{t}$ ($\tilde{t}$=0.1 in FIG.4-4), which at $\tilde{t}=t_{dwell}$ ($\tilde{t}$=4 in FIG.4-4) becomes very flat and disappears for $\tilde{t} \gg t_{dwell}$ ($\tilde{t}$=60 in FIG.4-4).

This means that towards the end of the 2nd burn time the concentration profile is practically eqivalent to a profile after one single burn time lasting

$$\hat{t}_{burn} = 2t_{burn} + t_{dwell}$$

with an averaged flux. For this reason it is appropriate to make the following generalization:

If $t_{dwell} \ll t_{burn}$

the concentration profile behaves towards the end of the n-th burn time as in the first burn time, provided it lasts

$$t_{burn} = n\, t_{burn} + (n-1)\, t_{dwell} \qquad (4.15a)$$

and a reduced flux

$$\overline{F_{implant}} = F_L \frac{t_{burn}}{t_{burn}+t_{dwell}} \qquad (4.15b)$$

is assumed instead of F_L. In the extremely dirty case this can be seen from the following:

during 1st burn time we have $C = F_L\, g(t)$

(see eq.(2.4))

with $g(t) = 2\sqrt{\frac{t}{\pi D}}\, \mathrm{eri}\left(\frac{x}{2\sqrt{D\,t}}\right)$;

during n-th burn time we have acc.to the superposition principle eq.(3.8)

$$C = F_L \left[g(t) - g(t-t_{burn}) + g(t-t_{burn}-t_{dwell}) - + \ldots \right]$$

which can re-arranged to give

$$C = F_L \frac{t_{burn}}{t_{burn}+t_{dwell}}\, g(t)$$

for large n.

Superposition

In the preceeding equations (4.9-14) we have written down the re-emission flux during the 1st dwell time in the following special cases:

1.) The time t elapsing since the first switching on is so long, that the profile built up in the preceeding burn time can be regarded as constant (see eq.(4.10a)).

2.) The irradiated surface is extremely clean (eq.(4.14))or extremely dirty (eq.(4.13)), so that the boundary conditions are linear and solutions can be superposed.

We now look for a solution for the case where both the time t elapsing since the first switching on and the release time t_A describing the degree of purity of the metal surface are finite. If the solution (4.6a) for the first burn time and (4.10a) for the dwell time are superposed, one obtains

$$\left.\frac{F}{F_L}\right|_{x=0} = \frac{1}{\sqrt{1+\tau}} - \frac{1}{1+\sqrt{\hat{\tau}}} \quad . \tag{4.16}$$

Numerical calculations now show that eq.(4.16) is a much better approximation than would have been expected from the crude simplifications contained in eq.(4.16). The reason for this is that eq.(4.16) contains two errors, which more or less compensate one another:

1.) the "substitution error" due to the substitution $\hat{b} = b = 1$ in the quasi-exact solutions (4.8) and (4.12) and

2.) the "superposition error" due to using the superposition principle (3.8) for cases with non-linear boundary conditions.

For small $\hat{\tau}$ the substitution error is dominant ,
and eq.(4.16) yields too large results;
for large $\hat{\tau}$ the superposition error is dominant
and eq.(4.16) yields too small results.
In many cases eq.(4.16) becomes useless, as can bee seen, when the right-hand side of eq.(4.16) is set =0 and solved:

$$\frac{1}{\sqrt{1+\tau_{burn}+\hat{\tau}}} - \frac{1}{1+\sqrt{\hat{\tau}}} = 0$$

$$\hat{\tau} = \tau_o = \frac{1}{4}\tau_{burn}^2 \tag{4.16a}$$

$$\tau_{burn} = \pi t_{burn}/t_A = \tau - \hat{\tau} \quad . \qquad \text{b)}$$

The flux F as calculated from eq.(4.16) thus becomes zero at $\hat{\tau} = \tau_o$. In many cases eq.(4.16) yields for

$$\hat{\tau} = 0.3\,\tau_o = 0.1\,\tau_{burn}^2 \qquad (4.16c)$$

a flux about half as large as that calculated numerically. Eq.(4.16c) is thus regarded as the validity limit of eq.(4.16).

The formulae for the substitution and the superposition errors are complicated and not particularly interesting. Instead, we calculated the re-emission flux numerically for various values of the parameters $\hat{\tau}$ and τ_{burn} and obtained the interpolation formula

$$\left.\frac{F}{F_L}\right|_{x=0} = \frac{-1 + \frac{1}{\sqrt{1+\tau_{burn}}}}{1 + 1.3\sqrt{\hat{\tau} + 6\hat{\tau}/\tau_{burn}} + 3.2\,\hat{\tau}^{1.33}/\tau_{burn}^{0.9}} \qquad (4.17)$$

The numerator gives the value of the normalized re-emission flux immediately after the start of the dwell time.
The factor 1.3 in the denominator is $=\hat{b}$ from eq.(4.12) for $\hat{\tau} \to 0$.
Eq.(4.17) has an inaccuracy of 5-10% in most practical cases and is also valid for values of $\hat{\tau}$ much higher than the zero (4.16a).
Fore more details, see FIG.6-2.

Eq.(4.17) is the re-emission flux law for the 1st dwell time. For the n-th dwell time t_{burn} has to be replaced by $\hat{t}_{burn}$ acc.to eq.(4.15a).

FIG.4-4d shows the re-emission flux calculating acc.to eq.(4.16) (dashed) and eq.(4.17) (solid) for two different burn times t_{burn}. As abscissa we use $\sqrt{\hat{\tau}}$ because this allows straightforward representation of a rather large time interval. The case $\tau_{burn}=3$ roughly corresponds to the case of INTOR with dirty surfaces (see table 4.20) during the 1st dwell time; this case can treated with eq.(4.16) only up to about $\hat{\tau} \leq 1$ or $\hat{t} \leq 4$ sec in FIG.4-6d. The zero transition is located at $\tau_o=2$. The case $\tau_{burn}=30$ roughly corresponds to INTOR with dirty surface during the 10.dwell time or else with a technically "clean" surface during the 1st dwell time. In this case the substitution and superposition errors cancel, so that eq.(4.16) is a good approximation.

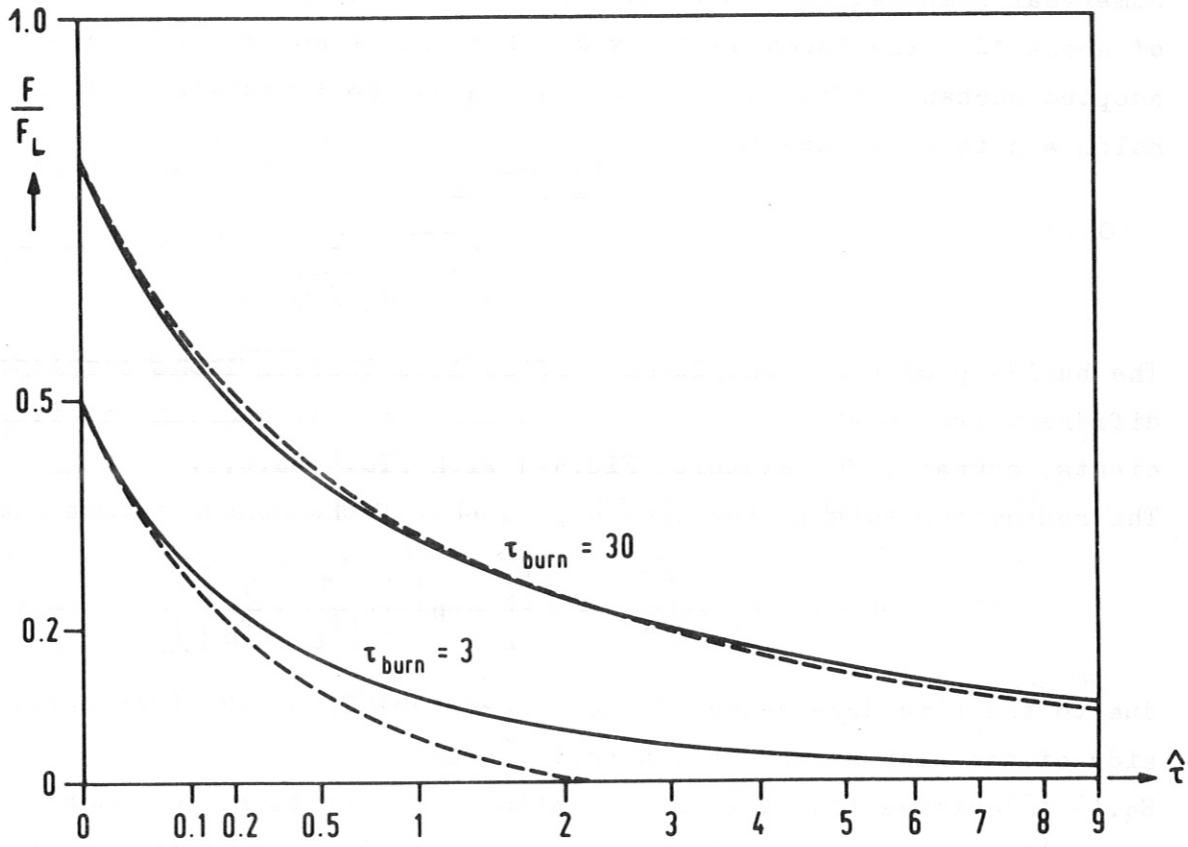

FIG.4-4d

Re-emission flux $|F/F_L|_{x=0}$ versus $\hat{\tau} = \pi \hat{t}/t_A$ during the 1st dwell time for the burn time lengths $\tau_{burn} = \pi t_{burn}/t_A = 3.$ and $\tau_{burn} = \pi t_{burn}/t_A = 30.$

Dashed: acc.to eq.(4.16)

Solid: acc.to eq.(4.17).

Remark: eq.(4.17) is almost exactly valid, while eq.(4.16) has only a limited range of validity.

The bottom left section $\hat{\tau} \leq 1$ and $|F/F_L| \leq 0.5$ corresponds to FIG.4-6d.

C Temperature-dependent coefficients

1st burn time

Numerical computations show that if one is content with an inaccuracy of about 10%, the formulae derived for constant coefficients can be adopted unchanged: for the concentration on the irradiated side it holds acc.to eq.(4.6b) that

$$C\big|_{x=0} = C_L\, W \qquad (4.18a)$$

$$W = \sqrt{1 - \frac{1}{\sqrt{1+\tau}}}\,, \qquad b)$$

The build-up of a concentration profile nevertheless looks completely different from what we have been accustomed to for constant coefficients; compare, for example, FIG.4-1 with FIG.4-5a,b,c.
The reason for this is the time dependence of the concentration limit

$$C_L = \sqrt{\frac{F_L}{K_L}} = \sqrt{\frac{F_L}{K_R}}\, \exp\left(\frac{E_K}{2}\left[\frac{1}{T_L} - \frac{1}{T_R}\right]\right) \qquad (4.18c)$$

due to the time dependence of the temperature T_L of the irradiated side of the slab at x=0 acc.to eq.(4.1h+k).
Eq.(4.18) states that the concentration rises at first for short times ($t < t_A$) acc.to eq.(4.18b), but at the same time the heating of the irradiated side of the slab produces a decrease in concentration acc. to eq.(4.18c). In some cases there exists a time

$$t_{max} = \frac{T_R^2}{E_K T_D}\sqrt{t_A\, t_{ST}} \qquad (4.19)$$

at which the two effects compensate one another; C(t) then assumes a maximum at $t=t_{max}$. For details see eq.(6.12-15).

In FIG.4-5 to 4-10 we present examples which are based on parameters deduced partly from INTOR or NET studies (see sec.5, Index I) partly from reactor studies (Index R). Both clean (subscript c) and dirty (subscript d) surfaces are considered.
We define these cases with the following data:

case	$K_o \left[\frac{cm^4}{atom\ sec}\right]$	$F_L \left[\frac{atoms}{cm^2 sec}\right]$	T_D
I_d	$1.6\ 10^{-20}$	$1.5\ 10^{16}$	80^o
I_c	$1.6\ 10^{-16}$	$1.5\ 10^{16}$	80^o
R_d	$1.6\ 10^{-20}$	$7.0\ 10^{16}$	200^o
R_c	$1.6\ 10^{-16}$	$7.0\ 10^{16}$	200^o

(4.20)

The data not contained in tab.(4.20) are presented in tab.(4.2). INTOR is water-cooled, from which it follows that $T_R=373^oK$. However, in order to compare reactor with INTOR conditions in all cases

$$T_R = 600^oK \qquad \text{s.(4.2h)}$$

is assumed.

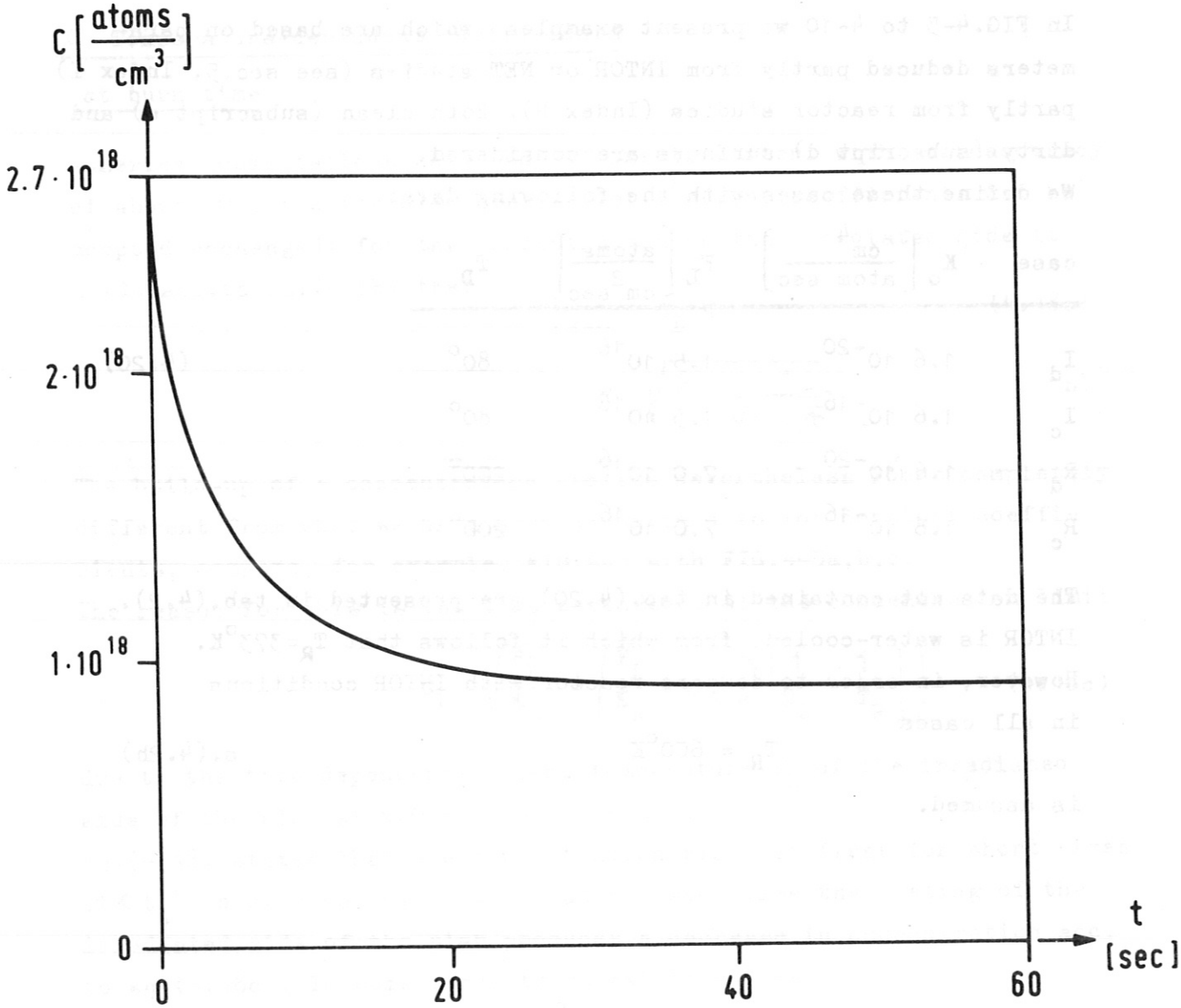

FIG.4-5a

H-concentration $C\big|_{x=0}$ versus t during the 1st burn time for the reactor with clean surfaces (case R_c in tab.(4.20)) acc.to eq.(4.18), which agrees with the numerical solution within the drawing accuracy.

The release time $t_A = 10^{-3}$ sec is so short that almost exactly

$$C\big|_{x=0} = C_L = \sqrt{F_L / K_L} \qquad (4.21)$$

is valid. The curve is a transformation of the temperature acc.to eq.(4.18c). The highest possible concentration

$$C_{max} = \sqrt{F_L / K_R} = 2.7\ 10^{18}\ \frac{\text{atoms}}{\text{cm}^3} \qquad (4.22)$$

is reached in the time interval $10^{-2} \leq t \leq 10^{-1}$ sec, which cannot be resolved in this figure.

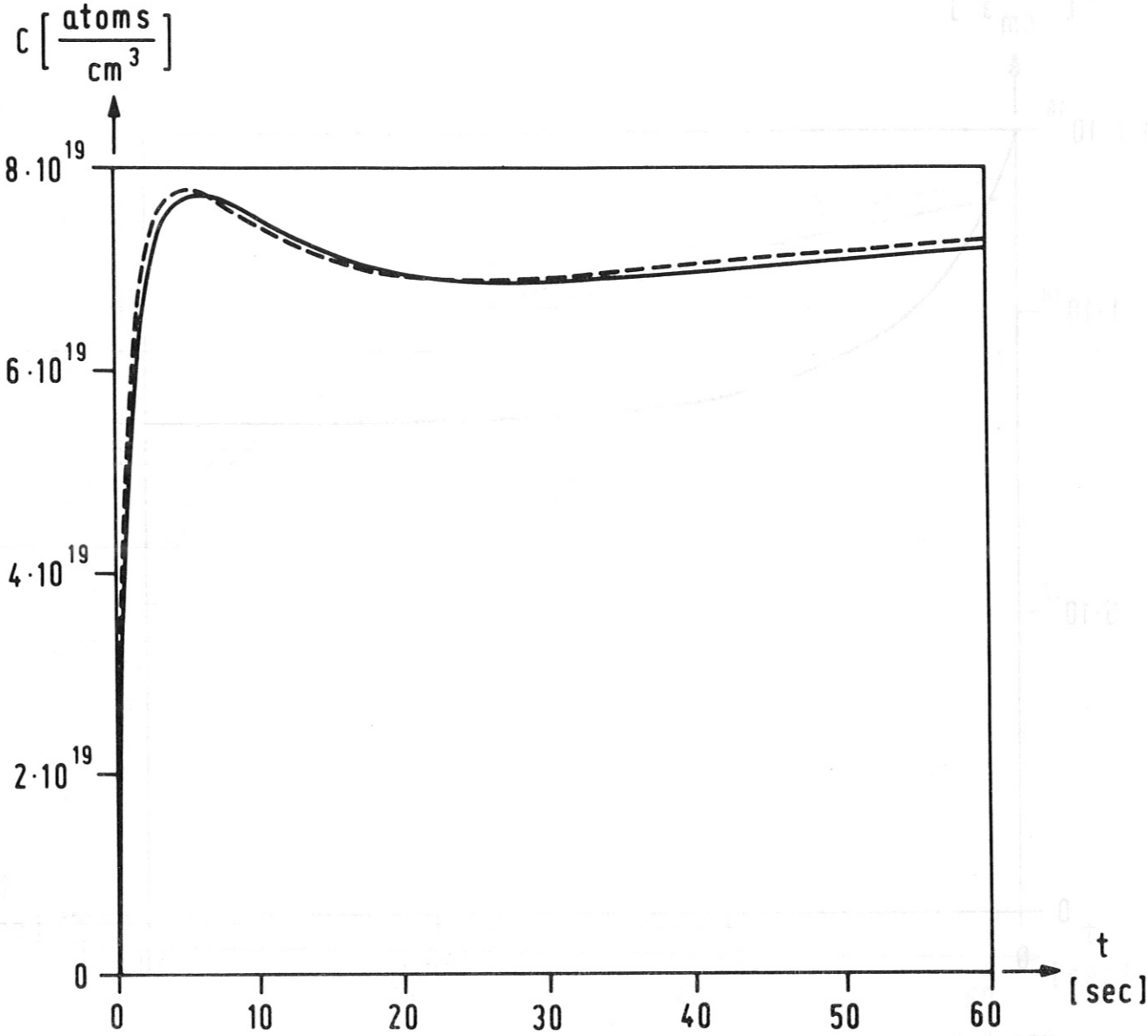

FIG.4-5b

H concentration $C\big|_{x=0}$ versus t during the 1st burn time for the reactor with dirty surfaces (case R_d in tab.(4.20))

Dashed: acc.to eq.(4.18)

Solid: numerically calculated.

The release time t_A=18 sec is about 2/3 as long as the temperature diffusion time t_{ST}=25 sec, so that the concentration build-up acc. to eq.(18b) and the reduction acc.to eq.(18c) roughly compensate one another, apart from short times. Eq.(4.19) yields

$$t_{max} = 6 \text{ sec}$$

for the location of the maximum.

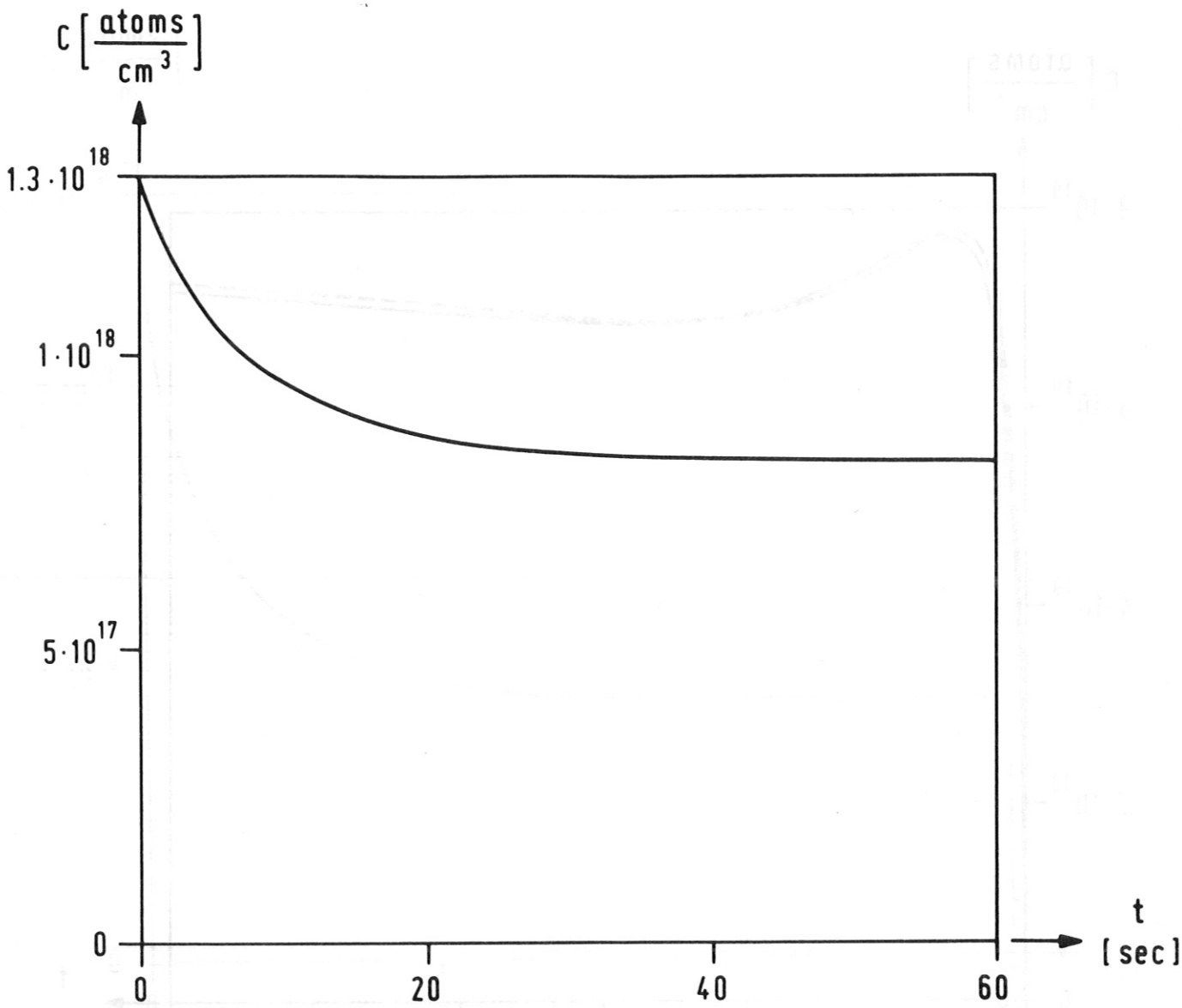

FIG.4-5c
H-concentration $C|_{x=0}$ versus t during the 1st burn time
for INTOR with clean surfaces (case I_c in tab.(4.20))
acc.to eq.(4.18), which is indistinguishable from the exact solution.
The release time is $t_A = 7\ 10^{-3}$ sec; it holds that

$$C|_{x=0} = C_L \qquad \text{s.(4.21)}$$

as in the case of FIG.4-5a.

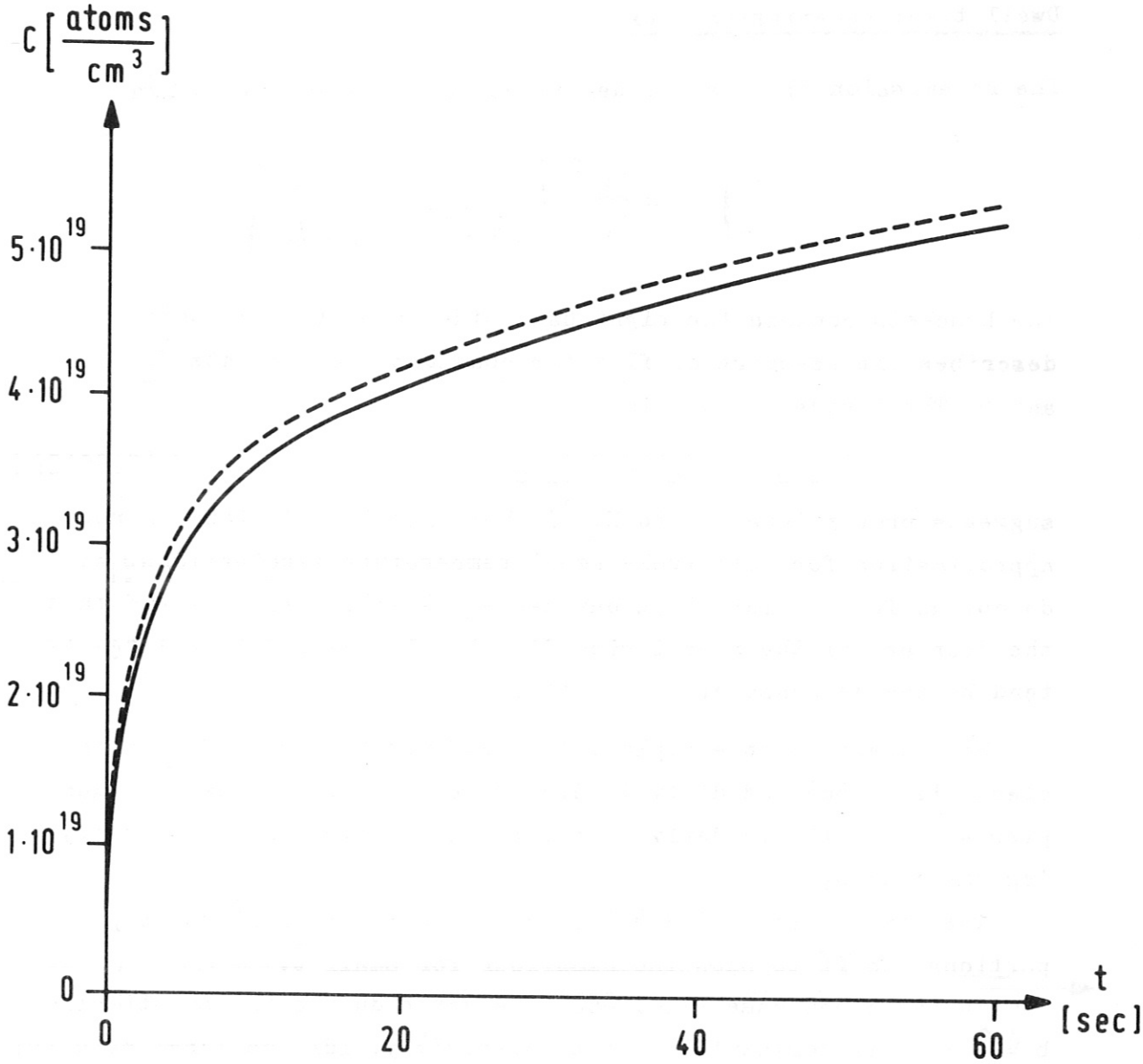

FIG.4-5d

H concentration $C|_{x=0}$ versus t during the 1st burn time for INTOR with dirty surfaces (case I_d in tab.(4.20)).

Dashed: acc.to eq.(4.18)

Solid: numerically calculated.

The release time t_A=75 sec is much longer than the temperature diffusion time t_{ST}=25 sec . The temperature and the coefficients are already nearly constant before the concentration build-up has got beyond its initial stage (eq.(4.5)). FIG.4-5d corresponds therefore to the left-hand part of FIG.4-1 for constant coefficients.

Dwell time: re-emission flux

The re-emission flux can be described in crude approximation by

$$\left.\frac{F}{F_L}\right|_{x=0} = \frac{K_L(\hat{t})}{K_L(0)}\left(\frac{1}{\sqrt{1+\tau}} - \frac{1}{1+\sqrt{\hat{\tau}}}\right) \qquad (4.23)$$

The brackets contain the right-hand side of eq.(4.16), which describes the re-emission flux for constant coefficients K_L and D. The boundary condition

$$F|_{x=0} = -K_L(\hat{t})\, C^2|_{x=0} \qquad \text{s.(4.1d+e)}$$

suggests proportionality to $K_L(\hat{t})$, but this is only true in rough approximation for relatively small temperature fluctuations. We do not go further into this but use eq.(4.23). Here we learn that the decrease of the re-emission flux is also caused to a large extend by the decrease of the coefficient K_L.

We present as an example INTOR (defined by tab.(4.20)) with clean (FIG.4-6c) and dirty (FIG.4-6d) surfaces. The reactor examples are essentially derived from the INTOR examples by multiplying the flux by 7.

The time scale in FIG.4-6 is distorted: the abscissa is proportional to $\sqrt{\hat{t}}$ to show the behaviour for small $\hat{t}$.

In the clean case (FIG.4-6c) the error due to the substitution $b = \hat{b} = 1$ is dominant, so that eq.(4.23) yields too large results; in the dirty case (FIG.4-6d) the superposition error (see page 25) is dominant, so that eq.(4.23) yields too small results.
The case INTOR dirty is already at the limit of applicability of eq.(4.23). The zero for F as calculated acc.to eq.(4.23) or (4.16) is at $\hat{t} \approx 10$ sec, see FIG.4-4d.

In the reactor case R_d in tab.(4.20) the superposition and substitution errors compensate one another to a certain extend, but then the factor $K_L(\hat{t})/K_L(0)$ from eq.(4.23) is too small, especially towards the end of the dwell time. Eq.(4.23) therefore also yields too small results.

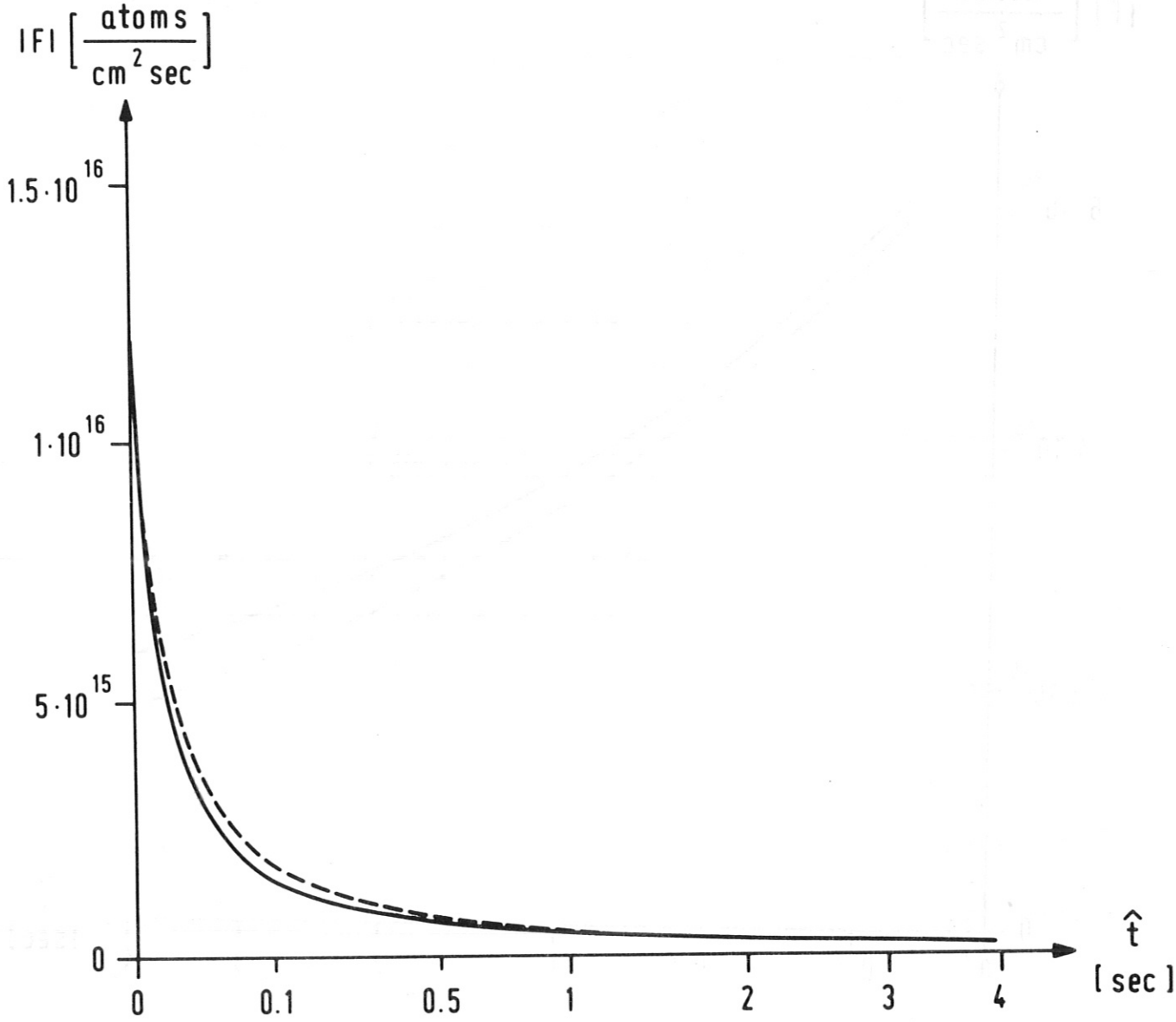

FIG.4-6c

Re-emission flux $|F|_{x=0}$ versus $\hat{t}$ for the 1st dwell time for INTOR with clean surfaces; data see tab.(4.20)+(4.2).

Dashed: calculated acc.to eq.(4.23)

Solid: numerically calculated.

$$K_L = \begin{cases} 2.3\ 10^{-20} & \text{cm}^4/(\text{atom sec}) \text{ at dwell time start} \\ 1.4\ 10^{-20} & \text{" " " " end;} \end{cases}$$

eq.(4.23) yields too large values owing to the substitution $\hat{b} = 1$ (see page 25 and 21)

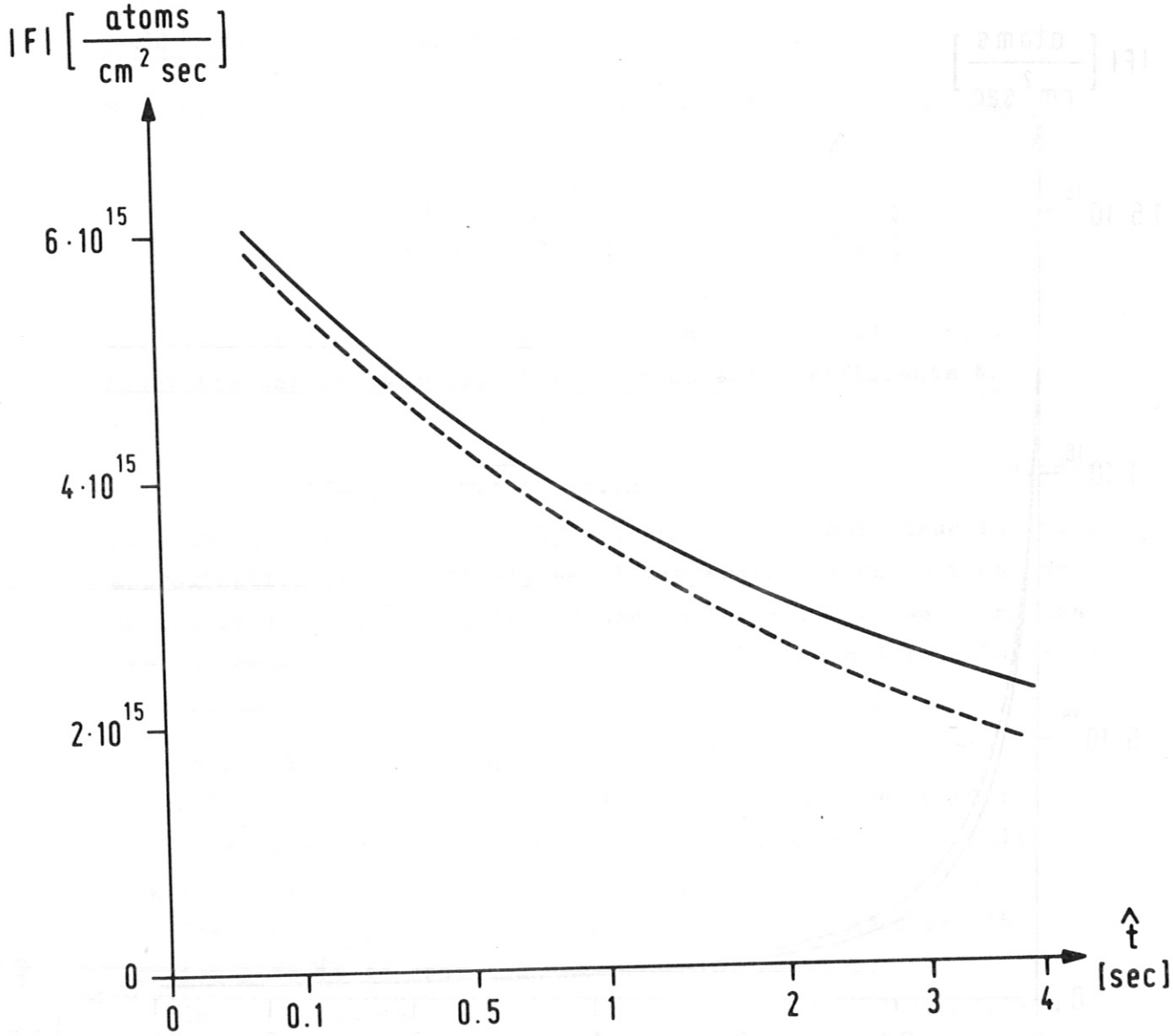

FIG.4-6d

Re-emission flux $|F|_{x=0}$ versus t for the 1st dwell time for INTOR with dirty surfaces; data see tab.(4.20)+(4.2).

Dashed: calculated acc.to eq.(4.23)

Solid: numerically calculated.

Eq.(4.23) yields too small values owing to the superposition error (see page 25) which is dominant in this example.

The flux at t=0 is barely half as large as in the clean case I_c, because the term deriving from the burn time

$$\frac{1}{\sqrt{1+\tau}} = \begin{cases} 0.6 \text{ in case } I_d \\ 0.0 \quad " \quad " \quad I_c \end{cases}$$

has to be substracted from 1 acc.to eq.(4.23)

Dwell time variation

The concentration C_{burn} at the end of the 1st burn time and $C = C_{burn} - C_{var}$ at the end of the 1st dwell time are calculated acc.to the following equations:

$$T = T_R + T_D \left[\sqrt{\frac{t_{burn}+t_{dwell}}{\sqrt[3]{0.485\, t_{ST}^3 + (t_{burn}+t_{dwell})^3}}} + \right.$$

$$\left. - \sqrt{\frac{t_{dwell}}{\sqrt[3]{0.485\, t_{ST}^3 + t_{dwell}^3}}} \right] \qquad (4.24a), s.(4.1k)$$

$$K_L = K_o \exp\left[- E_K / T\right] = K_L(t_{dwell}) \qquad (4.24b), s.(4.1h)$$

$$D = D_o \exp\left[- E_D / (T_R+T_D)\right] = D(0) \qquad c), s.(4.1g)$$

$$t_A = \frac{D}{F_L K_L} \qquad d), s.(4.3a)$$

$$H_{burn} = 2\sqrt{D\, t_{burn}} \qquad e), s.(2.3h)$$

$$H_{dwell} = 2\sqrt{D\, t_{dwell}} \qquad f), s.(4.3d)$$

$$\tau_{burn} = \pi t_{burn}/t_A \qquad g), s.(4.5d)$$

$$\tau_{dwell} = \pi t_{dwell}/t_A \qquad h)$$

$$C_B = \sqrt{\frac{F_L}{K_L(0)}} \sqrt{1 - \frac{1}{\sqrt{1+\tau_{burn}}}} \qquad i), s.(4.6b)$$

$$C_{burn} = C_B \operatorname{erfc}\left(\frac{x}{H_{burn}}\right) \qquad j), s.(4.7b)$$

$$F_o = \frac{K_L(t_{dwell})}{K_L(0)} \left[\frac{F_L}{1+\sqrt{\tau_{dwell}}} - \frac{F_L}{\sqrt{1+\tau_{burn}+\tau_{dwell}}} \right] \qquad k), s.(4.23)$$

$$C_D = \sqrt{\frac{F_o}{K_L(t_{dwell})}} \qquad l), s.(4.1d+e)$$

$$C_{var} = (C_B - C_D) \operatorname{eri}\left(\frac{x}{H_{dwell}}\right) = \text{"dwell time variation"} \qquad m), s.(4.9c)$$

$$C = C_{burn} - C_{var} \qquad n), s.(4.9)$$

Eq.(4.24) connects the formulae for the behaviour of the solution at x=0 with the space functions

erfc for the burn component and

eri for the dwell component.

We present as examples INTOR with clean (FIG.4-7c) and dirty (FIG.4-7d) surfaces. The corresponding reactor examples are derived from these by multiplying the concentration by 1.4 in the dirty case and 1.1 in the clean case. The poor agreement in the dirty case is essentially due to the superposition error (page 25).

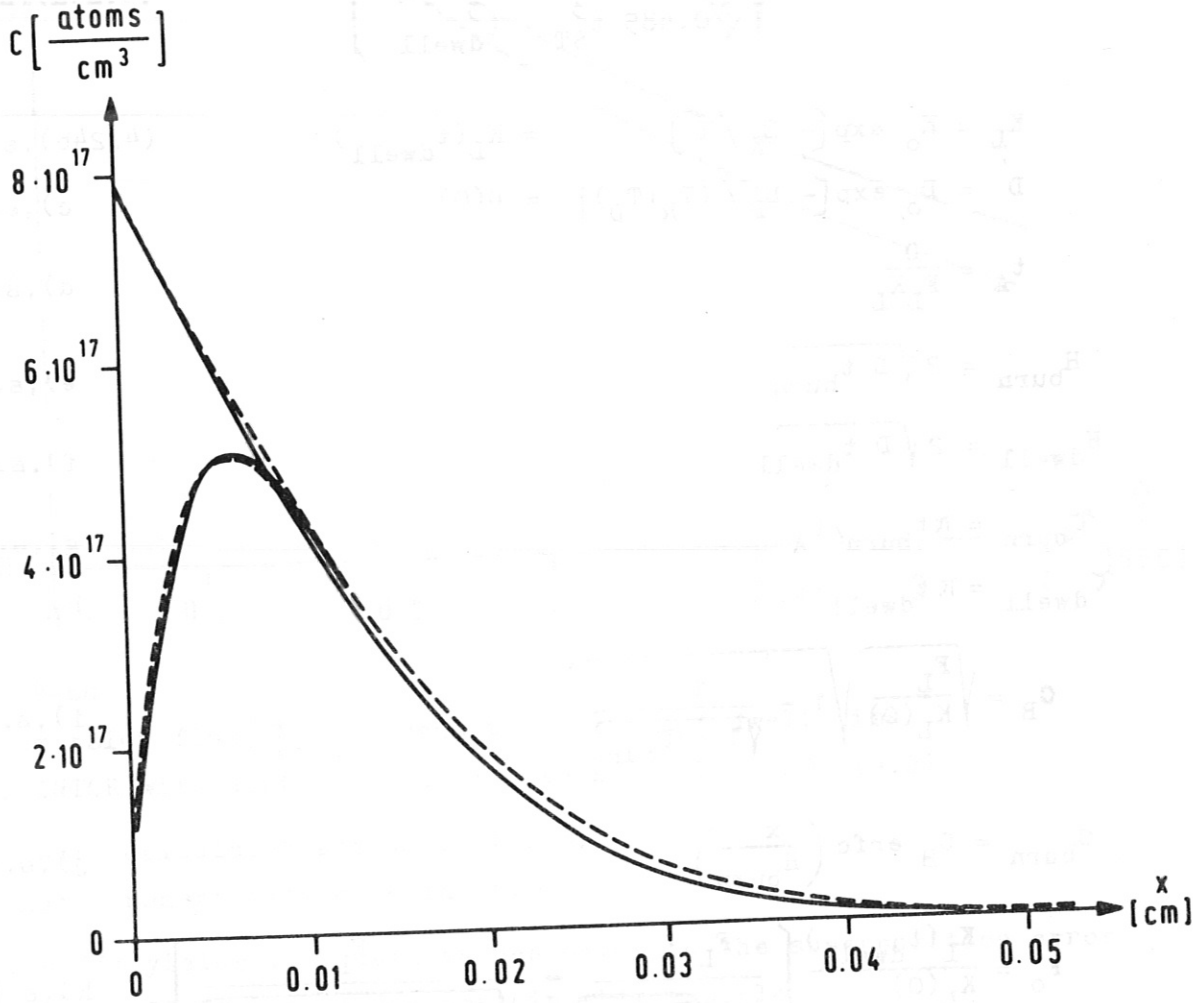

FIG.4-7c

Concentration C versus x at the start and the end of the 1st dwell time for INTOR with clean surfaces (case I_c in tab.(4.20))

Dashed: acc.to eq.(4.24)

Solid: numerically calculated

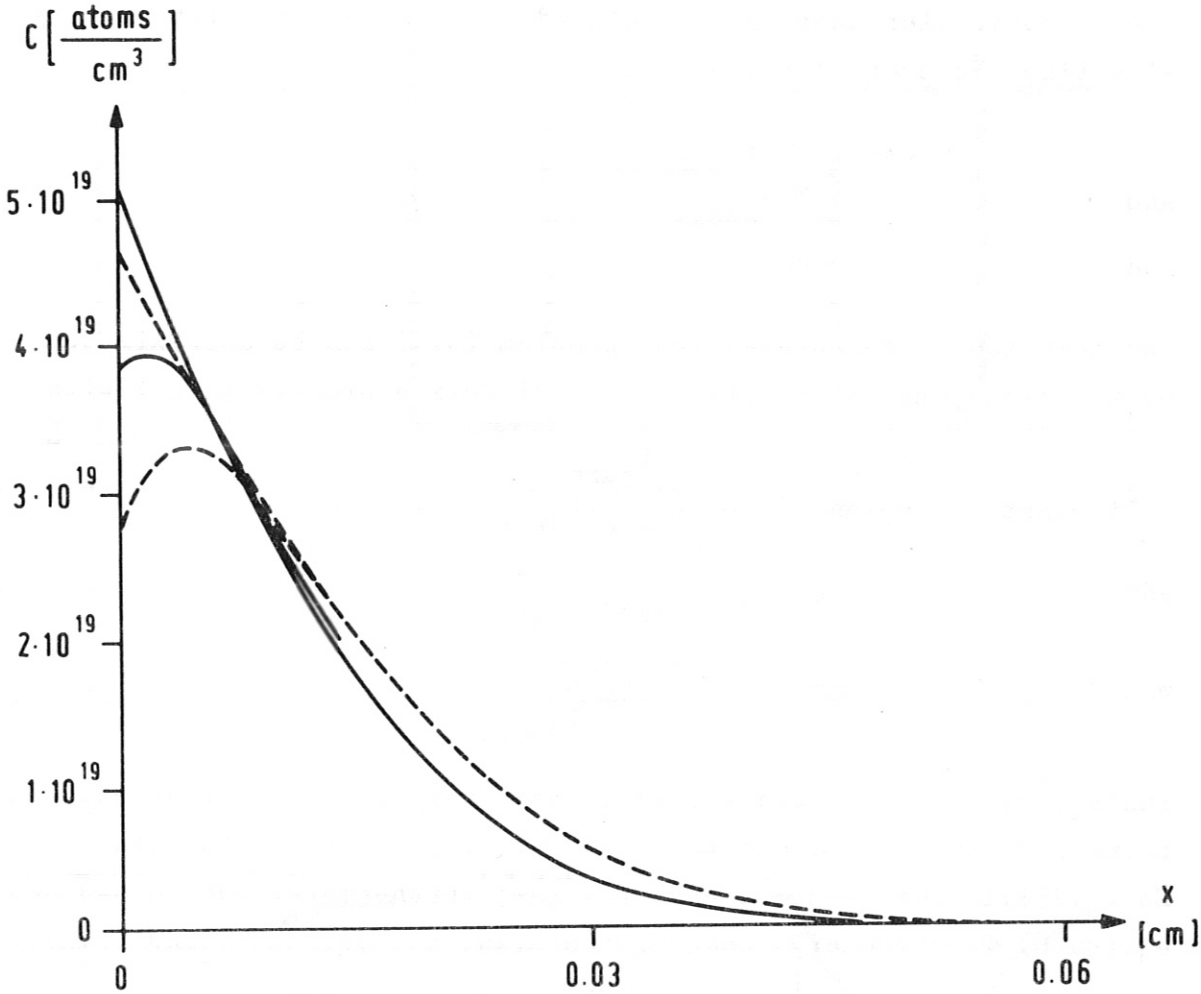

FIG.4-7d

Concentration C versus x at the start end the end of the 1st dwell time for INTOR with dirty surfaces (case I_d in table 4.20)

Dashed: acc.to eq.(4.24)

Solid: numerically calculated.

For $x \to 0$ the superposition error (page 25) is dominant.
The discrepancy at $x \approx 0.03$ arises from the choice of erfc as space function in eq.(4.24) for C_{burn}, which in this case ($t_A > t_{burn}$; t_A=80 sec ; t_{burn}=60 sec) is not justified.

The steady-state problem

The diffusion problem (4.1) has no steady-state solution. Even for very long times t the alternation of burn and dwell times causes the concentration near the irradiated side x=0 of the slab to vary with time. However, for conditions

$$t_{dwell} \ll t_{burn}$$

and $$x \gtrsim H_{dwell}$$

and $$t \gg t_{SC}$$

the solution as calculated from problem (4.1) can be approximated by the steady-state solution of the diffusion problem (4.25) with

$$F_{implant} = \overline{F_{implant}} = F_L \frac{t_{burn}}{t_{burn}+t_{dwell}} \qquad (4.25e)$$

and $$T = T_R + \overline{T_D}(1 - \frac{x}{a}) \qquad (4.25k)$$

with $$\overline{T_D} = T_D \frac{t_{burn}}{t_{burn}+t_{dwell}} \qquad (4.26)$$

instead of eq.(4.1e) and (4.1k) respectively with all other equations being left unchanged: one thus has eq.(4.25a) = eq.(4.1a) etc.. Eq.(4.25k)is the mass conservation law; furthermore, due to U=const eq.(4.26) is the energy conservation law, see eq.(3.3b) and (5.2).

The steady-state solution is treated in eq.(4.27). Beforehand, however, let us view the parameters $F_{implant}$, $\overline{F_{implant}}$, F_L, T_D, $\overline{T_D}$ in FIG.4-8 .

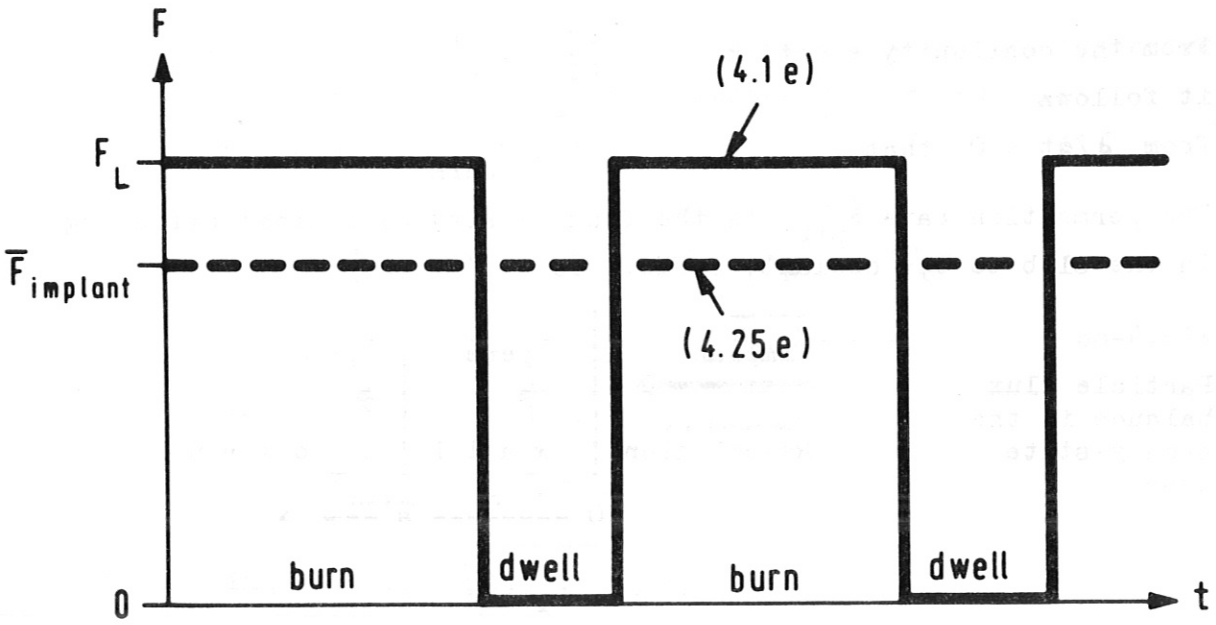

FIG.4-8a

The flux $F_{implant}$ of the implanted particles versus t

Solid: acc.to eq.(4.1e)

Dashed: ac.to eq.(4.25e).

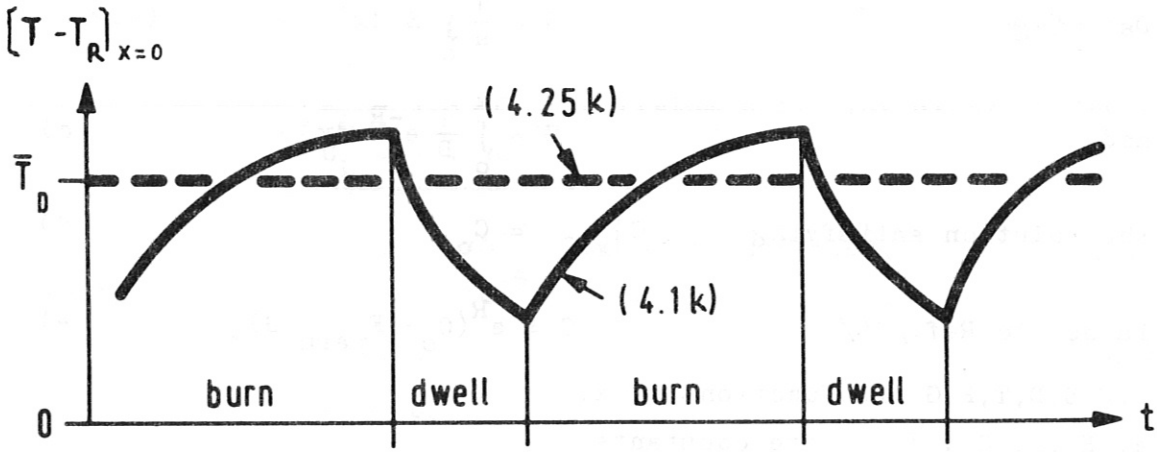

FIG.4-8b

The temperature of the irradiated side of the slab

T versus t (schematic)

Solid: acc.to eq.(4.1k)

Dashed: acc.to eq.(4.25k).

General solution

From the continuity equation $\frac{\partial C}{\partial t} = - \frac{\partial F}{\partial x}$ s.(4.1a)

it follows

from $\partial/\partial t = 0$ that $F = F_{perm} = const.$

The permeation rate F_{perm} is the flux density of H atoms diffusing in the slab to the coolant; s.FIG.4-8c

FIG.4-8c
Particle flux balance in the steady-state case

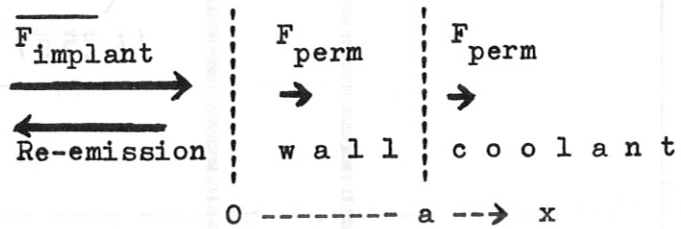

Taking into account the SORET effect (Ref./1/,eq.(4)) we have

from FICK's law $\frac{\partial C}{\partial x} - \frac{S}{a} C = - F_{perm} \frac{1}{D}$ (4.25b)

instead of eq.(4.1b)

with $S = - a E_{SOR} \frac{\partial T/\partial x}{T^2}$. (4.27a)

Defining $R = \frac{1}{a} \int_o^x S \, dx'$ (4.27b)

and $G = \int_o^x \frac{1}{D} e^{-R} \, dx'$ c)

the solution satisfying $C|_{x=0} = C_o$ d)

is acc.to Ref./14/ $C = e^R (C_o - F_{perm} G)$. e)

C,F,S,D,T,R,G are functions of x;

a, E_{SOR}, C_o, F_{perm} are constants.

The integration constants C_o and F_{perm} are determined from the boundary conditions

$F_{perm} = \overline{F_{implant}} - K_L C_o^2$ (4.28a)

and $F_{perm} = K_R e^{2R_a} \left[C_o - F_{perm} G_a\right]^2$ b)

with $R_a = R|_{x=a}$ c)

$G_a = G|_{x=a}$. d)

For more details s.eq.(6.17).

Special cases

In the following we treat simplificated cases which are characterized by dimensionless constants. The formulae are derived in §6.
In the most simple case we have

$$D = \text{const} \qquad \text{resp. } E_D = 0 \tag{4.29a}$$

$$C\big|_{x=a} = 0 \qquad " \quad K_R \gg D/(C_o a) \tag{b}$$

$$R = 0 \qquad " \quad E_{SOR} = 0 \,. \tag{c}$$

The solution is $C = C_o(1 - \frac{x}{a})$ (d)

$$F_{perm} = C_o \, D/a \,. \tag{e}$$

Introducing $\overline{C_L} = \sqrt{F_{implant}/K_L}$ (f)

and $A = D/(2aK_L\overline{C_L})$ (g)

we have $C_o = \overline{C_L}\left(\sqrt{1+A^2} - A\right)$. (h)

Sample application: INTOR as defined in tab.(4.20)+(4.2):

$D = 1.5\ 10^{-6}$ cm^2/sec
$a = 1.$ cm
$K_L = 1.3\ 10^{-24}$ cm^4/(atom sec) for dirty surfaces
$C_L = 1.1\ 10^{20}$ atoms/cm^3 " " "

$A = 5\ 10^{-3}$ for dirty surfaces; (4.29i)
similar, $A = 5\ 10^{-5}$ " clean " .

If $A \ll 1$ (4.30a)
we have $C_o \approx \overline{C_L}$ b)
and $A \approx \frac{1}{2} \, F_{perm}/\overline{F_{implant}}$. c)

In the following example (4.31) we take into account finite values of K_R. Therefore $C|_{x=a}/C_o$ has a value $h > 0$.

Assuming $D = \text{const}$ resp. $E_D = 0$ (4.31a)

and $R = 0$ " $E_{SOR} = 0$ b)

yields $$C = C_o\left[1 - \frac{x}{a}(1-h)\right] \quad \text{c)}$$

$$F_{perm} = C_o \frac{D}{a}(1-h) \quad \text{d)}$$

with $$h = \sqrt{p + \frac{1}{4}p^2} - \frac{1}{2}p \quad \text{e)}$$

and $$p = \frac{D}{K_R C_o a} \quad \text{f)}$$

Sample application: INTOR as defined in tab.(4.20)+(4.2):

$D = 1.5\ 10^{-6}\ cm^2/sec$

$a = 1.0\ cm$

$K_R = 0.7\ 10^{-24}\ cm^4/(atom\ sec)$ for dirty surfaces

$C_o = 1.1\ 10^{20}\ atoms/cm^3$ " " "

$p = 0.02$ for dirty surfaces (4.31g)

$h = 0.14$ " " "

similar $p = 0.0002$ for clean surfaces

$h = 0.014$ " " " .

From eq.(4.29g) we have $$\frac{A}{p} = \frac{K_R}{2K_L} \quad \text{(4.31h)}$$

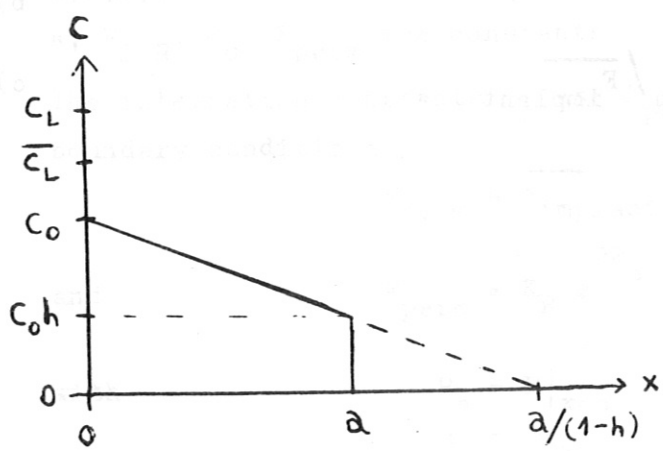

FIG.4-8d
C versus x in case (4.31)
with C_L , $\overline{C_L}$, C_o , h
indicated schematically

SORET-effect

Assuming $D = \text{const}$ resp. $E_D = 0$ (4.32a)

and $C|_{x=a'} = 0$ b)

yields for $|\bar{S}| \leq 1$ $C = C_o(1 - \frac{x}{a'})(1 + \frac{\bar{S}}{2}\frac{x}{a})$ c)

$$F_{perm} = C_o \frac{D}{a'} (1 + \frac{\bar{S}}{2}\frac{a'}{a}) \quad \text{d)}$$

with $\bar{S} = E_{SOR}\, \bar{T}_D / T_M^2$ e)

$$T_M = T_R + \frac{1}{2}\bar{T}_D \quad \text{f)}$$

$$a' = \frac{a}{1-h} \quad \text{g)}$$

s.eq.(6.20).

The dimensionless SORET constant $\bar{S}$ is approximately the space average of S (s.eq.(4.27a)) with $T = T_R + \bar{T}_D(1 + \frac{x}{a})$. s.(4.251)

h is the relative height of the C profile at x=a (see FIG.4-8d):

$$h = \frac{C|_{x=a}}{C|_{x=0}} \quad (4.32i)$$

Sample application:

steel slabs in INTOR as defined in tab.(4.20)+(4.2)+(5.4):

For steel one has $E_{SOR} = -800^o$

" INTOR " " $T_D = 80^o$

and $T_M = 640^o K$

It follows that $\bar{S} = -0.16$; (4.32j)

the SORET-effect thus causes C(x) to drop about 4-8% as compared with case (4.31) without SORET effect.

Temperature-dependent diffusion coefficient D

If the diffusion coefficient depends on temperature:

$$D = D_o \exp(- E_D / T) \qquad \text{s.(4.1g)}$$

$$T = T_R + \overline{T}_D(1- \frac{x}{a}) \qquad \text{s.(4.25K)}$$

we have two "new" parameters E_D / T_R and $\overline{T}_D / T_R$.

However, if $E_D / T_R \lesssim 15$, s.(6.25)

the problem can be described in good approximation by a set of equations (4.33) containing only one new parameter

$$B = \frac{E_D \overline{T}_D}{T_R^2} \qquad (4.33a)$$

B is the characteristic constant describing phenomena induced by the temperature dependence of the diffusion coefficient D.

Assuming $E_{SOR} = 0$ (4.33b)

yields $$C \approx C_o \left[1 - \frac{x}{a}(1-h) \exp\left(\frac{B}{2}\left(\frac{x}{a} -1\right)\right)\right] \qquad c)$$

and $$F_{perm} \approx C_o \frac{1-h}{a} \tilde{D} \qquad d)$$

with $$\tilde{D} = D_o \exp(- E_D / \tilde{T}) \qquad e)$$

$$\tilde{T} = T_R + \frac{\overline{T}_D}{2 + 0.2\, B} \qquad f)$$

$$h = \sqrt{p + \frac{1}{4}p^2} - \frac{1}{2}p \qquad g)$$

$$p = \frac{\tilde{D}}{K_R C_o a} \qquad h)$$

For more details s.eq.(6.21-25).

Permeation rates and hydrogen inventory

The total hydrogen inventory of the slab can be conceived as composed of hydrogen caught in traps and hydrogen diffusing in the direction of the coolant:

$$I_{total} = I_{trap} + I_{diff} \qquad (4.34a)$$

In this report we can only say something about the component I_{diff}, which can be defined by

$$I_{diff} = \int_0^a dx\, C(x) \,. \qquad (4.34b)$$

In the steady-state examples here (s.FIG.4-9) one has

$$\frac{I_{diff}}{a\, C_L} = \begin{cases} 0.65 \text{ for INTOR} \\ 0.75 \text{ " reactor} \end{cases} \qquad (4.34c)$$

but I_{trap} may be several times as large as I_{diff} if the slab has been exposed to the irradiation for a lengthy period, so that a large number of traps is present.

In tab.(4.35) the permeation rate F_{perm} and C_L are listed for the examples INTOR and reactor with dirty and clean surfaces as defined in tab.(4.20)+(4.2). The specification of grammes/(m^2 day) only applies to ordinary hydrogen; for tritium this value has to be multiplied by 3. With water cooling (T_R=373°K) the permeation rates are about 100 times as small as in tab.(4.35). I_{diff} need not be specified since the numerical value of C_L is also a measure of I_{diff} owing to a=1 (see eq.(4.2a)).

case	F_{perm} $\left[\frac{atoms}{cm^2 sec}\right]$	F_{perm} $\left[\frac{grammes}{m^2 day}\right]$	C_L $\left[\frac{atoms}{cm^3}\right]$
I_d	$1.0\ 10^{14}$	0.14	$8.1\ 10^{19}$
I_c	$1.1\ 10^{12}$	0.0016	$8.1\ 10^{17}$
R_d	$1.9\ 10^{14}$	0.27	$8.9\ 10^{19}$
R_c	$2.2\ 10^{12}$	0.0032	$8.9\ 10^{17}$

tab.(4.35)

The data in grammes/(m^2day) only apply to the isotope H^1; for tritium the values in the 2nd column should be multiplied by 3; see sec.6, page 76.

Concentration profiles in the steady-state

If the diffusion coefficient D depends on the temperature and/or the SORET effect is taken into account, the concentration profile C(x) is no longer linear in x, as can be seen from eq.(4.32c) and eq.(4.33b). Fortunately the combination

$$\frac{C}{C_o} = \left[1 - \frac{x}{a}(1-h)\ \exp\left(\frac{B}{2}\left(\frac{x}{a} - 1\right)\right)\right]\left[1 + \frac{\bar{S}}{2}\frac{x}{a}\right] , \qquad (4.36)$$

of eq.(4.32c) and (4.33b) gives a good fit for our examples. In the following figures (FIG.4-9;4-10;4-11) numerically calculated C-profiles are compared with C calculated acc.to eq.(4.36) for our examples from tab.(4.20)+(4.2)+(5.4) INTOR and reactor with dirty or clean surfaces without or inclusive SORET effect. It is found that eq.(4.36) fits the numerical results fairly well, s.FIG4-9 and 4-10.

In the case of positive E_{SOR} and strong temperature dependence E_D of the diffusion coefficient it is possible that hydrogen runs against grad C driven by grad T, s.FIG.4-11.

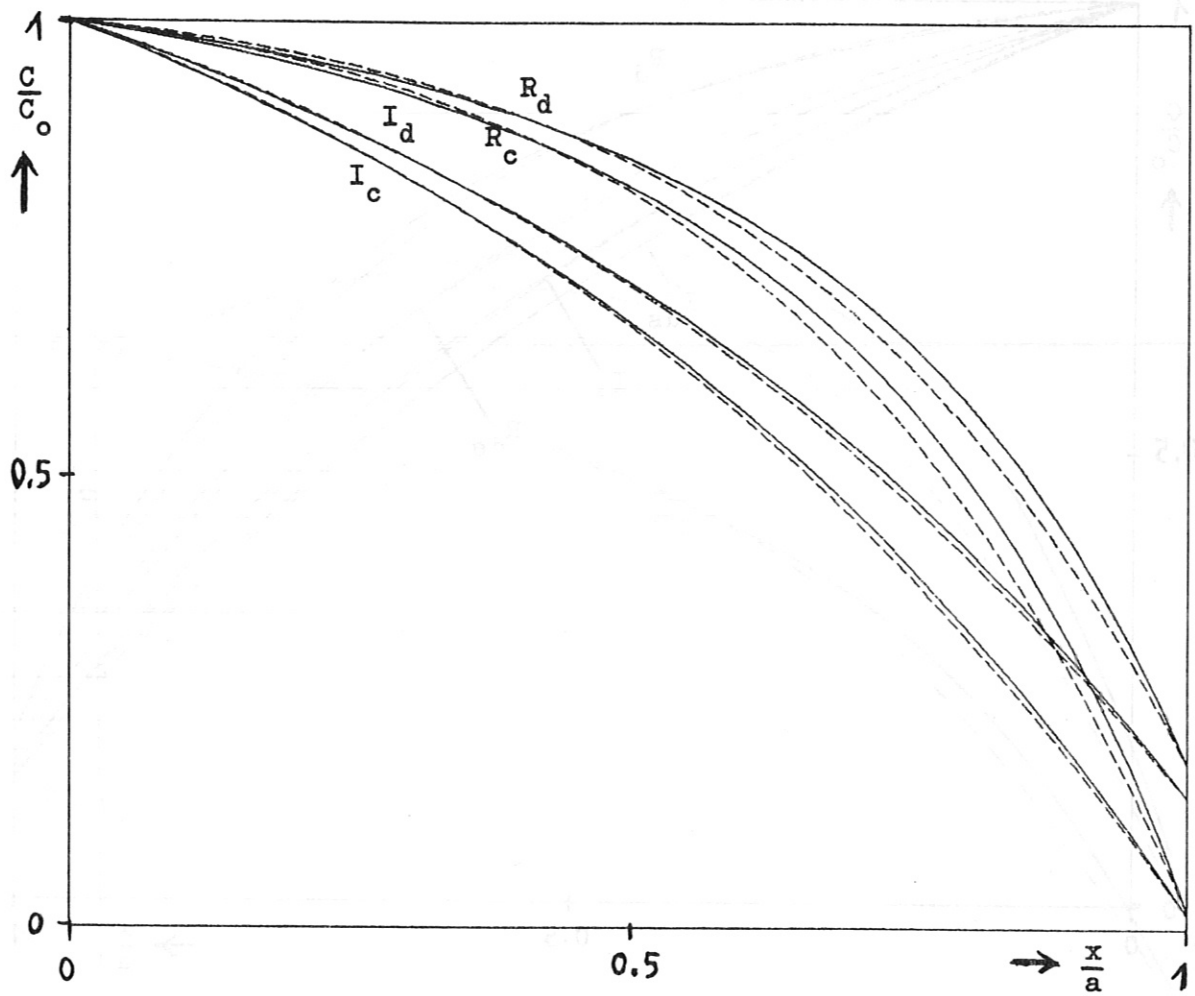

FIG.4-9

C/C_o versus x/a in the steady-state for the examples from tab.(4.20)

I_c = INTOR with clean surfaces
I_d = " " dirty "
R_c = reactor " clean "
R_d = " " dirty " ;

The SORET effect is neglected: $E_{SOR} = 0$.

Solid: numerically
Dashed: acc.to eq.(4.36).

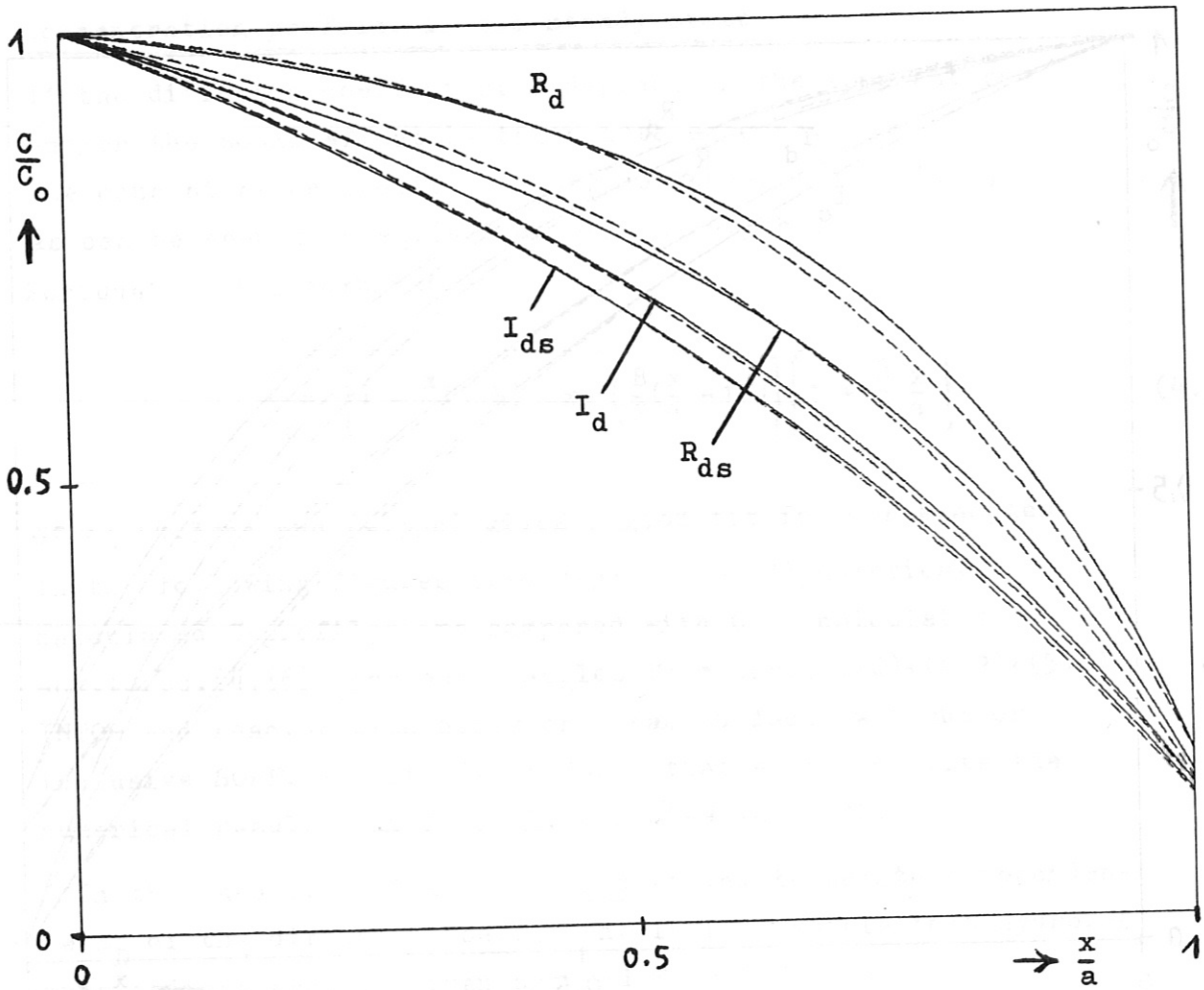

FIG.4-10

C/C_o versus x/a in the steady-state for the examples

I_d = INTOR with dirty surfaces; E_{SOR} = 0 ;

R_d = reactor " " " " ;

I_{ds} = INTOR " " " $E_{SOR} = -800^o$

R_{ds} = reactor " " " " .

Solid: numerically

Dashed: acc.to eq.(4.36).

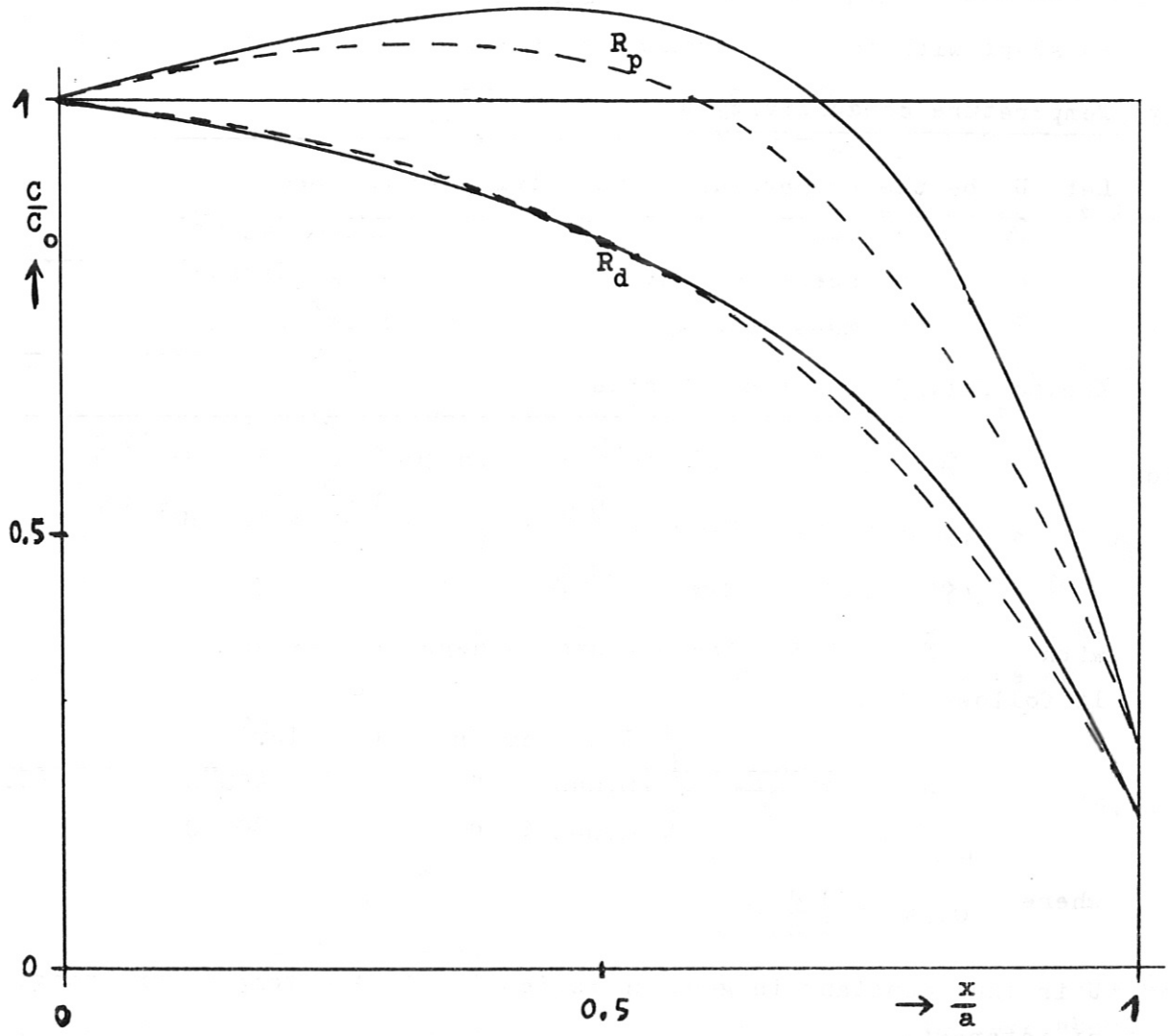

FIG.4-11

C/C_o versus x/a in the steady-state for the reactor with dirty surfaces;

R_d without SORET effect;
R_p with positive $E_{SOR} = 2000^o$;

Solid: numerically

Dashed: acc.to eq.(4.36)

Appendix

5. On the origin of the parameters

In this section we describe how the numerical values of the material parameters U, Q_L, F_L, E_D, E_K, E_{SOR}, D_o, K_o were obtained.

We start with the heat conduction data.

Temperature conductivity U

Let U be the temperature conductivity in cm^2/sec

λ " heat " $W/(cm\ degree)$

c " specific heat $cal/(gr\ degree)$

ϱ " mass density gr/cm^3 .

Acc.to Ref./3/ one then obtains

$$\lambda = 0.127 + 9.63\ 10^{-5}\ \tilde{T} - 7.8\ 10^{-9}\ \tilde{T}^2 - 3.3\ 10^{-13}\ \tilde{T}^3$$

$$c = 0.107 + 6.03\ 10^{-5}\ \tilde{T} - 4.4\ 10^{-8}\ \tilde{T}^2 + 1.4\ 10^{-11}\ \tilde{T}^3$$

$$\varrho = 7.98 - 2.96\ 10^{-4}\ \tilde{T}$$

with $\tilde{T} = T - 273$ = temperature in degrees Celsius .

It follows that

$$U = 0.24\ \frac{\lambda}{\varrho\, c} = \begin{cases} 0.035\ cm^2/sec & \text{for } T=0^oC \\ 0.040 \quad " & " \quad 400^oC \\ 0.045 \quad " & " \quad 800^oC \end{cases} \qquad (5.1)$$

where $0.24 = \frac{1\ J}{1\ cal}$.

U is thus constant in good approximation in the temperature range of interest.

Temperature flux

The heat flux $\dot{q}$ for INTOR is taken from Ref./7/; on page 43, Table II-13, it is stated:

surface heat flux from plasma = $11.6\ W/cm^2$.

This yields

$$Q_L = 0.24\ \dot{q}_L\ /(\varrho\ c) = 0.24\ \ 11.6\ /(7.9\ \ 0.11) = 3.2 \text{ degrees cm/sec} \qquad (5.2)$$

for the temperature flux.

Flux density F_L of the implanted atoms

According to Ref./7/, Table II-13, page 43, the INTOR plasma emits $1.3\ 10^{23}$ atoms per sec during burn periods.
The surface area of the 1st wall is 380 m^2.
It follows that the flux density of the incident particles (H-atoms) during burn periods is

$$F_{incident} = \frac{1.3\ 10^{23}\ \text{atoms}}{380\ \ m^2\ \ \text{sec}} = 3\ 10^{16}\ \frac{\text{atoms}}{cm^2 \text{sec}}\ . \qquad (5.3a)$$

Some of the incident particles are reflected and the rest are implanted:

$$F_{implant} = (1 - R_N)\ F_{incident}.$$

We recall the definition of F_L as the flux density of the implanted H atoms during burn periods, see eq.(4.1e). It follows that

$$F_L = (1 - R_N)\ F_{incident} \qquad (5.3b)$$

As an example of determining the particle reflection coefficient R_N we use the computer simulation computations Ref./13/,FIG.2.5 for the case where nickel is bombarded with deuterium. Acc.to W. ECKSTEIN the values obtained for Fe or steel are about the same as for Ni. The results are approximatively

$$R_N(E) = \begin{cases} 0.7 & \text{for E = 10 eV} \\ 0.5 & \text{" 100 "} \\ 0.3 & \text{" 1000 "} \\ 0.1 & \text{" 10000 "} \end{cases} \qquad (5.3c)$$

where E is the energy of the incident H atoms in eV.
In this report we choose arbitrarily

$$R_N = 0.5 \qquad (5.3d)$$

since the bombarding particles for INTOR are expected to have about 100 eV ; from which it follows that

$$F_L = 1.5\ 10^{16}\ \frac{\text{atoms}}{cm^2 \text{sec}} \qquad (5.3e)$$

Diffusion and recombination coefficients

The data for the H diffusion and recombination are taken from Refs./1/ and /8/. First we express the quantities E_D, E_S and Q^* from Ref./1/, Table 1-1, in units of temperature:

Ref./1/	this paper
$E_D = 0.61$ eV	$E_D = 7000^o$
$E_s = 0.091$eV	$E_D - E_K = 1000^o$
$-Q^* = 0.065$eV	$E_{SOR} = -800^o$

(5.4)

In addition, Ref./1/,Table 1-1 contains the diffusion coefficient

$$D_o = 0.085 \text{ cm}^2/\text{sec}.$$

To determine the recombination coefficient K_o we use Fig.1-1 from REF./1/, which is identical with FIG.5-1 of this report. This figure presents limiting curves labelled "THEORY" which characterize a very clean and a very dirty surface. They can be desribed by the equations

$$K_{clean} = 1.6\ 10^{-16} \exp(-6000/T) \quad \text{cm}^4/(\text{atom sec})$$
$$K_{dirty} = 1.6\ 10^{-20} \exp(-6000/T) \quad "$$

from which we have taken

$$K_o = \begin{cases} 1.6\ 10^{-16} \text{ cm}^4/(\text{atom sec}) \text{ for clean surfaces} \\ 1.6\ 10^{-20} \quad " \quad " \text{ dirty } " \end{cases} \qquad (5.5)$$

The parameter α used in Ref./1/ is proportional to the parameter K_o used in this report. In addition we compared WAELBROECK`s series of measurements with the exponential law

$$K_{waelb} = 10^{-15} \exp(-8860/T) \text{ cm}^4/(\text{atom sec})$$

In sec.4 we only used K_{clean} and K_{dirty}.

Finally, in FIG.5-2 we plotted for the particle diffusion coefficient the exponential law (4.1g) used here into fig.17 from Ref./8/, which contains experimental data.

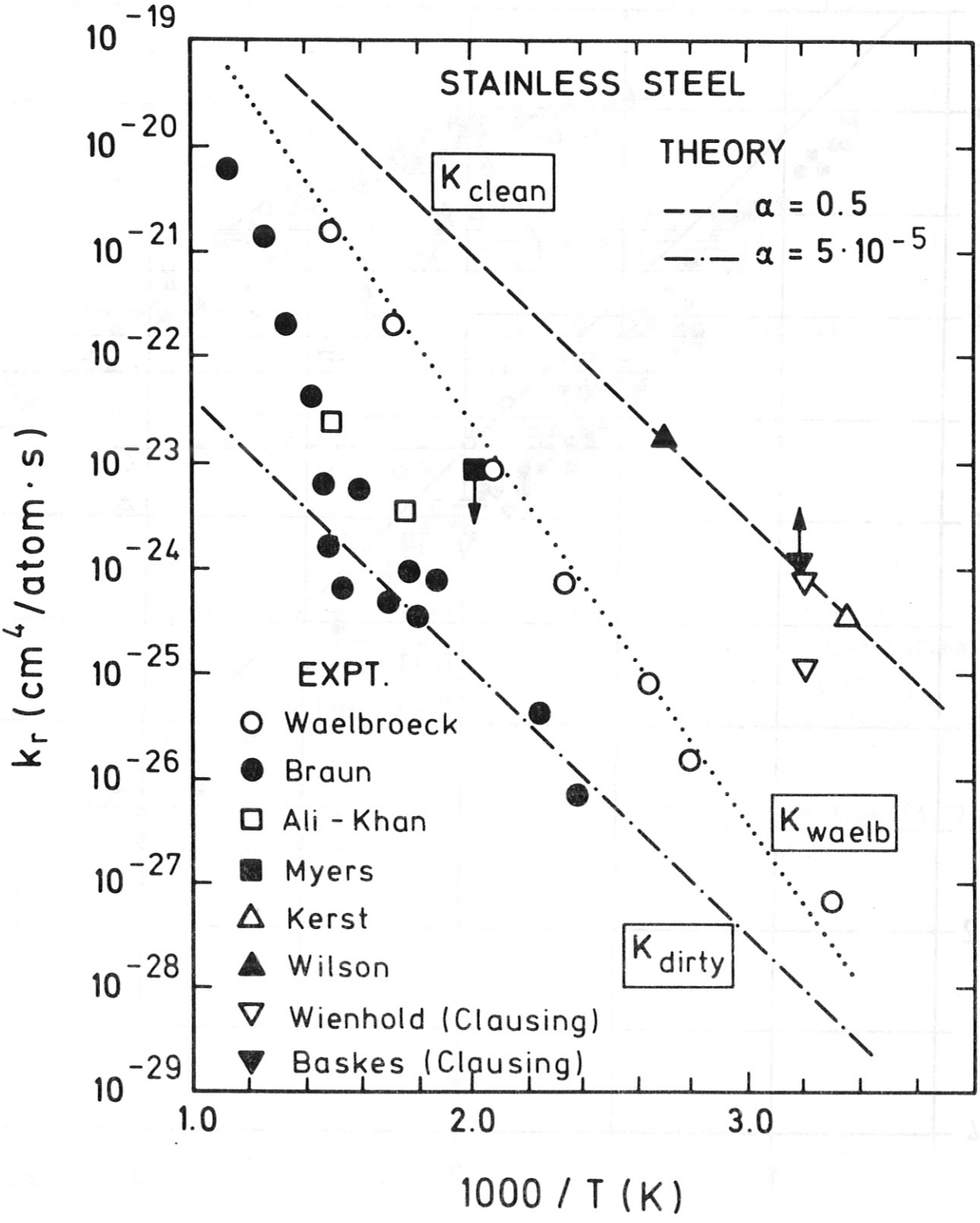

FIG.5-1

Reproduction of Ref./1/, Fig.1-1 with K_{clean}, K_{dirty} and K_{waelb}

Fig. 5-1

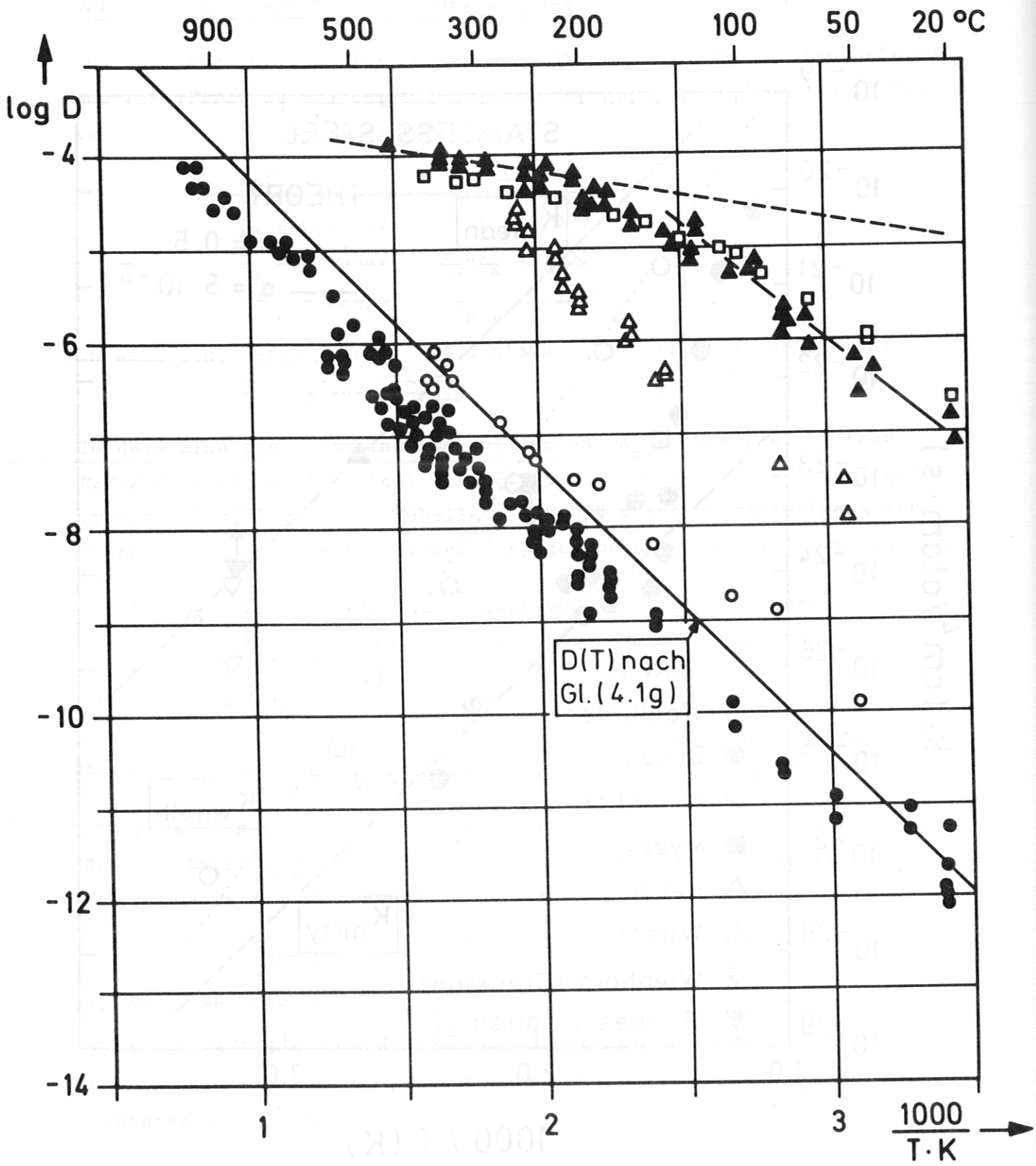

FIG.5-2

Reproduction of Ref./8/, Fig.17

with D(T) for some types of steel and acc.to eq.(4.1g)

- □ 4135
- ▲ 20 CrNiMo 10
- △ 430 α SS
- ○ 326 (α + γ) SS
- ● γ SS in general

Fig. 5 - 2

Appendix

6. Remarks on the formulae

Re. eq.(3.5-7) temperature

The numerator of eq.(3.5)

$$\text{numerator} = 2\, Q_L \sqrt{\frac{t}{\pi U}} \left[\text{eri}\left(\frac{x}{2\sqrt{U\,t}}\right) - \text{eri}\left(\frac{2a - x}{2\sqrt{U\,t}}\right)\right] \qquad (6.1)$$

solves the differential eq.(3.1a+b) exactly for T = numerator, but yields at x=0 the boundary condition

$$Q\big|_{x=0} = Q_L \left[1 + \text{erfc}\left(\frac{a}{\sqrt{U\,t}}\right)\right] \qquad (6.2)$$

instead of

$$Q\big|_{x=0} = Q_L \,, \qquad \text{s.(3.1d)}$$

Eq.(3.5) is formed by dividing the right-hand side of eq.(6.1) by the right-hand side of eq.(6.2). Consequently, T satisfies the boundary condition $Q\big|_{x=0} = Q_L$ exactly, but the differential eq. (3.1a+b) only approximately; comparison with numerical calculations shows that T acc.to eq.(3.5) can turn out to be up to 6% too small.

In FIG.6-1 eq.(3.5) is compared with the quasi-exact solution (3.7) for the temperature at the irradiated side x=0 of the slab.

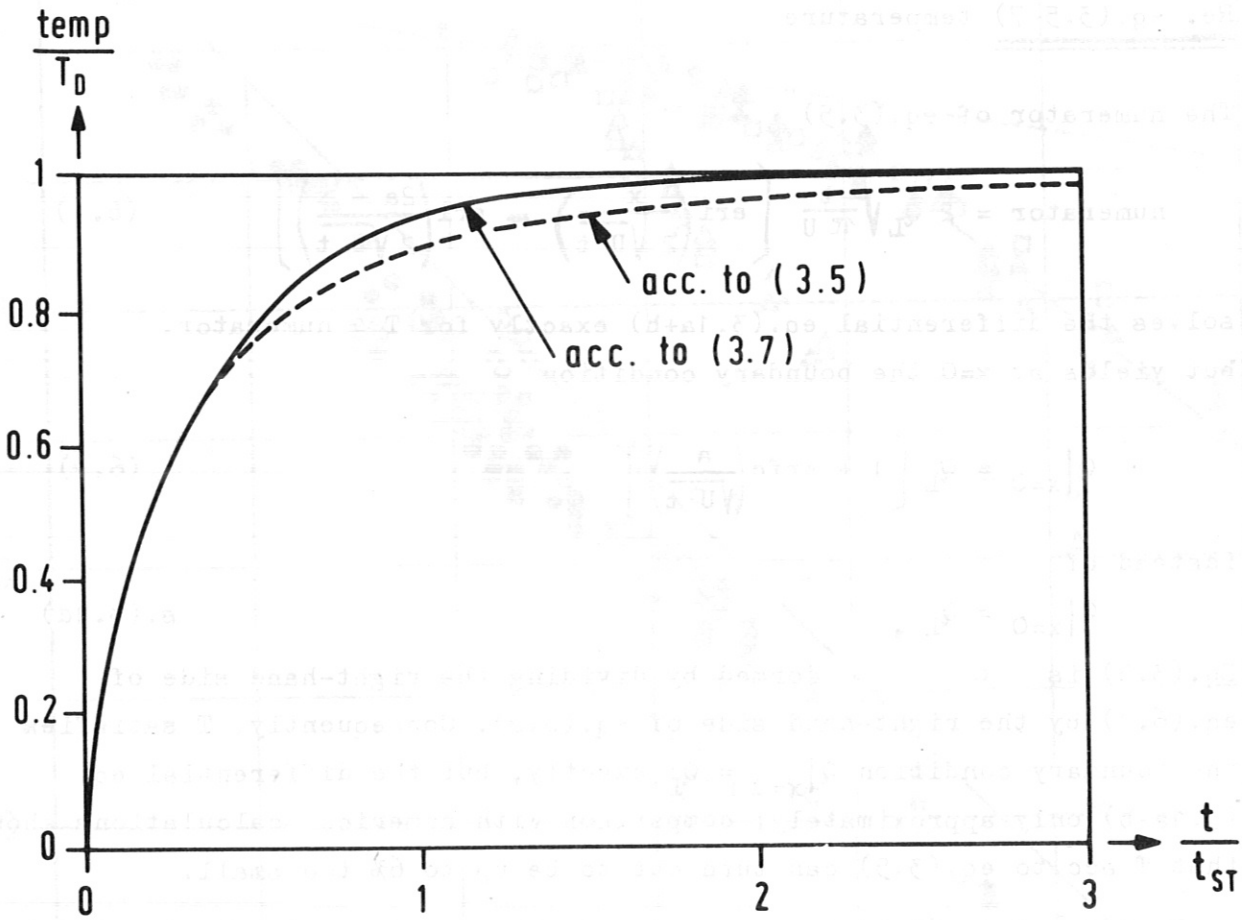

FIG.6-1
The normalized temperature temp/T_D versus t/t_{ST} at x=0

Dashed:
acc.to

$$\frac{temp(x,t)}{T_D} = \frac{2}{\sqrt{\pi}}\sqrt{\frac{t}{t_{ST}}}\;\frac{eri\left(\frac{x/a}{2\sqrt{t/t_{ST}}}\right) - eri\left(\frac{2 - x/a}{2\sqrt{t/t_{ST}}}\right)}{1 + erfc(\sqrt{t_{ST}/t})}$$

s.(3.5)

Solid:
acc.to

$$\frac{temp(0,t)}{T_D} = \sqrt{\frac{1}{\sqrt[3]{0.485\,(t_{ST}/t)^3 + 1}}}$$

s.(3.7)

Re. eq.(4.13-15) Extreme limiting cases

Exact analytical solutions relevant to our problem (4.1) (H diffusion) only exist for the following boundary conditions:

"Right": $C\big|_{x\to\infty} = 0$ (6.3c)

"Left": $C\big|_{x=0}$ or $F\big|_{x=0}$ piecewise constant .

The solutions for these cases are obtained by superposing the solutions given in sec.2 in the same fashion as in eq.(3.8).

At times not too long ($t < t_{SC}$) no significant concentration will yet have formed at x=a, so that boundary condition (4.1c) can be replaced by (6.3c) in good approximation. This applies not only to the extreme limiting cases but also to all solutions with $t \ll t_{SC}$ (s. eq.(4.3b)). Consequently, the parameters a and K_R do not appear in eq.(4.5) till (4.24) inclusive.

The extreme limiting cases are obtained for parameters for which the boundary condition at x=0 can be put in the form

$$F\big|_{x=0} = \begin{cases} 0 & \text{during dwell times} \\ F_L & \text{during burn times} \end{cases} \qquad (6.3d)$$

or

$$C\big|_{x=0} = \begin{cases} 0 & \text{during dwell times} \\ C_L & \text{during burn times} \end{cases} \qquad (6.4d)$$

For nomenclature:
Problem (6.3) is defined by replacing in problem (4.1)
(4.1c) by (6.3c) and (4.1d) by (6.3d) ;
problem (6.4) is defined by replacing in problem (4.1)
(4.1c) by (6.3c) and (4.1d) by (6.4d) ;
with all other eqs. being unchanged: one thus has (6.4a) = (4.1a) etc..

The extremely dirty limiting case

This case is defined by boundary condition (6.3d) (s.page 59) and can be achieved in two ways:

Either the recombination coefficient is made to vanish:

$$K_L = 0 \ ,$$

which is why this case is called "extremely dirty",

Or the H concentration $C \approx 0$, as is the case immediately after the start of the 1st burn period, even with finite values of the recombination coefficient, which is why this case is called "short time case" (s.eq.(4.5)).

In eq.(6.5) we give the solution for the 2nd burn period.

$$C = \frac{2 F_L}{\sqrt{\pi D}} \left[\sqrt{t}\ \operatorname{eri}\left(\frac{x}{2\sqrt{D\,t}}\right) - \sqrt{\hat{t}}\ \operatorname{eri}\left(\frac{x}{2\sqrt{D\,\hat{t}}}\right) + \sqrt{\tilde{t}}\ \operatorname{eri}\left(\frac{x}{2\sqrt{D\,\tilde{t}}}\right) \right] \qquad (6.5a)$$

$$F = F_L \left[\operatorname{erfc}\left(\frac{x}{2\sqrt{D\,t}}\right) - \operatorname{erfc}\left(\frac{x}{2\sqrt{D\,\hat{t}}}\right) + \operatorname{erfc}\left(\frac{x}{2\sqrt{D\,\tilde{t}}}\right) \right] \qquad b)$$

With $\hat{t} = t - t_{burn}$

$\tilde{t} = t - t_{burn} - t_{dwell}$;

Reproduction of FIG.3-1:

the time scales used in this report: t ,

$\hat{t} = t - t_{burn}$

and $\tilde{t} = t - t_{burn} - t_{dwell}$

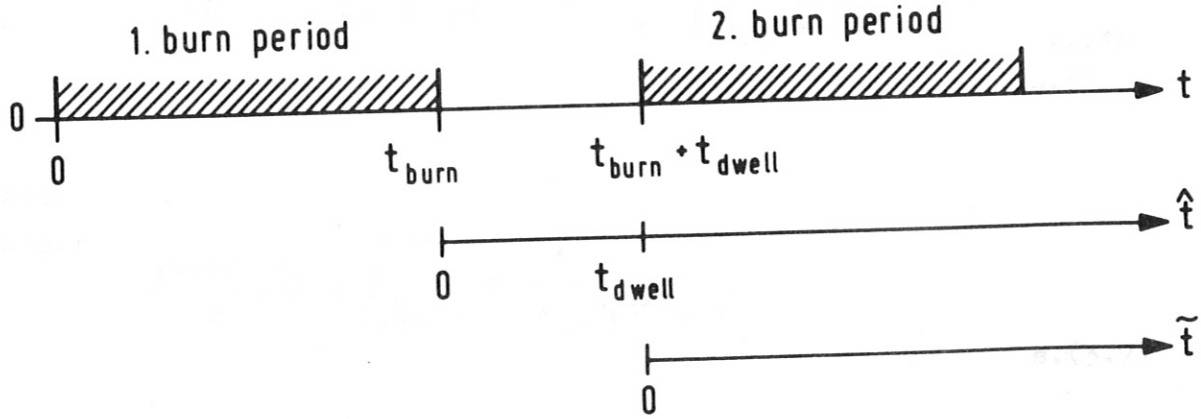

The extremely clean limiting case

This case is defined by boundary condition (6.4d) (s.page 59), which is obtained from eq.(4.1d) by setting $K_L \to \infty$ or

$$F|_{x=0} = 0 .$$

This is approximately achieved if

$$t_A \ll \tilde{t},\ \hat{t},\ t,\ t_{dwell},\ t_{burn}$$

is satisfied, i.e.
for very large values of K_L, hence the name "extremely clean", and/or for large $\tilde{t}, \hat{t}, t$ which is why this case is also named "long time case".
The solution for the 2nd burn period is analog to eq.(6.5)

$$C = C_L \left[\operatorname{erfc}\left[\frac{x}{2\sqrt{D\,t}}\right] - \operatorname{erfc}\left(\frac{x}{2\sqrt{D\,\hat{t}}}\right) + \operatorname{erfc}\left(\frac{x}{2\sqrt{D\,\tilde{t}}}\right)\right]$$

$$F = \frac{C_L}{\sqrt{\pi\,D}}\left[\frac{1}{\sqrt{t}}\exp\left[-\left(\frac{x}{2\sqrt{Dt}}\right)^2\right] - \frac{1}{\sqrt{\hat{t}}}\exp\left[-\left(\frac{x}{2\sqrt{D\hat{t}}}\right)^2\right] + \frac{1}{\sqrt{\tilde{t}}}\exp\left[-\left(\frac{x}{2\sqrt{D\tilde{t}}}\right)^2\right]\right] .$$

(6.6)

Re. eq.(4.5) - (4.12) **Analogies between**

1st burn period and nth dwell period for constant coefficients

Here we compare the concentration build-up during the 1st burn period with the drop during the n-th dwell period, making n large enough to set

$$C(x)\big|_{\hat{t}=0} = C_L \qquad (6.7a)$$

$$F(x)\big|_{\hat{t}=0} = 0 \qquad b)$$

at the start t=0 of the n-th dwell period. Let the coefficients D and K_L be finite constants. We are interested here only in C and F at x=0 and introduce the dimensionless quantities

$$c_o = \frac{C}{C_L}\Big|_{x=0} \quad \text{and} \quad f_o = \frac{F}{F_L}\Big|_{x=0} . \qquad (6.8)$$

Because of the quadratic boundary condition (4.1d) there is no exact analytical solution; we thus have to describe numerical results with arbitrary approximation formulae. The arbitrariness in the choice of approximation formulae is, however, severely restricted by the requirement that the approximation formulae have to contain the extreme limiting cases short time (eq.(4.5) and (4.9c)) and long time (eq.(4.7) and (4.11)) as special cases.
If the flux is written in the form

$$f_o = \begin{cases} 1/\sqrt{1+b\tau} & \text{for the 1st burn time} \\ 1/(1+\hat{b}\sqrt{\hat{\tau}} & \text{" " n-th dwell "} \end{cases} \qquad (6.9h)$$

it follows from numerical results that

$$b = 1 - 0.19/\sqrt{1+\tau} \quad \text{for the 1st burn time} \qquad (6.9k)$$
$$\hat{b} = 1 + 0.27/\sqrt[6]{1+\hat{\tau}} \quad \text{" " n-th dwell "}$$

In tab.(6.9) it is shown why the factors 0.19 and 0.27 have to occur in the short-time case. Both are small relative to 1, and so everywhere in sec.4 except in eq.(4.8) and (4.12) we use the approximation $b = \hat{b} = 1$ (s.(6.9j)).

Explanation	1st burn period	n-th dwell period	
Initial condition	$c_o = 0$	$c_o = 1$	(6.9a)
Short-time solution acc.to (4.5b)+(4.9c)	$c_o = \frac{2}{\pi}\sqrt{\tau}$	$c_o = 1 - \frac{2}{\pi}\sqrt{\hat{\tau}}$	b)
Substitution of the short-time solution into the bound.cond.	$f_o = 1-c_o^2$	$f_o = - c_o^2$	c)
yields	$f_o = 1- \frac{4}{\pi^2}\tau$	$f_o = -1 + \frac{4}{\pi}\sqrt{\hat{\tau}}$	d)
This is interpreted as a power series expansion of	$f_o = \frac{1}{\sqrt{1+\frac{8}{\pi^2}\tau}}$	$f_o = \frac{-1}{1+\frac{4}{\pi}\sqrt{\hat{\tau}}}$	e)
since these functions also give within factors of the order 1 acc.to (4.7)+(4.11) the long-time solution	$f_o = \frac{1}{\sqrt{\tau}}$	$f_o = - \frac{1}{\sqrt{\hat{\tau}}}$	f)
This is interpreted as an expansion of	$f_o = \frac{1}{\sqrt{1+\tau}}$	$f_o = - \frac{1}{\sqrt{1+\hat{\tau}}}$	g)
The exact solution is	$f_o = \frac{1}{\sqrt{1+ b\tau}}$	$f_o = - \frac{1}{1+ \hat{b}\sqrt{\hat{\tau}}}$	h)
where in the short-time case	$b = \frac{8}{\pi^2} = 1-0.19$	$\hat{b} = \frac{4}{\pi} = 1+0.27$	i)
and in the long-time case	$b = 1$	$\hat{b} = 1,$	j)
For arbitrary times we have from numerical results approx.	$b = 1 - \frac{0.19}{\sqrt{1+\tau}}$	$\hat{b} = 1 + \frac{0.27}{\sqrt[6]{1+\hat{\tau}}}$	k)

Re. eq.(4.16-(4.17) Superposition

We look for an approximation formula for the re-emission flux during the 1st dwell period for the case where the length of the preceding burn period t_{burn} is finite. If $t_{dwell} \ll t_{burn}$, this formula can also be used for arbitrary dwell times by replacing t_{burn} with $\hat{t}_{burn}$ from eq.(4.15a).

The re-emission flux

$$\left.\frac{F}{F_L}\right|_{x=0} = f_o \qquad \text{s.(6.8)}$$

depends on the parameters

$$\hat{\tau} = \pi \hat{t}/t_A \qquad \text{s.(4.9e)}$$

and

$$\tau_{burn} = t_{burn}/t_A$$

Acc.to eq.(4.8a) the concentration during the 1st burn period is

$$\left.\frac{c}{c_L}\right|_{x=0} = c_o = \sqrt{1 - \frac{1}{\sqrt{1+ b\tau}}} \qquad \text{s.(4.8a)}$$

We use this value for c_o as initial condition and modify the right-hand column of tab.(6.9) for the dwell period as follows:

Explanation	1st dwell time
initial condition	$c_o = \sqrt{1 - \frac{1}{\sqrt{1+ b\hat{\tau}}}}$
Short-time solution	$c_o = \sqrt{1 - \frac{1}{\sqrt{1+ b\tau}}} - \frac{2}{\pi}\sqrt{\hat{\tau}}$
Substitution in the bound.cond.at x=0	$f_o = - c_o^2$
yields	$f_o = - 1 + \frac{4}{\pi}\sqrt{\hat{\tau}} + \frac{1}{\sqrt{1+ b\tau}}$
This equation is interpreted as an expansion of	$f_o = - \frac{1}{1 + \hat{b}\sqrt{\hat{\tau}}} + \frac{1}{\sqrt{1+ b\tau}}$ (6.10a)
with	$\left.\hat{b}\right\|_{x=0} = \frac{4}{\pi} = 1.27$.

Substituting $\hat{b} = b = 1$

into eq.(6.10a) yields eq.(4.16).
For $\hat{\tau} \lesssim 0.001 \tau_{burn}^2$ this substitution causes the re-emission flux to be about 10% too high ("substitution error", s.FIG.4-6c).
For $\hat{\tau} \gtrsim 0.1 \tau_{burn}^2$ eq.(6.10a) is no longer the correct interpretation of the short-time solution

$$f_o = -1 + \frac{1}{\sqrt{1+ b\tau}} + \frac{4}{\pi}\sqrt{\hat{\tau}} \qquad \text{(s.page 64)}$$

One can interpret this e.g. as an expansion of

$$f_o = \frac{-1 + \frac{1}{\sqrt{1+ b\tau}}}{1 + \frac{4}{\pi}\sqrt{\hat{\tau}} \Big/ \left[1 - \frac{1}{\sqrt{1+ b\tau}}\right]} \qquad (6.10b)$$

This goes much too slowly $\to 0$ for large $\hat{\tau}$, but was useful for obtaining

$$\left.\frac{F}{F_L}\right|_{x=0} = \frac{-1 + \frac{1}{\sqrt{1 + \tau_{burn}}}}{1 + 1.3\sqrt{\hat{\tau} + 6\hat{\tau}/\tau_{burn}} + 3.2\ \hat{\tau}^{1.33}/\tau_{burn}^{0.9}} \qquad \text{s.(4.17)}$$

from numerical results.

For $\tau_{burn} \geq 1$ and $\hat{\tau} \geq 0.1\, \tau_{burn}$

we have in crude approximation

$$f_o = 0.043\, \tau_{burn}^{1.04}\ \hat{\tau}^{-\hat{E}} \qquad (6.10c)$$

with

$$\hat{E} = 1.06 + 0.031 \ln \tau_{burn} .$$

For very large values of $\hat{\tau}$ eq.(6.10c) is a better approximation than eq.(4.17).

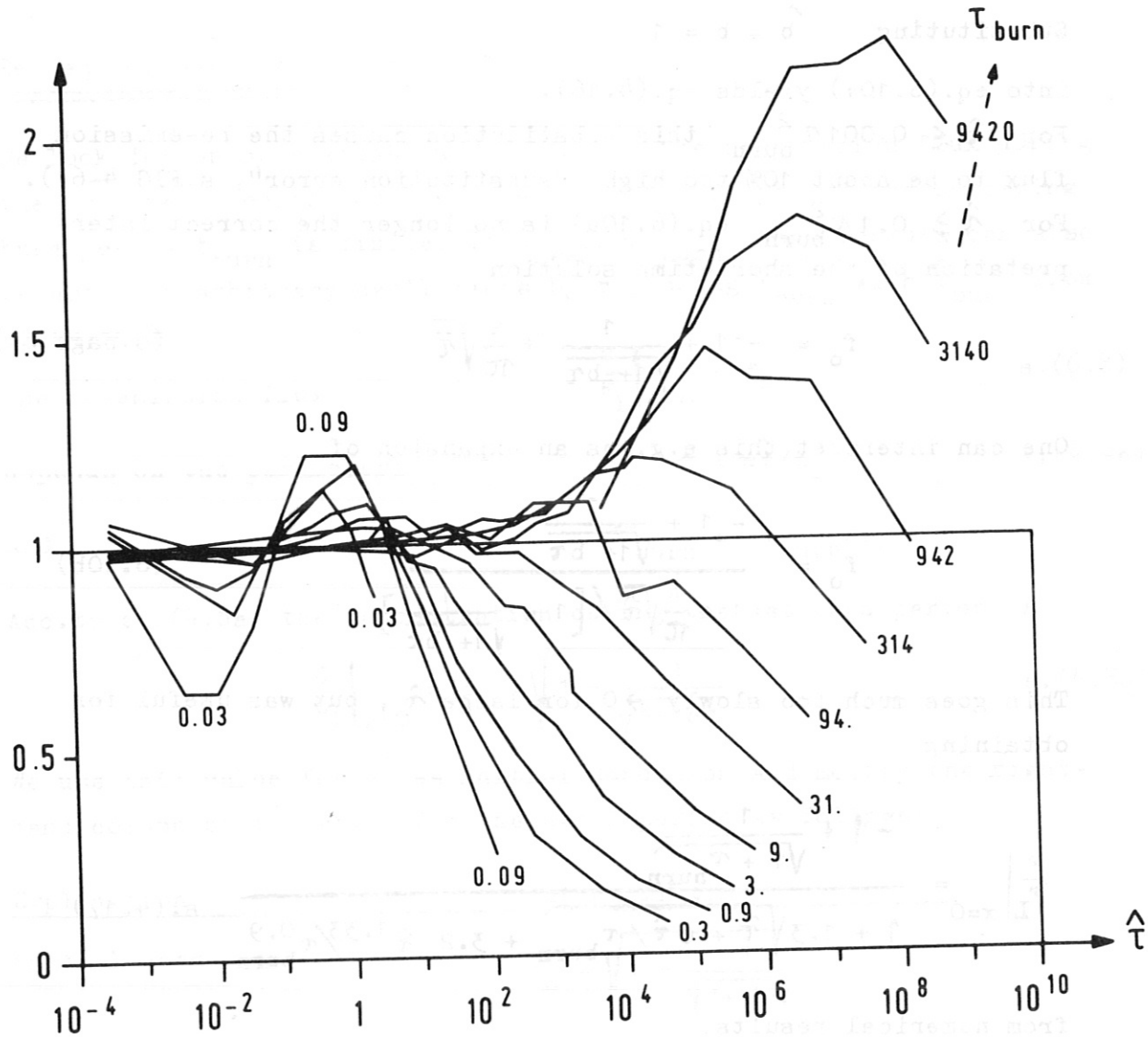

FIG.6-2

To test the interpolation formula (4.17)

the quotient $$\hat{q} = \frac{\text{F calculated acc.to eq.(4.17)}}{\text{F numerically calculated}}$$

is plotted as a function of $\hat{\tau}$ and τ_{burn}

Re. eq.(4.19) Maximum of $C(t)\big|_{x=0}$

First we give an approximation for the time dependence of C:

$$C_L = \sqrt{F_L / K_L} \qquad \text{s.(4.3c)}$$

$$= \sqrt{F_L / K_o}\ \exp\left[\tfrac{1}{2} E_K / T_L\right] \qquad \text{s.(4.1h)}$$

$$= \sqrt{F_L / K_o}\ \exp\left[\tfrac{1}{2} E_K / \left(T_R + \tfrac{2}{\sqrt{\pi}} T_D \sqrt{\frac{t}{t_{ST}}}\ \right)\right] \qquad \text{s.(3.5a)}$$

$$= \sqrt{F_L / K_o}\ \exp\left[\tfrac{1}{2} E_K / T_R\right] \left(1 - \hat{A}\sqrt{\tau}\ \right) . \qquad (6.11)$$

The last two lines contain the short-time expansion (3.5a) for the temperature and, consequently, are only valid if $t < t_{ST}$;

the parameter
$$\hat{A} = 0.3 \frac{T_D E_K}{T_R^2} \sqrt{\frac{t_A}{t_{ST}}} \qquad (6.12)$$

essentially describes the decrease of the H concentration on the irradiated side of the slab due to the rising temperature.
Apart from constant factors, it follows from eqs.(6.11) and (4.6b)

that
$$c = (1 - \hat{A}\sqrt{\tau}) \sqrt{1 - \frac{1}{\sqrt{1+\tau}}} \qquad (6.13)$$

and
$$\frac{dc}{d\tau} = \frac{1}{2} \sqrt{1 - \frac{1}{\sqrt{1+\tau}}} \sqrt{\frac{1}{1+\tau}} \left\{ \frac{1}{1+\tau} - \left[\sqrt{1+\tau} - 1\right] \frac{\hat{A}}{\sqrt{\tau}} \right\} .$$

It holds approximately (approx. 20% inaccuracy) that

$$\frac{(1+\tau)\left(\sqrt{1+\tau} - 1\right)}{\sqrt{\tau}} \approx \tau \qquad (6.14)$$

so that from $\frac{dc}{d\tau} = 0$

we have
$$\tau = \frac{1}{\hat{A}} \qquad (6.15)$$

and hence
$$t_{max} = \frac{T_R^2}{E_K T_D} \sqrt{t_A t_{ST}} \ . \qquad \text{s.(4.19)}$$

The inaccuracy is about 20%-50%. Eq.(4.19) is no longer valid, if $t_A \gtrsim t_{ST}$, because there is then mostly no maximum, as in the case of, for example, INTOR with dirty surfaces, s.FIG.4-5d.

Re. eq.(4.27) Steady-state, general solution

Comparison of our formulae with those of Ref./14/

This paper	Ref./14/
$\frac{\partial C}{\partial x} - \frac{S}{a} C = - F_{perm} \frac{1}{D}$	$y' + f\, y = g$
$C = e^{R}(C_o - F_{perm}\, G)$	$y = e^{-F}\left(\eta + \int_o^x g\, e^{F}\, dx`\right)$
$R = \frac{1}{a} \int_o^x S\, dx`$	$F = \int_o^x f\, dx`$

Re.eq.(4.28) C_o and F_{perm} from boundary conditions

Eq.(4.28) arises from eq.(4.1c+d) with $F_{implant} = \overline{F_{implant}}$ and $F = F_{perm}$.

Eq.(4.28) is a 4th order algebraic system and very difficult to solve exactly. However, in most practical cases it holds that

$$F_{perm} \ll \overline{F_{implant}} \,. \tag{6.16}$$

Thus we have

from eq.(4.28a) $$C_o \approx \sqrt{\overline{F_{implant}} / K_L} \tag{6.16a}$$

Defining $$F_p = \frac{e^{-2R_a}}{2K_R G_a^2} + \frac{C_o}{G_a} \tag{6.17a}$$

yields

from eq.(4.28b) $$F_{perm} = F_p - \sqrt{F_p^2 - (C_o/G_a)^2} \,. \tag{b}$$

If condition (6.16) is not valid, eq.(6.16a)-(6.17b) can be used as 1st step of an iteration. The next step is the more accurate calculation of C_o from

$$C_o = \sqrt{\left[\overline{F_{implant}} - F_{perm}\right] / K_L} \tag{6.17c}$$

which arises from rearranging eq.(4.28a).

Re. eq.(4.29) $C\big|_{x=a} = 0$

This case is approximatively realized for very large values of K_R i.e. clean surfaces. From eq.(6.17b+a) we have

$$F_{perm} = + C_o / G_a \quad . \tag{6.18a}$$

In this case eq.(4.28) is only a 2nd order algebraic equation

$$C_o / G_a = \overline{F_{implant}} - K_L C_o^2$$

which can be exactly solved to give

$$C_o = \left[-\frac{1}{2G_a} + \sqrt{\frac{1}{4G_a^2} + \overline{F_{implant}}} \right] \Big/ \sqrt{K_L} \quad . \tag{6.18b}$$

Defining $$\overline{C}_L = \sqrt{\overline{F_{implant}} / K_L} \qquad \text{s.(4.29f)}$$

and $$A = \frac{1}{2G_a K_L \overline{C}_L} \tag{6.18c}$$

yields $$C_o = \overline{C}_L \left[\sqrt{1+A^2} - A \right] \quad . \qquad \text{s.(4.29h)}$$

Eq.(6.18) holds also if SORET effect and temperature dependence of D is taken into account.

Now let us furthermore assume: $D = \text{const}$

and $R = 0.$

In this case we have $$G = \int_o^x \frac{dx}{D} \, e^{-R} = \frac{x}{D}$$

In eq.(6.16-18) is $$G_a = G\big|_{x=a} = \frac{a}{D} \; ; \tag{6.19a}$$

Inserting eq.(6.19a) into eq.(6.18a) yields $$F_{perm} = C_o \frac{D}{a} \qquad \text{s.(4.29e)}$$

Inserting eq.(6.19a) into eq.(6.18c) yields $$A = \frac{D}{2aK_L \overline{C}_L} \quad . \qquad \text{s.(4.29g)}$$

Re. eq.(4.31) Finite K_R

From $D = \text{const}$ s.(4.31a)

and $R = 0$ b)

it follows that $G = + x/D$. s.(6.19a)

Inserting this into $F_p = \frac{1}{2K_R G_a^2} + \frac{C_o}{G_a}$ s.(6.17a)

yields $F_p = C_o \frac{D}{a}\left[\frac{p}{2} + 1\right]$

with $p = \frac{D}{K_R C_o a}$. s.(4.31f)

Inserting this into $F_{perm} = F_p - \sqrt{F_p^2 - (C_o/G_a)^2}$ (6.17b)

gives $F_{perm} = C_o \frac{D}{a'}$

with $a' = \frac{a}{1-h}$

and $h = \sqrt{p + \frac{1}{4}p^2} - \frac{1}{2}p$.

From the general solution $C = C_o - F_{perm} \frac{x}{D}$ s.(4.27e)

we have $C = C_o\left[1 - \frac{x}{a'}\right]$

$C = C_o\left[1 - \frac{x}{a}(1-h)\right]$ s.(4.31c)

and from this $h = \frac{C|_{x=0}}{C|_{x=a}}$ = relative height at x=a.

The equations given here on p.70 are part of the iteration (6.17), because C_o is not exactly known. However, in most practical cases one may forgot this taking $\overline{C_L}$ for C_o .

Re. eq.(4.32) SORET effect

In order to get an estimate easy to handle we replace

the x-dependent $$S = - a\, E_{SOR} \frac{\partial T/\partial x}{T^2}$$ s.(4.27a)

by the

constant average value $$\bar{S} = E_{SOR}\, \overline{T}_D / T_M^2 \,.$$ s.(4.32e)

From the general solution

it follows that

$$R = \frac{1}{a} \int_o^x S\, dx' = \bar{S}\, \frac{x}{a}$$ s.(4.27b)

$$G = \int_o^x \frac{1}{D}\, e^{-R} dx' = \frac{a}{\bar{S}\, D} \left[1 - e^{-R}\right]$$ s.(4.27c)

$$C = e^{R}(C_o - F_{perm} G)$$ s.(4.27e)

$$= e^{R}(C_o - F_{perm} \frac{a}{\bar{S}\, D}) + F_{perm} \frac{a}{\bar{S}\, D} \,.$$

From the boundary condition

$$C\big|_{x=a'} = 0$$ s.(4.32b)

we have $$F_{perm} = C_o \frac{D}{a} \frac{\bar{S}}{1 - \exp(-\bar{S}\, \frac{a'}{a})}$$ (6.20a)

$$C = C_o \frac{1 - \exp\left[\bar{S}(\frac{x}{a} - \frac{a'}{a})\right]}{1 - \exp\,(-\bar{S}\, \frac{a'}{a})} \,.$$ b)

Expanding yields

$$C = C_o \left[1 - \frac{x}{a'}\right]\left[1 + \frac{\bar{S}}{2} \frac{x}{a} + ..\right]$$ s.(4.32c)

$$F_{perm} = C_o \frac{D}{a'} \left[1 + \frac{\bar{S}}{2} \frac{a'}{a} + ..\right] \,.$$ d)

Note that C/C_o acc.to the exact solution (6.20) is ≤ 1 ; the case $C/C_o > 1$ with hydrogen running against grad C driven by grad T (s.FIG.4-11) can only occur if the diffusion coefficient D depends on the temperature .

Numerical calculations show that G as calculated from page 71 becomes too small due to replacing S by $\bar{S}$; the relative error is about

$$\varepsilon = \begin{cases} \bar{S}\ \overline{T}_D / T_M & \bar{S} \lesssim 1 \\ \overline{T}_D / T_M & \bar{S} \gtrsim 1 . \end{cases} \qquad (6.20c)$$

Furthermore, the expansions (4.32c+d) induce an error about $\bar{S}/3$; the applicability of eq.(4.32) is therefore limited by

$$\frac{\overline{T}_D}{T_M} \lesssim 0.3 \qquad \bar{S} \lesssim 1 . \qquad (6.20d)$$

Sample application:
steel slabs in the reactor as defined in tab.(4.2)+(4.20)+(5.4):

for steel one has $E_{SOR} = 800^\circ$
for the reactor one has $T_D = 200^\circ$
and $T_M = 700^\circ$

It follows that $|\bar{S}| = 0.3$
$\varepsilon \approx 5\% - 10\%$.

From this it can be expected that eq.(4.32) is a good approximation; s.FIG.4-10

Re. eq.(4.33) Temperature-dependence of D

Neglecting the SORET effect $R = E_{SOR} = 0$

we have $$C(x) = C_o - F_{perm} \int_o^x \frac{dx`}{D(x`)} \qquad \text{s.(4.27b+e)}$$

$$C(x) = C_o - F_{perm} \frac{x}{D(\tilde{x})} \; . \qquad (6.21)$$

$\tilde{x}$ is defined by $$\frac{x}{D(\tilde{x})} = \int_o^x \frac{dx`}{D(x`)} \; ;$$

in the following we estimate $\tilde{x}$ from numerical results.

In the case $$D = D_o \exp(-E_D / T) \qquad \text{s.(4.1g)}$$

with $$T = T_R + \bar{T}_D \left(1 - \frac{x}{a}\right) \qquad \text{s.(4.25k)}$$

we have approximatively

$$\tilde{x} = x \left[1 - \frac{1}{2 + 0.2\, E}\right] \qquad (6.22a)$$

with $$E = \frac{(T_R + \bar{T}_D - T)\, E_D\, x}{T^2 \quad a} \; . \qquad b)$$

In FIG.6-3 we test the applicability of the approximation (6.22) by representing

$$q = \frac{\int_o^x \frac{dx`}{D(x`)} \quad \text{numerically calculated}}{\frac{x}{D(\tilde{x})} \quad \text{with } \tilde{x} \text{ from eq.(6.22a)}} \qquad (6.22c)$$

as a function of the two dimensionless parameters

$$z = \bar{T}_D x / \left[(T_R + \bar{T}_D)\, a\right] \qquad (6.22d)$$

and

$$A_D = E_D / (T_R + \bar{T}_D) \qquad e)$$

The deviation q-1 is a measure of the relative error.
It is found that the numerical results are almost exactly (< 1%) reproduced for our examples INTOR and reactor with clean or dirty surfaces. There are, however, other examples for which approximation (6.21) is not very applicable or not at all, e.g. $A_D \geq 30$ and $z \geq 0.7$

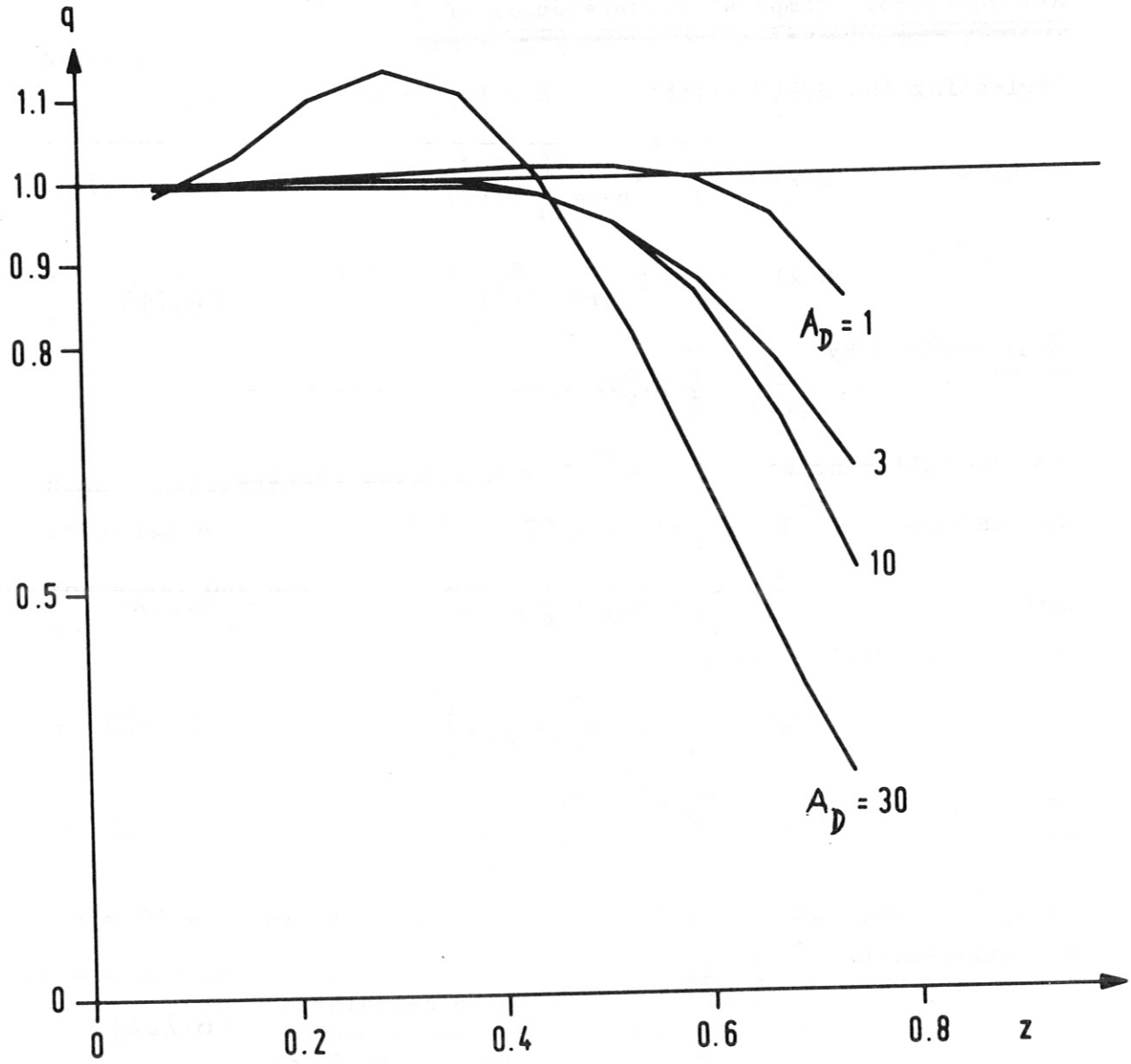

FIG.6-3
To test the approximation (6.22)

the quotient $$q = \frac{\int_0^x \frac{dx`}{D(x`)} \quad \text{numerically calculated}}{\frac{x}{D(\tilde{x})} \quad \text{with } \tilde{x} \text{ from eq.(6.22)}}$$

is plotted as a function of the parameters

$$z = \overline{T}_D x / [(T_R + \overline{T}_D)\ a]$$

and

$$A_D = E_D / (T_R + \overline{T}_D).$$

The examples INTOR and reactor are located at $5 \leq A \leq 10$
and $0 \leq z \leq 0.3$

If we know how to calculate $\tilde{x}$ from x,
we also can calculate the solution with the
boundary condition

$$C|_{x=0} = C_o$$
$$C|_{x=a} = C_o h$$

from eq.(6.21): one has

$$C = C_o \left[1 - \frac{x}{a}(1-h) \frac{D(\tilde{a})}{D(\tilde{x})} \right] \qquad (6.23a)$$

with $$\tilde{a} = a\left[1 - \frac{1}{2 + 0.2B}\right] \qquad b)$$

and $$B = E_D \overline{T}_D / T_R^2 \ . \qquad c)$$

$$F_{perm} = C_o \frac{1-h}{a} D(\tilde{a}) \qquad d)$$

$$= C_o \frac{1-h}{a} D_o \exp\left[- E_D / T(\tilde{a})\right] \qquad e)$$

with $$T(\tilde{a}) = T_R + \overline{T}_D / (2 + 0.2B), \qquad f)$$

However, in general the calculation of $D(\tilde{x})$ is a tedious matter;
therefore we look for simplifications.

Neglecting E in eq.(6.22a): $\tilde{x} = \frac{x}{2}$

and assuming small temperature gradient $\overline{T}_D \ll T_R$

we can approximate $$\frac{D(\tilde{a})}{D(\tilde{x})} \approx \exp\left[\frac{B}{2}\left(\frac{x}{a} - 1\right)\right]. \qquad (6.24)$$

Numerical calculations show that
the range of validity of eq.(6.24) is approximatively

$$E_D / T_R \lesssim 15 \quad \text{and} \quad \overline{T}_D / T_R \lesssim 1 \qquad (6.25)$$

$$E_D / T_R \lesssim 20 \quad \text{and} \quad \overline{T}_D / T_R \lesssim 0.2 \ .$$

For our examples INTOR and reactor with steel slabs eq.(6.24)
is a good approximation. Inserting eq.(6.24) into eq.(6.23a)
yields eq.(4.33c). Furthermore, $T(\tilde{a})$ from (6.23f) = $\tilde{T}$ from (
(4.33f).

Example for eq.(4.33c)

Permeation rates for INTOR with dirty surfaces

"INTOR" is defined in this report
acc.to tab.(4.20) by the data

$F_L = 1.5\ 10^{16}$ atoms/(cm^{2}sec)
$T_D = 80^o$
$T_R = 600^oK$;
$K_o = 1.6\ 10^{-20}$cm^4/(atom sec);

"Dirty" is defined by
in addition, one has ac.to (4.2)

$a = 1$ cm
$D_o = 0.085$ cm^2/sec
$E_D = 7000^oK$
$E_K = 6000^oK$.

From this we get
the averaged temperature

$\overline{T} = 640^oK$

and

$D = D_o \exp(-E_D / \overline{T}) = 1.5\ 10^{-6}$ cm^2/sec
$K_L = K_o \exp(-E_K / T_L) = 2.4\ 10^{-24}$cm^4/(atom sec)
$K_R = K_o \exp(-E_K / T_R) = 7.3\ 10^{-25}$ "
$C_o = \sqrt{F_L / K_L} = 7.9\ 10^{19}$ atoms/cm^3

$p = D / (K_R\ C_L\ a) = 0.026$

$h \approx \sqrt{p} = 0.16$

$F_{perm} = C_o \frac{D}{a} (1-h) = 1.0\ 10^{14}$ atoms/(cm^{2}sec)
$= 0.14$ gramm / (m^{2}day)

in the case of 1 atom $= 1.67\ 10^{-24}$gramm (H^1)

Comparison with Ref./6/

Reference /6/ presets formulae and examples for the steady-state problem, which are compared here in tabular form with the formulae used in this report

ref/6/		this paper
$F_i = - D \frac{\partial n}{\partial x}$	(1)	$F_{perm} = - D \frac{\partial C}{\partial x}$
$n(0) - n(x) = F_i \int_0^x \frac{dz}{D(T(z))}$	(2)	$C_L - C(x) = F_{perm} \int_0^x \frac{dx`}{D(x`)}$
$n(0) = \sqrt{\frac{F_o}{K(0)}}$	(3)	$C_L = \sqrt{\frac{F_L}{K_L}}$
$n(d) = \sqrt{\frac{F_i}{K(d)}}$	(4)	$C(a) = \sqrt{\frac{F_{perm}}{K_R}}$
$\sqrt{\frac{F_o}{K(0)}} - \sqrt{\frac{F_i}{K(d)}} = F_i \int_0^d \frac{dz}{D(T(z))}$	(5)	$C_L - C(a) = F_{perm} \int_0^a \frac{dx`}{D(x`)}$
$\varphi\xi = z/d$		
$\int_0^d \frac{dz}{D(T(z))} = d \int_0^1 \frac{d\varphi\xi}{D(T(\xi))}$	(6)	$\int_0^a \frac{dx`}{D(x`)} = \frac{a}{D(\tilde{a})}$
$F_i = \sqrt{\frac{F_o}{K(0)}} \; \frac{1}{d} \left[\int_0^1 \frac{d\varphi\xi}{D(T(\xi))} \right]^{-1}$	(7)	$F_{perm} = C_L \frac{D(\tilde{a})}{a}$
$F_i = \sqrt{\frac{F_o}{K(0)}} \; \frac{D(T(0))}{d} \; R$		$F_{perm} = C_L \frac{D(0)}{a} \tilde{R}$
$R = \left[\int_0^1 d\varphi\xi \frac{D(T(0))}{D(T(\varphi\xi))} \right]^{-1}$	(8)	$\tilde{R} = \frac{D(\tilde{a})}{D(0)}$

7. Outline of numerical calculation

Here we outline the numerical calculation of the H concentration and flux near the irradiated side x=0 of the slab during the 1st burn and dwell periods. The method described only deals with distances x from the irradiated side that are small relative to the slab wide a. We therefore neglect the spatial dependence of the temperature and take only its time dependence into account.
We start with the 1st burn time. The long-time solution

$$C = C_L \, \mathrm{erfc}\left(\frac{x}{H}\right) \qquad \text{s.(4.7b)}$$

is also valid for time-dependent diffusion coefficient D, if

$$H = 2\sqrt{\int_0^t dt' D(t')} \qquad (7.1)$$

is used instead of eq.(4.5e) as profile depth. With time-dependent t, the short-time solution (4.5) also remains at least qualitatively correct. Both in the long-time and in the short-time solution x only appears in the combination

$$V = \frac{x}{H} \quad ; \qquad (7.2)$$

we therefore use V instead of x as independent variable. This gives the symbol $\partial C/\partial t$ a different meaning to that in problem (4.1) because V depends on time via H. It holds that

$$\left.\frac{\partial C}{\partial t}\right|_{x=\text{const}} = \left.\frac{\partial C}{\partial t}\right|_{V=\text{const}} + \frac{\partial C}{\partial V}\,\frac{\partial V}{\partial t} \qquad (7.3a)$$

with

$$\frac{\partial V}{\partial t} = -\frac{2VD}{H^2} \; . \qquad \text{b)}$$

Now to the boundary conditions:
the boundary condition at x=0 is left unchanged.
In order to write down the boundary condition "right"
we introduce a parameter

$$V_{max} \approx 2 \text{ or } 3 \qquad (7.4a)$$

so that $\mathrm{erfc}(V_{max})$ and $\mathrm{eri}(V_{max}) \ll 1$. b)

From this we have $\left. C \right|_{V=V_{max}} = 0$ c)

in good approximation if $t \leq t_{SC} / (4V_{max}^2)$. d)

We use eq.(7.4c) as boundary condition "right" instead of (4.1c), which is justified if (4.7d) is valid. t_{SC} is the particle diffusion time introduced in eq.(4.3b).

For our examples (steel) we have $t_{SC} \approx$ a few days s.(4.3b)

and from this $t \lesssim$ a few hours s.(4.7d)

as the range of applicability for the program described in this section.

Furthermore, the initial condition ought not to be defined at t=0 but should be set at a somewhat later time

$$^{10}\log t_{begin} = {}^{10}\log t_A - KFINE \qquad (7.5)$$

with t_A = release time s.(4.3a)

and KFINE = 2 or 3

as a further accuracy parameter. For the initial distribution we use the short-time solution (4.5), which at time t_{begin} is still a good approximation solution.

Substituting eq.(7.1-5) in problem (4.1) yields

$$\frac{\partial C}{\partial t} = -\frac{1}{H}\left[2VF + \frac{\partial F}{\partial V}\right] \qquad (7.6a)$$

$$F = -\frac{D}{H}\frac{\partial C}{\partial V} \qquad b)$$

$$C\big|_{V=V_{max}} = 0 \qquad c)$$

$$F\big|_{V=0} = F_L - K_L C^2\big|_{V=0} \qquad d)$$

$$C\big|_{t=t_{begin}} = \frac{2}{\sqrt{\pi}}\sqrt{\frac{t}{D}}\, F_L\, \mathrm{eri}\left(\frac{x}{H}\right) . \qquad e)$$

The rest of the equations of problem (4.1) remains unchanged.

To form a difference scheme for problem (7.6), we divide the V interval $(0;V_{max})$ into sub-intervals of equal length ΔV. Acc.to RICHMYER MORTON`s stability criterion this yields a time step

$$\Delta t = Z_2 \, (H \, \Delta V)^2 / D \qquad (7.7a)$$

with $$Z_2 \leq 0.5 \, . \qquad b)$$

Our program contains altogether the four accuracy parameters V_{max} , KFINE , ΔV and Z_2 .

Δt increases roughly in proportion to the time t. The time mesh points are thus approximately equidistant on the log t axis. For example, the number of t mesh points in the interval $(10^{-3};1)$ is the same as in the interval $(1;10^{3})$. From this we can see that the use of V instead of x is well adapted to the abrupt change of burn and dwell times.

During the 1st dwell period we have to solve the problem

$$\frac{\partial C}{\partial t} = - \frac{1}{H} \left[2VF + \frac{\partial F}{\partial V} \right] \qquad (7.8a)$$

$$F = - \frac{D}{H} \frac{\partial C}{\partial V} \qquad b)$$

$$C\big|_{V=V_{max}} = C_{burn} \qquad c)$$

$$F\big|_{V=0} = - K_L C^2\big|_{V=0} \qquad d)$$

$$C\big|_{\hat{t}=t_{begin}} = C_{burn} - \frac{2}{\sqrt{\pi}} \sqrt{\frac{\hat{t}}{D}} \; F_L \; \mathrm{eri}\left(\frac{x}{\hat{H}} \right) \qquad e)$$

where C_{burn} denotes the profile built up during the preceding burn period; for $\hat{t}$, $\hat{H}$ see eq.(4.9f+g).

List of all symbols used in this report

A Capital letters

Symbol		remarks
A	eq.(4.29g)	steady state: $A \approx \frac{1}{2} F_{perm} / \overline{F_{implant}}$
$\hat{A}$	eq.(6.12)	C-decrease due to rising temperature
A_D	eq.(6.22e)	
B	eq.(4.33a)	steady state: temperature dependence
C	eq.(4.1)	H concentration (atoms/cm^3)
C_o	eq.(4.27d)	steady-state: $C_o = C\|_{x=0}$
C_{burn}	eq.(4.9)	dwell time: H concentration built up at the end of the preceding burn time
C_L	eq.(4.3c)	$C_L = \sqrt{F_L / K_L}$
$\overline{C_L}$	eq.(4.29f)	$\overline{C_L} = \sqrt{\overline{F_{implant}} / K_L}$ (steady-state)
C_{var}	eq.(4.9)	dwell time variation: $C_{var} = C - C_{burn}$
D	eq.(4.1)	particle diffusion coefficient
D_o	eq.(4.1g)	
E	eq.(6.22b)	steady state: temperature dependence
$\hat{E}$	eq.(6.10c)	exponent in a superposition formula
E_D	eq.(4.1g)	temperature dependence of diffusion
E_K	eq.(4.1h)	" " " recombination
E_{SOR}	eq.(5.4)	SORET constant: $E_{SOR} = -800^o$ for steel
F	eq.(4.1)	hydrogen flux in the slab
$F_{implant}$	(4.1e)	flux of the implanted H-atoms
$\overline{F_{implant}}$	(4.25e)	time average of $F_{implant}$
$F_{incident}$	(5.3a)	flux of the incident H-atoms
F_L	(4.1e)	$F_{implant}$ during burn times
F_p	eq.(6.17a)	
F_{perm}	eq.(4.27)	permeation rate
G	eq.(4.27)	steady state: $G = \int (e^{-R} / D)\, dx$
G_a	eq.(4.28)	$G_a = G\|_{x=a}$

Symbol		remarks
H	eq.(4.5e)	profile depth during 1st burn period
$\hat{H}$	eq.(4.9g)	outgassing " " 1st dwell "
H_{dwell}	eq.(4.3d)	penetration depth of dwell time variation
I_c	tab.(4.20)	INTOR with clean surfaces
I_d	"	INTOR with dirty "
I_{diff}	eq.(4.34)	inventory of H diffusing towards coolant
I_{trap}	eq.(4.34)	" " caught in traps
I_{total}	eq.(4.34)	$I_{total} = I_{diff} + I_{trap}$
K_o	eq.(4.1h)	
KFINE	eq.(7.5)	accuracy parameter
K_L	eq.(4.1h)	recombination coefficient "Left" at x=0
K_R	eq.(4.1i)	" "Right" " x=a
K_{clean}	FIG.5-1	" " for clean surfaces
K_{dirty}	"	" " " dirty "
K_{waelb}	"	" measured by WAELBROECK
Q	eq.(3.1)	temperature flux
Q_L	eq.(3.1d)	$Q_L = Q\|_{x=0}$ during burn times
R	eq.(4.27)	SORET term in the steady-state general solution
R_a	eq.(4.28)	$R_a = R\|_{x=a}$
R_c	tab.(4.20)	Reactor with clean surfaces
R_d	"	Reactor " dirty "
R_N	eq.(5.3)	particle reflection coefficient
S	eq.(4.27a)	SORET term in FICK`s law
$\bar{S}$	eq.(4.32e)	space average of S
T	eq.(3.1)	temperature
$\tilde{T}$	eq.(4.33f)	steady state: $\tilde{T} = T(\tilde{a})$ from eq.(6.23f)
T_D	eq.(3.3b)	maximal temperature difference towards the end of a burn time
$\overline{T_D}$	eq.(4.26)	time average of $T_D(t)$ prop. $Q\|_{x=0}$
T_L	eq.(4.1k)	temperature "Left" at x=0
T_R	eq.(3.2c)	coolant temperature "Right" at x=a
U	eq.(3.2b)	temperature conductivity

Symbol		remarks
V	eq.(7.2)	V = x/H
V_{max}	eq.(7.4)	bound.cond. $C\big\|_{V=V_{max}} = 0$
W	eq.(4.18a)	
Z_2	eq.(7.7b)	accuracy parameter

B Small letters

Symbol		remarks
a	eq.(3.1)	slab thickness
a'	eq.(4.32g)	zero of C(x)
$\tilde{a}$	eq.(6.23b)	steady-state
b	eq.(4.8)	1st burn time: quasi-exact correction
$\hat{b}$	eq.(4.12)	1st dwell " " " "
c	eq.(5.1)	specific heat
c_o	eq.(6.8)	$C/C_L\big\|_{x=0}$
erfc	eq.(2.1a)	error function complement
eri	eq.(2.2)	error function integrated
f_o	eq.(6.8)	$F/F_L\big\|_{x=0}$
h	eq.(4.31e)	steady state: $h = C\big\|_{x=a} / C\big\|_{x=0}$
p	eq.(4.31f)	steady state: $h \approx \sqrt{p}$
q	FIG.6-3	steady state
$\hat{q}$	FIG.6-2	superposition
$\dot{q}_L$; $\dot{q}$	eq.(5.2)	heat flux
t	eq.(3.1)	time elapsed since 1st switching on
$\hat{t}$	eq.(4.9f)	" " " 1st dwell time start
$\tilde{t}$	FIG.3-1	" " " 2nd burn " "
t_A	eq.(4.3a)	release time $D/F_L K_L$
t_{begin}	eq.(7.5)	
t_{burn}	FIG.3-1	burn time length
t_{dwell}	"	dwell " "

Symbol		remarks
t_{max}	eq.(4.19)	time when $C\|_{x=0}$ (t) reaches its maximum
t_{SC}	eq.(4.3b)	particle diffusion time a^2/D
t_{ST}	eq.(3.3a)	temperature " " a^2/U
x	eq.(3.1)	distance from the irradiated side of the slab
$\tilde{x}$	eq.(6.22)	steady-state
z	eq.(6.22d)	" "

C Greek symbols

Symbol		remarks
Δt	eq.(7.7a)	time step
ΔV	eq.(7.7b)	V-step
ε	page 72	error induced by replacing S by $\bar{S}$
λ	eq.(5.1)	heat conductivity
ϱ	eq.(5.1)	mass density
τ	eq.(4.5d)	dimensionless time $\pi t/t_A$
$\hat{\tau}$	eq.(4.9e)	" " $\pi\hat{t}/t_A$
τ_{burn}	eq.(4.16b)	" " $\pi t_{burn}/t_A$

References

/1/ INTOR Phase II^{A} U.S.A Contributions to the 3rd Workshop Meeting Dec.1981 Brussels/Vienna
1. Tritium Permeation in INTOR (M.I.BASKES et al.,Sandia,Liv.)

/2/ U.GRIGULL, H.SANDNER, Wärmeleitung, Gl.(6.1)

/3/ UC-20d
WFPS-TME-096
October, 1978
Structural Evaluation of a Tokamak Reactor
Cylindrical Module Blanket Concept
T.V.PREVENSLIK

/4/ R.D.RICHTMYER, K.W.MORTON
Difference Methods for Initial Value Problems
Interscience Publishers, John Wiley & Sons
New York 1957

/5/ M.I.BASKES , J.Nucl.Mat.92(1980),318

/6/ J.BOHDANSKY and F.POHL
Tritium Permeation and Inventory for INTOR
in steady state conditions
European Contributions INTOR Workshop Phase 2A Session 4
(22.3.-2.4.1982) Wien

/7/ International Tokamal Reaktor Phase One
Report of the International Tokamak Reactor Workshop
held in seven sessions in Vienna during 1980 and 1981
Vienna 1982
Summary, Table II-13, page 43

/8/ CEA N- 2231 (1981)
Investigation of Phenomena which with Diffusion
can control metals permeability to H Isotops
P.TISON and J-P.FIDELLE

/9/ F.WAELBROECK et al., J.Nucl.Mat.103&104(1981), 471-476

/10/ INTOR Phase II^{A} Critical Issues
European Contributions to the INTOR Phase II^{A} Workshop
Volume III,p.VIII-27

/11/ P.WIENHOLD et al., J.Nucl.Mat.93&94 (1980), 866-870

/12/ M.I.BASKES Report SAND 80-8201 (1980)

/13/ R.A.LANGLEY et al.
Data Compendium for Plasma Surface Interaction
Nuclear Fusion, special issue 1984

/14/ E.KAMKE Differentialgleichungen
Lösungsmethoden und Lösungen
I. Gewöhnliche Differentialgleichungen
Leipzig 1961 Akademische Verlagsgesellschaft